

PEOPLE'S DEMOCRATIC REPUBLIC OF ALGERIA
MINISTRY OF HIGHER EDUCATION AND SCIENTIFIC RESEARCH



UNIVERSITY OF BLIDA 1

Faculty of Technology

Civil Engineering Department



MASTER'S THESIS

Speciality: Materials

MODELLING THE RHEOLOGICAL BEHAVIOUR OF CEMENT
PASTES

By:

Badia HOUAOURA

Younes CHAMAINE

In front of a jury composed of:

Pr.Balkacem MENADI	U. Saad Dahleb-Blida	President
Pr.Abdelmalek BRAHMA	U. Saad Dahleb-Blida	Examiner
M ^{em} .Karima MEGUENNI	U. Saad Dahleb-Blida	Promoter
Dr.Walid YAHIAOUI	U. Saad Dahleb-Blida	Co-Promoter

Blida, June 2023

ملخص:

النمذجة الدقيقة للمعلومات الريولوجية أمر بالغ الأهمية لتحسين قابلية التشغيل والأداء لمعاجين الأسمنت في تطبيقات الهندسة المدنية.

في هذه الدراسة ، نركز على نمذجة المعلومات الانسيابية لنوعين من معاجين الأسمنت المصاغة بواسطة CEMI42.5 و CEMII A 42.5-CPJ و CRS ، معدلة بثلاثة أنواع مختلفة من الملدنات الفائقة المتاحة تجارياً. الهدف من هذه الدراسة هو التحقق من تأثير ثلاثة مواد الملدنة متميزة على السلوك الانسيابي لمعاجين الأسمنت. تم تقدير البيانات التجريبية باختبار ريولوجي باستخدام مقياس اللزوجة الدورانية مع الأسطوانات المحورية ، مما يسمح لنا بجمع البيانات حول إجهاد القص ولزوجة البلاستيك. بعد ذلك ، تم اختبار العديد من النماذج الرياضية ، بما في ذلك نماذج مثل Sisko ، و Bingham المعدلة ، و Herschel-Bulkley ، ونماذج Casson المعممة التي تم استكشافها لتأسيس العلاقات بين التركيب والجرعة من الملدنات الفائقة المقترحة للنهج لتحديد المعلومات الريولوجية المختلفة. تم تقييم أداء النماذج الريولوجية من خلال حساب معامل التحديد R^2 لكل نموذج. تظهر النتائج أن R^2 يعتمد على النموذج المستخدم. تحتوي معظم النماذج التي تمت دراستها على R^2 مشترك أعلى ، لكن معظمها لم يناسب البيانات بشكل أفضل. تم العثور على نموذج Herschel-Bulkley الأنسب لالتقاط منحنى البيانات التجريبية. يأخذ هذا النموذج في الاعتبار بشكل فعال السلوك غير النيوتوني لمعاجين الأسمنت الفائقة اللدائن ، مما يضمن تمثيلاً أكثر دقة لخصائصها الانسيابية.

الكلمات الرئيسية: الريولوجيا؛ الملدن المتفوق؛ نماذج ريولوجية؛ عجينة الأسمنت؛ الأسمنت.

Résumé

La modélisation précise des paramètres rhéologiques est cruciale pour l'optimisation de l'ouvrabilité et de la performance des pâtes de ciment dans les applications de génie civil.

Dans cette étude, nous nous concentrons sur la modélisation des paramètres rhéologiques de deux types de pâtes de ciment formulées par CEMI 42.5 et CEMII A 42.5, modifiées avec trois super plastifiants différents disponibles dans le commerce. L'objectif de cette étude est d'étudier l'impact de trois super plastifiants distincts sur le comportement rhéologique des pâtes de ciment. Les données expérimentales ont été estimées par un test rhéologique utilisant un viscosimètre rotatif avec des cylindres coaxiaux, ce qui nous permet de collecter des données sur la contrainte de cisaillement et la viscosité plastique. Par la suite, divers modèles mathématiques ont été testés, y compris des modèles comme Sisko, Bingham modifié, Herschel-Bulkley, et les modèles de Casson généralisés sont explorés pour établir des corrélations entre la composition et le dosage des super plastifiants proposés pour l'approche afin de déterminer les différents paramètres rhéologiques. La performance des modèles rhéologiques a été évaluée en calculant le coefficient de détermination R^2 pour chaque modèle. Les résultats montrent que le R^2 dépend du modèle utilisé. La plupart des modèles étudiés présentaient un R^2 commun plus élevé, mais la plupart d'entre eux n'étaient pas les mieux adaptés aux données. Le modèle de Herschel-Bulkley s'est avéré le mieux adapté pour capturer la courbe des données expérimentales. Ce modèle tient effectivement compte du comportement non newtonien des pâtes de ciment super plastifiantes, ce qui garantit une représentation plus précise de leurs propriétés rhéologiques.

Mots clés : Rhéologie ; super plastifiant, modèles rhéologiques ; pâte de ciment ; ciment

ABSTRACT

Accurate modelling of rheological parameters is crucial for the optimisation of workability and performance of cement pastes in civil engineering applications.

In this study, we focus on modelling the rheological parameters of two types of cement pastes are formulated using CEMI 42.5 and the CEMII A 42.5, modified with three different commercially available superplasticizers are selected. The goal of this study is to investigate the impact of three distinct superplasticizers on the rheological behaviour of the cement pastes. Experimental data were estimated by rheological test using rotary viscometer with coaxial cylinders, which allows us to collected data of shear stress, plastic viscosity. Subsequently, various mathematical models were tested; including models like Sisko, the modified Bingham, Herschel-Bulkley, and Generalised Casson models are explored to establish correlations between the composition and dosage of the superplasticizers proposed for approach to determine the different rheological parameter. The performance of the rheological models was evaluated by calculating the coefficient of determination R^2 for each model. The results show that the R^2 depended on the model used. There was a common higher R^2 for most all models investigated, but not the best fitting for the data for most of them. The Herschel-Bulkley model demonstrated the best fit for capturing the curve of the experimental data. This model effectively accounted for the non-Newtonian behaviour of the superplasticizer cement pastes, ensuring a more accurate representation of their rheological properties.

Keywords: Rheology; superplasticizer, rheological models; cement paste; cement

ACKNOWLEDGEMENTS

Firstly, we would like to thank Almighty and Merciful God, who has given us the strength and patience to carry out this modest work.

It takes a lot of motivation, rigour and enthusiasm to complete this thesis, then this research work needed the contribution of several people, whom we would like to thank!

Our supervisor, Mrs K. MEGUENNI and Dr W. YAHYAOUI for all their valuable advice, their active listening and their availability. Indeed, starting this and finishing the whole dissertation in such a short time was not an easy task, and we would not have succeeded so much if we had not received their advice, as well as their persuasiveness.

Our parents and close friends, who supported us during the moments of doubt and abandonment, who believed in us more than ever,

To our library advisers, who will probably never read this dissertation but who helped us to reflect on our dissertation plan and provided us with all the necessary documentation.

We would also like to thank the professors and administrative staff of the University of SAAD Dahlab Blida 1, who provided us with the tools we needed to succeed in our university studies. we would like to thank them in particular.

Thanks to them, we were able to have a solid basis on which to carry out our research and analysis.

We would also like to thank the members of the jury who agreed to be my referees.

Dedicate

In the name of Allah the Merciful

(Work and God will see your work, as well as His messenger and the believers)

The great truth of Allah

A Allah who makes the night good only by thanking Him, and who makes the day good only by obeying Him... and who makes the moments good only by remembering Him...

Almighty Allah

To him who conveyed the message and fulfilled the trust ... and advised the nation to the Prophet of Mercy and Light of the Worlds

Our prophet Muhammad, may peace be upon him.

The journey is over... it wasn't easy and it's not meant to be... and however long it takes, it will go smoothly

Moving on, here I am now, with the help of Almighty Allah, completing this work.

I dedicate this work to my first model and the meaning of love and devotion... To the smile of life and the secret of existence, to her whose plea was a secret, the one who raised me and fought for me... to the light that lit my path... and

My success and her tenderness ... To her who has guided and accompanied me in all my life's endeavours and who continues to do so to this day... Oh Lord, protect her and grant her forgiveness and well-being... My beloved mother,

To the one whose name I bear with pride... a long wait and...

Your words will remain the stars that guide me today, tomorrow and always... My dear father

To my dear sisters and nieces and to the support of my life

To my close friends who they believed in me more than ever,

CHAMAINE Younes

Dedicate

To the pillars of my life, who inspire me to reach for the stars... my loving parents, who have been my unwavering source of support and encouragement throughout my academic journey. Their unconditional love, sacrifices, and belief in my abilities have been the driving force behind my pursuit of knowledge.

To my siblings, who have been my lifelong companions and best friends,

To my dear friends, who have stood by my side,

Houaoura Badia.

List of Figures

Figure 1. 1: Typical heat of hydration curve of Portland cement.	26
Figure 1. 2: Action of superplasticizer on cement particles. (a) Flocculated cement particles; (b) dispersing cement particles by a repulsive force generated by negatively charged superplasticizer; (c) releasing of entrapped water.	29
Figure 1. 3: Effect of SP dosage on the rheological parameters of SCC.	30
Figure 1. 4: Shear stress in terms of strain rate during a rheometers test for all percentages of superplasticizer.	31
Figure 1. 5: Variation of the flow time for various superplasticizer dosages.	31
Figure 1. 6: Variation of the yield stress for various superplasticizer dosages.	32
Figure 1. 7: The Two-Plate-Model Definition of Viscosity (Coghill, 2003; Paterson & Cooke, 2000 Slatter et al, 2002).	36
Figure 1. 8: Schematisation of shear rate.	36
Figure 1. 9: The Newtonian model.	38
Figure 1. 10: Schematisation of shear stress-shear strain plot for Newtonian and Non-Newtonian fluids.	39
Figure 1. 11: Evolution of the structure of a cement paste without additives under various shear rates.	40
Figure 1. 12: Thixotropy versus anti-thixotropy.	40
Figure 1. 13: Typical common constitutive models for non-Newtonian fluids.	44
Figure 1. 14: Correlation between the Bingham yield stress and that estimated by the Modified Bingham, Herschel-Bilkley, and Casson models (a) tested by coaxial cylinders, (b) tested by vane rotor, (c) tested by smooth plate, (d) tested by serrated plate.	45
Figure 1. 15: Correlation between the modified Bingham, and Herschel Bulkley and Casson model yield stress for parallel plates test geometries. Herschel-Bulkley and Casson model yield stress versus modified Bingham model yield stress (b) tested by coaxial cylinders.	46
Figure 2. 1: The DSR testing configuration.	55
Figure 2. 2: Cross-section of Oscillating Piston Viscometer.	56
Figure 2. 3: Rotational viscometer.	57
Figure 2. 4: Schematic representation of the operating principle of rotary rheometers with coaxial cylinders.	58
Figure 2. 5: Functional principle of the instrument used.	59
Figure 2. 6: Comparative analysis of Shear rate -Shear stress behaviour in cement paste 1 with different superplasticizers: (a) SP1, (b) SP2, (c) SP3.	64
Figure 2. 7: Comparative analysis of Shear rate -Shear stress behaviour in cement paste 2 with different superplasticizers: (a) SP1, (b) SP2, (c) SP3.	65
Figure 2. 8: Viscosity behaviour for cement paste 1 with different superplasticizers: (a) SP1, (b) SP2, (c) SP3.	66
Figure 2. 9: Viscosity behaviour for cement paste 2 with different superplasticizers: (a) SP1, (b) SP2, (c) SP3.	67
Figure 2. 10: Evolution of the shear stress in function of time for cement paste 1 with different superplasticizers: (a) SP1, (b) SP2, (c) SP3.	68
Figure 2. 11: Evolution of the shear stress in function of time for cement paste 2 with different superplasticizers: (a) SP1, (b) SP2, (c) SP3.	69

Figure 3. 1: Curves of C1 and C2 with a 1.5% dosage of SP1 followed by the predicted curve of the rheological models.....	75
Figure 3. 2: Yield stress histogram of C1 and C2 with a 1.5% dosage of SP1 obtained by rheological model tested.	77
Figure 3. 3: Yield Stress Curves for C1 and C2 with Different Superplasticizers:(a) Generalized Casson, (b)Sisko, (c)Modified Bingham.	80
Figure 3. 4: Herschel-Bulkley yield Stress Curves for C1 and C2 with Different Superplasticizers.	81
Figure 3. 5: Yield stress as a function of solid PCE content.	82
Figure 3. 6: Yield stress as a function of W/C.	82
Figure 3. 7: Experimental and predicted Herschel-Bulkley curves for C1 C2 SP1.....	83
Figure 3. 8: Experimental and predicted Herschel-Bulkley curves for C1 C2 SP2.....	84
Figure 3. 9: Experimental and predicted Herschel-Bulkley curves for C1 C2 SP3.....	85
Figure 3. 10: Yield stress as a function of SP dose level.	88
Figure 3. 11: Curves of Herschel-Bulkley model rheological parameters of C1 and C2 with the superplasticizer dosage.	89
Figure 3. 12: Yield stress in relation to the SP dosages.....	90
Figure 3. 13: The Consistency Index k with 3 Superplasticizer Dosage for C1 and C2.	91
Figure 3. 14: Flow Index “n” Variation with 3 Superplasticizer Dosage in C1 and C2.	93
Figure 3. 15: Flow index as a function of W/C.	95

Table of Tables

Table 1. 1: Approximate oxide composition limits of Portland cement.	23
Table 1. 2: Characteristics of the main hydrates at a young age.....	25
Table 1. 3: Summary of rheological equations for non-Newtonian fluids.	44
Table 2. 1: Chemical analysis of the two clinkers.....	60
Table 2. 2: Mineralogical composition of the two clinkers.	61
Table 3. 1: The coefficient of determination R ² for rheological models tested.	73
Table 3. 2: Tested Rheological models Yield Stress for C1.....	76
Table 3. 3: Tested Rheological Model Yield Stress for C2.	77
Table 3. 4: Herschel-Bulkley parameters results obtained for C1 with different dosages of the three types of superplasticizers.	86
Table 3. 5: Herschel-Bulkley parameters results obtained for C2 with different dosage of the three types of superplasticizers.	87
Table 3. 6: The parameters of the suggested model for the yield stress.	89
Table 3. 7: The parameters of the model suggested for the consistency index.	92
Table 3. 8: The parameters of the model suggested for the flow index (C1).	94
Table 3. 9: The parameters of the model suggested for the flow index (C2).	94

List of Symbols

EN: European norms

ASTM: American Society for Testing and Materials

SP: Superplasticizer

SCC: Self-Compacting Concrete

W/C: Water Cement ratio

τ : Shear stress

γ : Shear strain

$\dot{\gamma}$: Shear rate

η : Dynamic viscosity

τ_0 : Yield stress

μ : Plastic viscosity

R^2 : Coefficient of determination

SSR: Regression Sum of Squares

SST: Total Sum of Squares

S: Standard error

DSR: Dynamic Shear Rheometer

CRS: Cement Resistant to Sulphates

Table of Contents

ملخص

RESUMÉ

ABSTRACT

ACKNOWLEDGEMENTS

Dedicate

List of Figures

List of Tables

List of Abbreviation and Symbols

General introduction

Chapter 1: bibliographical research

Part A: Rheology of cement pastes

1	Introduction.....	21
2	Cement.....	21
2.1	History	21
2.2	Portland cement	21
2.3	Portland manufacturing.....	22
2.4	Cements additives	22
2.4.1	Fly-ash	22
2.4.2	Blast-furnace slag	22
2.4.3	Silica fume	23
2.5	Chemical Composition	23
2.6	Mineralogical Composition	23
2.7	Hydration of Portland cement.....	24
2.7.1	Hydration of C ₃ S.....	25
2.6.2	Hydration of C ₂ S.....	26
2.6.3	Hydration of C ₃ A.....	26
2.6.4	Hydration of C ₄ AF.....	27
3	Superplasticizer.....	28
3.1	Working mechanism	28
3.2	Uses of Superplasticizer.....	29
3.3	The effect of superplasticizers on Rheology.....	29
4	Rheology.....	33
4.1	Introduction.....	33

4.2	Rheological parameters.....	35
4.2.1	Viscosity	35
4.2.2	Shear stress	36
4.2.3	Shear rate	36
4.2.4	Yield stress.....	37
4.3	Types of Fluids	37
4.3.1	Newtonian fluid	37
4.3.2	No-Newtonian fluid	38
4.3.3	Time Independent Fluid.....	38
	• Shear-thinning fluids.....	39
	• Shear-thickening fluids	39
4.3.4	Time-Dependent Fluid.....	39
	• Thixotropic Fluid	39
	• Non-Thixotropic Fluid.....	40
5	Rheology of cement pastes	41
5.1	Rheological Models for cement pastes	41
5.1.1	The Bingham model.....	41
5.1.2	The Herschel-Bulkley model	42
5.1.3	The power law model	42
5.1.4	Modified Bingham Model:	42
5.1.5	The Sisko model	43
5.1.6	The Generalized Casson model	43
1	Generalities	47
2	Regression and Modelling	47
2.1	Model Building	48
2.2	Simple Linear Regression	48
2.3	Multiple Linear Regression	49
2.4	Nonlinear regression	49
3	Choice of model.....	50
3.1	Coefficient of Determination	50
3.2	The error	50
3.3	Identification of the model parameters	51
	• The least square method	51
	• Gauss-Newton Algorithm	52
	• Maximum Likelihood Estimation.....	53

Chapter 2: Test and experimental

1	Introduction.....	55
2	Rheological test.....	55
2.1	Types of viscometer:.....	55
2.1.1	Dynamic Shear Rheometer (DSR):.....	55
2.1.2	Oscillating rheometer.....	56
2.1.3	Ultrasonic Rheometer:	56
2.1.4	Coaxial cylinder rheometer:.....	56
3	Equipment and materials	58
3.1	The experimental instrument used.....	58
3.2	Materials used	60
3.2.1	Cement.....	60
3.2.2	Superplasticizers	61
4	Mixture proportion.....	62
5	Results and Discussion	62
5.1	Rheological Curves.....	62

Chapter 3: Modelling and Interpretation

1	Introduction.....	72
2	The choice of model	72
2.1	The choice based on R^2	73
2.2	The choice based on the model parameters	74
3	The chosen model	81
4	The model parameters.....	86
4.1	The yield stress " τ_0 "	89
4.2	The consistency index "k"	91
4.3	The flow index "n"	93

Conclusion

References List

Annex

Introduction

The use of superplasticizers in cement materials has revolutionized the construction industry by significantly improving the workability and the performance of concrete. Superplasticizers are chemical admixtures that improve the flow behaviour of cement pastes, making them easier to work with and improving their strength. Understanding and predicting accurately the rheological behaviour of cement pastes containing superplasticizers is an important part of optimizing the mix design and the performance of concrete mixes.

The rheological parameters of cement pastes, including yield stress, plastic viscosity and thixotropy, play a fundamental role in determining the flow characteristics and stability of the mix. Traditionally, experimental procedures and approaches based on test and failure have been used to estimate the rheology of cementitious systems containing superplasticizers. These methods, are time-consuming, demanding and resource-intensive, and do not provide an understanding of the fundamental mechanisms that determine the flow behaviour.

In recent years, there has been growing interest in developing mathematical models and computer simulation techniques to both predict and characterise the rheological parameters of cement pastes which contain superplasticizers. These models aim to provide a quantitative relationship between the composition of the mix, including the type and dosage of superplasticizer, and its rheological response under different conditions. By being able to describe rheological parameters accurately, engineers and researchers can improve the workability, durability and overall performance of concrete mixtures for specific purposes.

The aim of this master's thesis is to compare different rheological parameters of cement pastes incorporating superplasticizers by developing a comprehensive and accurate model to predict the rheological parameters of cement pastes incorporating superplasticizers. The proposed model will consider the composition of the cement paste, including cement type, water-cement ratio and superplasticizer dosage, as well as environmental factors such as temperature and curing conditions. Experimental data from laboratory tests will be used to validate and refine the model, to ensure its reliability and applicability in practical scenarios.

This research will help to advance understanding of the complex interaction between cement particles, water and superplasticizer molecules in determining the rheological properties of cement pastes. The model studied will be a valuable tool for engineers and researchers involved in concrete design, construction and optimisation processes. By accurately

predicting the rheological behaviour of cement pastes containing superplasticizers, this study aims to improve the efficiency, durability and performance of cement-based materials, which will ultimately benefit the construction sector as a whole.

Chapter 1: bibliographical research

Part A: Rheology of cement pastes

1 Introduction

Cement, as a fundamental construction material, plays a crucial role in the development of various structures. The behaviour and properties of cement and its pastes have a direct impact on the performance and durability of concrete. Therefore, understanding the rheological behaviour of cement pastes, including those with the incorporation of superplasticizers in particular, holds significant importance in optimizing their application in construction.

2 Cement

2.1 History

The history of cement dates back thousands of years to the ancient Egyptians, who used a mixture of mud and straw to bind together bricks to build structures such as the pyramids [1].

In the 19th century, the development of Portland cement revolutionized the building industry. Joseph Aspdin of England patented the process in 1824, and it quickly became the most widely used type of cement. The key ingredient in Portland cement is a mixture of limestone and clay, which is ground into a powder and then heated to a high temperature to form a substance known as clinker. The clinker is then ground into a fine powder to create the final product [1].

Over the years, many variations and improvements have been made to the production process of cement, making it more efficient and environmentally friendly. For example, the use of alternative raw materials and the implementation of energy-saving measures in the production process have become increasingly common [2].

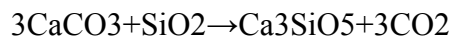
2.2 Portland cement

Hydraulic cement is a construction material most used nowadays, it is known as Portland cement. It is the basic ingredient in making concrete; Portland cement is suitable for wet climates and can be used underwater. Different types or blends of Portland cement include Portland blast furnace slag cement, Portland fly-ash cement, Portland pozzolan cement, Portland-silica fume cement, masonry cement, expansive cement, white blended cement, coloured cement, and very finely ground cement.

In a close interpenetrating association, the Portland cement clinker substantially of the four crystalline clinker phase's alite, belite, calcium aluminate, and calcium aluminoferrite. In addition, clinker contains voids ("pores") and usually some free (uncombined) lime; more rarely periclase is present [3].

2.3 Portland manufacturing

Portland cement is a vital and dominant construction material in the world. It is a mixture of about 80% burning limestone and 20% clay. Cement clinker is manufactured by calcining limestone (calcium source), clay, or sand (silica and alumina source) in a rotary kiln at a temperature of about 1450 °C [4]. Raw materials such as limestone and chalk for calcium and clay for silica are easily available. The grinding of clinker combined with around 5% of gypsum (calcium sulfate) forms Portland cement. Calcination is the decomposition of calcium carbonate (limestone) into calcium oxide (CaO) and CO₂. In the cement industry, the product of calcination is called clinker. The calcination process occurs when calcium carbonate (CaCO₃) and silicon dioxide SiO₂ are combined in the furnace at 1450 °C, which results in the formation of the following products, i.e., alite (tricalcium silicate) [5].



2.4 Cements additives

2.4.1 Fly-ash

Cement can contain up to 40% fly ash, as per ASTM standards (ASTM C595) and up to 35% according to EN standards (EN 197-1). The fly ash is pozzolanic and helps to maintain the ultimate strength of the cement. Using fly ash also reduces the water content in concrete, resulting in improved early strength. When cost-effective fly ash is readily available, it can be a more economical option compared to ordinary cement.

2.4.2 Blast-furnace slag

According to ASTM C595 and EN 197-1, blast furnace slag cement can contain up to 95% ground granulated blast furnace slag, with the remainder being clinker and a small amount of gypsum. This type of cement has high ultimate strength and improved sulfate resistance as the slag content increases, but may have reduced early strength and diminished heat evolution. It is often used as a cost-effective alternative to Portland sulfate-resisting and low-heat cement.

2.4.3 Silica fume

Silica fume addition can result in significantly higher strengths in cement, with cement containing 5-20% silica fume being produced occasionally and the maximum limit being 10% as per EN 197-1. However, it is more common for silica fume to be added to Portland cement during mixing at the concrete mixer.

2.5 Chemical Composition

Lime (CaO), silica (SiO₂), alumina (Al₂O₃), and iron oxide are the primary constituents of Portland cement (Fe₂O₃). The four oxides are typically referred to as the "major oxides" since their combined concentration makes up around 90% of the weight of cement[6]. The remaining 10% is made up of gypsum, titania (TiO₂), phosphorus pentoxide (P₂O₅), alkali oxides (Na₂O and K₂O), and magnesia (MgO). These are known as "minor components." Over the years, Portland cement's composition has gradually changed. The rise in lime content and the small reduction in silica content are the key indicators of this alteration. The specifics of the cement's composition rely on both the kind and the specifics of the raw materials employed in it [7].

The approximations listed in Table 1.1 provide a general understanding of the composition of Portland cement used today.

Table 1. 1: Approximate oxide composition limits of Portland cement.

Oxide	Composition (%)
CaO	60-67
SiO ₂	17-25
Al ₂ O ₃	3-8
Fe ₂ O ₃	0.5-6
MgO	0.1-5.5
Na ₂ O+K ₂ O	0.5-1.3
TiO ₂	0.1-0.4
P ₂ O ₅	0.1-0.2
SO ₃	1-3

2.6 Mineralogical Composition

The major minerals found in regular cement clinker are C₃S, C₂S, C₃A, and C₄AF. To grind cement, a suitable amount of gypsum is added to the clinker. Each mineral composition has a different rate of hydration and water requirement. It is reasonable to assume that the

mineral compositions of cement may have an impact on the rheological characteristics of cement paste.

According to Bogue, all of the iron oxides are assumed to be present in the calculation as a solid solution of composition C_4AF for an aluminium-ferrite, and all of the aluminas that is not necessary to satisfy the iron in this ferrite is assumed to be present as a solid solution of composition C_3A . The leftover lime is divided between C_3S and C_2S in proportion after the amount needed for these compounds has been subtracted from the combined lime. The total found through chemical analysis is simply subtracted from the free lime, which may be identified by its extraction with ethanediol, to yield the mixed lime [8].

The general solution to the calculation is expressed in the following equations:

$$C_4AF = 3.04 Fe_2O_3$$

$$C_3A = 2.65AL_2O_3 - 1.96Fe_2O_3$$

$$C_2S = 8.60SiO_2 + 1.08Fe_2O_3 + 5.07AL_2O_3 - 3.07CaO$$

$$C_3S = 4.07CaO - 7.60SiO_2 - 1.43Fe_2O_3 - 6.72AL_2O_3$$

For ordinary Portland cement, the mineralogical constituents are within the following limits


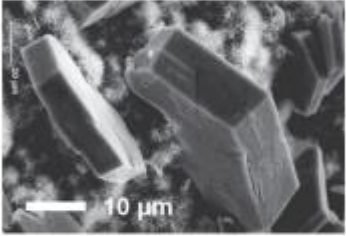


C_3S	50-75 %
C_2S	7-30 %
C_3A	0-16 %
C_4AF	0-20 %

2.7 Hydration of Portland cement

Hydration encompasses a broad range of processes occurring upon the contact between cement powder and water, culminating in the formation of hydrates. Le Chatelier's theory postulates that the "hydration" process of cement is contingent upon cyclic phenomena involving the dissolution and precipitation of ionic species inherent to distinct phases. Analogous to other minerals, these species exhibit a propensity to dissolve in water until their solubility product is attained. Beyond this threshold, the solution becomes supersaturated, thereby thermodynamically promoting the precipitation of hydrates. Consequently, the consumption of ions diminishes, resulting in the dissolution of other constituents within the material [9][10]. The kinetics governing this process are phase-

specific. Notably, Table 1.2 provides an overview of the principal hydrates formed during the initial stages, and the ensuing reactions delineate their formation [11].

Table 1. 2: Characteristics of the main hydrates at a young age.[11]

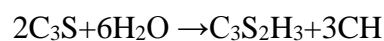
Hydrates			Morphology
Calcium Silicates Hydrates	C-S-H	$x \text{ CaO}, \text{ SiO}_2, y \text{ H}_2\text{O}$	
Portlandite	CH	$\text{Ca}(\text{OH})_2$	 
Ettringite	$\text{C}_6\text{A}\bar{\text{S}}_3\text{H}_{32}$	$\text{Ca}_6\text{Al}_2(\text{SO}_4)_3(\text{OH})_{12}, 26 \text{ H}_2\text{O}$	
Calcium monosulfoaluminae	$\text{C}_4\text{A}\bar{\text{S}}_3\text{H}_{12}$	$3\text{CaO} \cdot \text{Al}_2\text{O}_3 \cdot \text{CaSO}_4, 12 \text{ H}_2\text{O}$	

2.7.1 Hydration of C₃S

Long fibres of gelatinous or virtually amorphous hydrated calcium silicates, as well as crystals of portlandite $\text{Ca}(\text{OH})_2$, are produced after the reaction of C_3S with water.

This calcium silicate gel is identified as C-S-H without conserving the composition given that it may alter during hydration depending on the water content (W/C) and cure temperature.

The following equation can be used to represent the reaction at full hydration [12]:



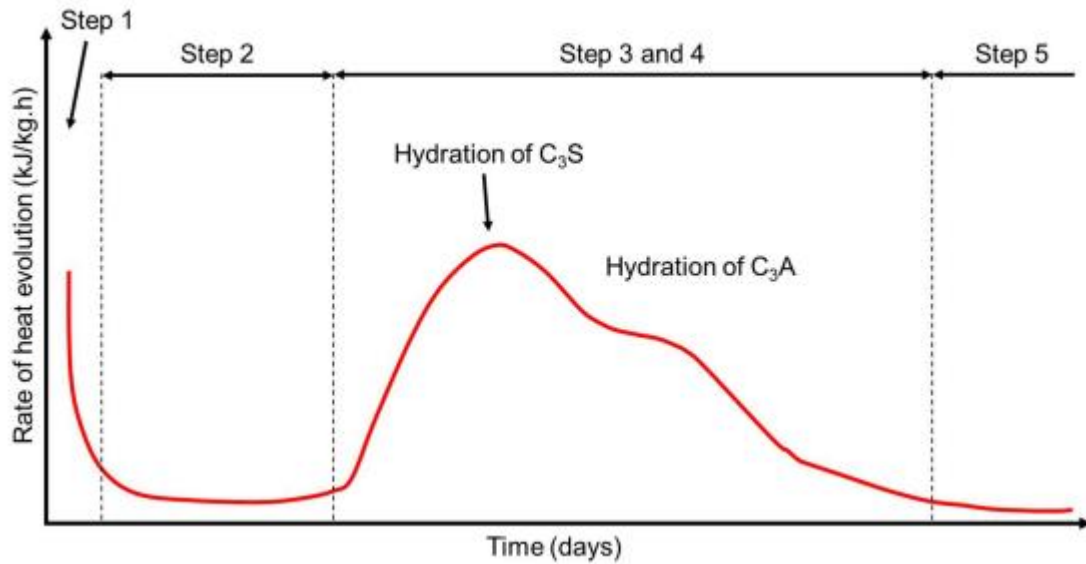


Figure 1. 1: Typical heat of hydration curve of Portland cement.[13]

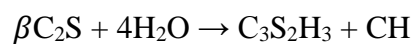
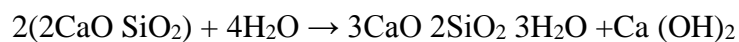
The previous reactions carry on steadily for a few hours, and the first product created (C-S-H) coats the C_3S grains. After a few hours, a layer forms on the surface of C_3S that is thick enough to slow down the passage of ions and water. The reaction still proceeds but at a slower and slower rate.

2.6.2. Hydration of C_2S

Four alternative kinds of dicalcium silicate hydration exist γ , β , α , and α' . However, in Portland cement, the form is typically the most common; it is this final shape that is drawn to water, whereas the forms α and α' are occasional.

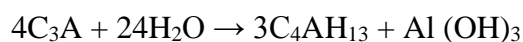
The same kind of compounds as those produced by C_3S are produced by the hydration process of C_2S , although at a considerably slower rate.

The complete hydration reaction can be given by the following equation [12] :



2.6.3. Hydration of C_3A

When the tricalcium aluminate C_3A is placed in the presence of water, a reaction is accelerated and results in the synthesis of a gel (hydrated alumina), and the hexagonal-shaped aluminates C_2AH_8 and C_4AH_{13} .



After a few hours, the hexagonal hydrates that were surrounding the C_3A grains disappear and are replaced by cubic C_3AH_6 crystals, which causes the hydration reaction to proceed more quickly



Tricalcium aluminate C_3A has fast precipitation, preventing the hydration of the other clinker constituents, particularly C_3S , and as a result, gypsum is added as a general catch regulator.

2.6.4. Hydration of C_4AF

Tetra calcium aluminoferrite (C_4AF) or a component of the $C_2A_{1-x}Fx$ family of solid solutions, i.e., a solid solution with a composition between C_6AF_2 and C_6A_2F , can both be used to illustrate the hydration process of the ferrite phase of Portland cement.

The synthesis of hydrated calcium sulfoaluminates and sulfoferrates from tetra calcium aluminoferrite is comparable to that of hydrated tricalcium aluminate C_3A , however, C_4AF hydrates more slowly than C_3A .

3 Superplasticizer

There are several types of superplasticizers, each with their unique properties and characteristics. These types include purified lignosulfonates, carboxylate synthetic polymers, sulfonated synthetic polymers, and synthetic polymers with mixed functionality in cementitious materials. Each of these types of superplasticizers offers distinct benefits and can be used in various construction applications depending on the specific needs and requirements of the project [14].

3.1 Working mechanism

In the process of cement mixing, superplasticizers are commonly added to the mixing water beforehand. When water comes into contact with cement particles, the molecules of superplasticizers play a role in saturating the surface charges, similar to other ions present in the solution. Research conducted by Ramachandran et al suggests that superplasticizers effectively prevent the formation of harmful agglomerates. Specifically, the molecules of superplasticizers undergo adsorption at the interface between cement particles and the mixing water. Once adsorbed, these superplasticizer molecules create a negative charge surrounding each cement particle, resulting in repulsion between them. As a result of this dispersion, the viscosity of the cement paste is reduced, leading to improved workability.

Figure 1.2 depicts the operating principle of superplasticizers. The image illustrates how the negatively charged superplasticizers generate a repelling force that acts upon the cement particles, effectively dispersing them and releasing any entrapped water in the process. This leads to an improvement in the flow characteristics of the concrete mixture, making it more fluid and workable. Overall, the use of superplasticizers serves to enhance the performance and ease of handling of concrete, making it a crucial component in many constructions and building projects [15].

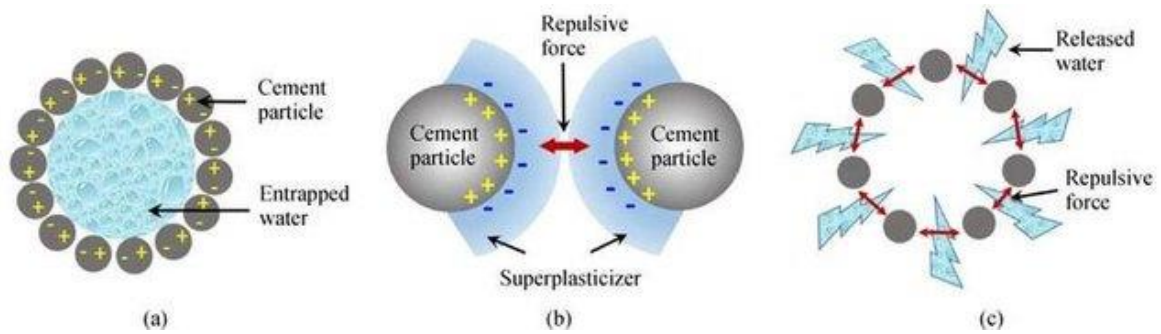


Figure 1. 2: Action of superplasticizer on cement particles. (a) Flocculated cement particles; (b) dispersing cement particles by a repulsive force generated by negatively charged superplasticizer; (c) releasing of entrapped water [15].

Ferrari et al. [16], suggest that the addition of SP in cement mixtures leads to the formation of a directional adsorption layer on the surface of the cement particles, which contributes to the even dispersion of fine particles. This occurs because the presence of SP molecules within the mixture releases free water due to the combined effects of electrostatic repulsion and steric hindrance. As a result, the increase in SP dosage leads to a decrease in yield stress.

3.2 Uses of Superplasticizer

Improving concrete workability: Superplasticizers can improve the fluidity of concrete, making it easier to pour and place, while reducing the water-cement ratio needed to achieve a given level of workability. This helps reduce the risk of cracking, bleeding, and segregation, and results in a higher-quality finished product [17].

Improving the strength and durability of concrete: By reducing the water-cement ratio, superplasticizers can also increase the compressive strength of concrete. This is because the reduction of the amount of excess water available to cause chemical reactions, results in a denser and stronger concrete structure [18].

Facilitating pumping of concrete: Superplasticizers can be used to reduce the viscosity of concrete, making it easier to pump over long distances, or through tight spaces. This can reduce labour costs and improve construction efficiency [19].

3.3 The effect of superplasticizers on Rheology

Rheology is an important aspect of materials science and engineering, as it helps to understand how materials behave when subjected to stress or strain. In the context of concrete, rheology plays a crucial role in determining the workability and spread ability of the mixture. The impact of superplasticizers on the composition and properties of cement

paste, as well as the rheological and mechanical characteristics of self-compacting concrete, is significant. Superplasticizers are chemical admixtures used in concrete to enhance its flowability and workability without affecting its strength. the chemical nature of the superplasticizer determines its effectiveness in increasing the slump[20][21]. By reducing the viscosity of the cement paste, superplasticizers allow for the creation of self-compacting concrete, which can flow into place and compact itself without the need for mechanical vibration. The use of superplasticizers can lead to improved rheological properties, such as increased fluidity and reduced segregation, as well as improved mechanical properties, including increased strength and durability. These enhancements can result in improved constructability and reduced construction time, making superplasticizers a valuable addition to the concrete mix [22].

The impact of Superplasticizers (SP) on the yield stress and plastic viscosity of self-compacting concrete (SCC) is depicted in Figure 1.3. As the amount of SP increases, it is noticeable that both the yield stress and plastic viscosity of the SCC mixtures decrease significantly [23].

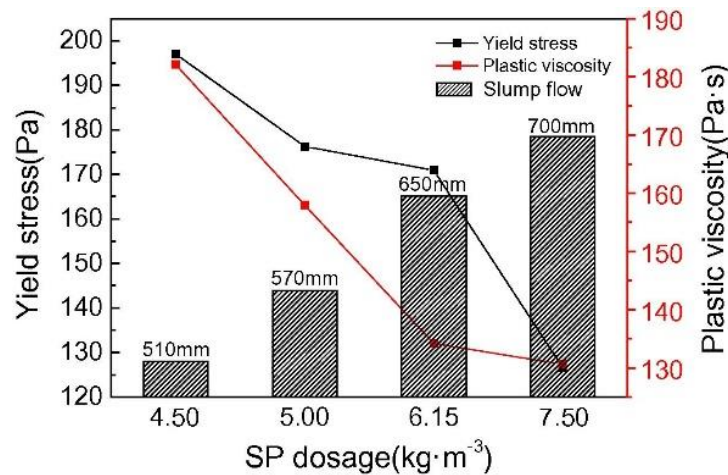


Figure 1. 3: Effect of SP dosage on the rheological parameters of SCC[23].

Measuring the shear stress and rate of grout using a rheometer is a standard approach used to quantify its rheological properties. This method enables the determination of the grout's viscosity, yield stress, and other relevant parameters that can be used to optimize its performance and ensure that it meets the requirements for the intended application.

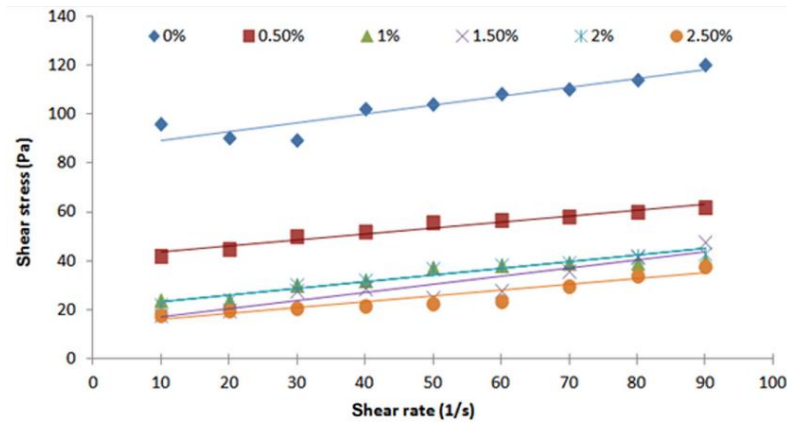


Figure 1. 4: Shear stress in terms of strain rate during a rheometers test for all percentages of superplasticizer[24].

Achieving the most stable fluidity depends greatly on the type and amount of superplasticizer used. Figure 1.5 illustrates the changes in flow time that occur with different dosages of superplasticizer about cement mass [24].

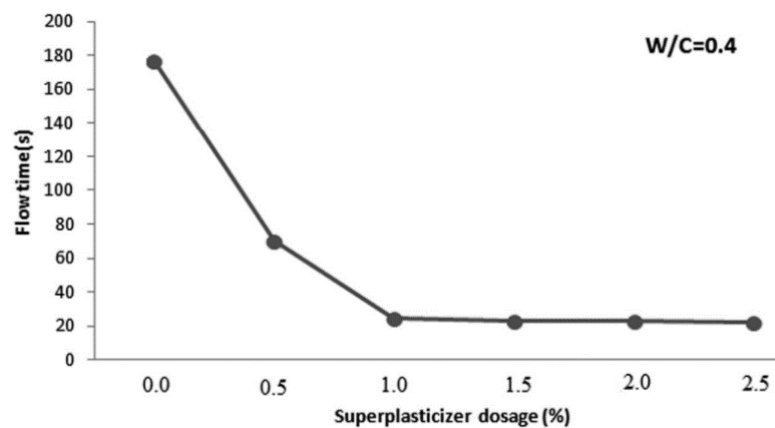


Figure 1. 5: Variation of the flow time for various superplasticizer dosages[24].

Chen. [25] investigated the impact of superplasticizer (SP) on the plastic viscosity of concrete using a customized rheometer. The findings indicated a slight increase in plastic viscosity with the addition of SP. Chen proposed that the cause of this was the weakening of the lubricating effect of the paste, which resulted from increasing the SP dose. The decrease in lubrication caused an increase in the friction resistance between the aggregate particles, leading to a rise in plastic viscosity. An increase in superplasticizers leads to an increase in the values of slump flow diameter. Additionally, they observed that this increase in superplasticizer causes a decrease in both yield stress and plastic viscosity values. The enhancement of the mixture's rheological properties can be attributed to the release of water between cement particles and the subsequent increase in water films coating the mixture particles [16][23][26].

The effectiveness of the superplasticizer does not continue beyond a saturation dosage [27][28], beyond this dosage, further water reduction is not possible. The water reduction also depends on the type of superplasticizer [29]. On the other hand, the amount of bleeding and segregation depends on the type of superplasticizer [20]. The use of stabilizing agents is necessary when excessive bleeding and segregation occur [30]. In addition, the increase in mechanical properties such as compressive and modulus of elasticity depends on the reductions in the water-to-cement ratio.

The amount of bleeding and segregation that occurs in concrete is dependent on the specific superplasticizer employed. In instances where excessive bleeding and segregation arise, the use of stabilizing agents becomes necessary. Furthermore, enhancing mechanical properties such as compressive and modulus of elasticity in concrete is tied to decreasing the water-to-cement ratio.

The breaking of links between cement particles by the superplasticizer is responsible for the various changes observed in the mixture. This mechanism allows water that is trapped between the grains to flow freely, resulting in increased fluidity and decreased yield stress Figure 1.6 It should be noted, however, that the efficiency of this process decreases as the dosage of the superplasticizer is increased.

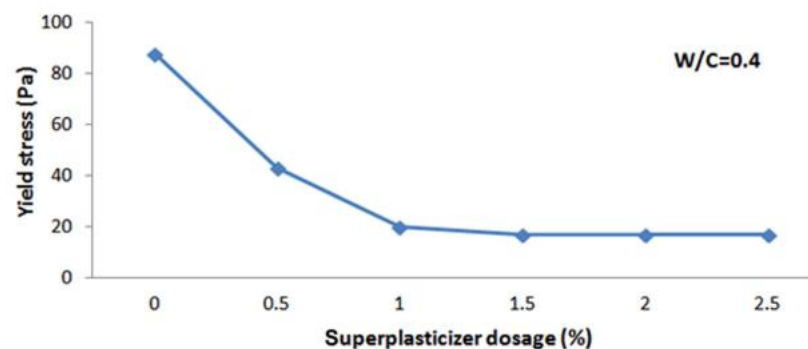


Figure 1. 6: Variation of the yield stress for various superplasticizer dosages[24].

Several researchers have proposed that increasing the dosage of superplasticizer and the water-to-cement (W/C) ratio enhances the long-term preservation of rheological behaviour. Aîtcin similarly demonstrated that the utilization of superplasticizers at high dosages can lead to a delaying effect on the hydration of cement grains, irrespective of the superplasticizer type, cement composition, or average grain size. Conversely, an excessive concentration of superplasticizer effectively offsets the depletion of the polymer by cement grains and its hydrates [31].

4 Rheology

4.1 Introduction

Rheology was first proposed by Professor Eugene Cook Bingham of Lafayette College (Bingham,1922). It is a branch of physics. The term rheology originates from the Greek words *rheo* indicating *flow* and *logia* meaning *the study of*. This definition has been accepted by the American Society of Rheology founded in 1929.

Rheology is the study of the flow and deformation of matters, it is principally concerned with the following question: “How does a material response to an externally applied force?” That is, rheology describes the relationship between force, deformation, and time[32].

The study of material rheology is necessary for two reasons.

First, rheology might be used to indicate the process window during which actions like mixing, transport, dispensing, and storage in the production process could be carried out. Second, rheology can be also used as a quality control technique to detect batch-to-batch variation during processing and manufacture. Rheological measurements can be used as a quality control technique because of how sensitive they are to even the smallest structural variations in materials can help to determine whether or not to accept the incoming material [33].

It is required to briefly introduce the elastic, viscous, and viscoelastic properties of solids and/or liquids from a historical viewpoint before exploring rheology.

Solid substances maintain a constant volume and shape, they are not compressible and do not flow, which distinguishes them from liquids in a very evident way. These macro-properties depict the interior configuration of the atoms, molecules, and ions that make up solids; these particles are closely packed and frequently arranged regularly.

Coussot distinguished five groups of solid materials based on their microscopical structure: (a) crystalline solids, (b) glasses, (c) reticulated polymers, (d) colloidal aggregates, and (e) concentrated foams or emulsions [34].

The most fundamental type of solid is a crystalline solid, and it is quite well understood how these solids behave when they are deformed. Most solid materials suffer a deformation when a modest load is applied that is linearly proportional to the amount of stress, and the material returns to its original shape when the load is removed. This deformation regime referred to

as elastic, is defined by Hooke's Law, described in its general form by [35]:

$$\sigma = E\varepsilon \quad (1.1)$$

$$\tau = G\gamma \quad (1.2)$$

where σ and τ are principal and shear stress, respectively, ε and γ are corresponding normal and shear strains, and E and G are material constants that define the amount of deformation for a corresponding load (i.e. Young's and shear moduli) [35].

At a specific load level, known as the yield point, a portion of the material's atoms receive a significant amount of energy and shift sufficiently from their initial positions to result in a dislocation in the crystalline structure. But because the remaining atoms exploit these dislocations to move into different positions, the substance continues to exist as an ordered structure. This process reflects the plastic characteristic, that many materials exhibit on a macroscopic level; plastic deformation is irreversible deformation. Since all materials produce persistent deformations upon load reduction, there are no fully linear-elastic materials. However, these deformations are frequently overlooked for engineering purposes [34].

Unlike solids, fluids do not maintain a consistent shape. They are very well defined by their deformation characteristics: they have zero shear modulus, which means that they flow continuously under applied shear stress provided that it is greater than the fluid's yield stress [35].

In the case of a perfect viscous liquid, the material constantly deforms in response to applied stress, and the distortion is irreversible after the load has been lifted. In this regard, Newton's viscous law was put forward by Isaac Newton in his 1687 publication *Philosophie Principia Mathematica*. A dashpot immediately begins to deform when an external stress is applied and continues to do so at a constant speed v (m/s) until the stress is removed. The shear rate, denoted by the symbol $\dot{\gamma}$ in s^{-1} can be determined as [32]:

$$\dot{\gamma} = v / h \quad (1.3)$$

Where

h : the gap height in m.

The coefficient of the applied stress and the shear rate is defined as shear viscosity or dynamic viscosity η in Pa. s, which can be described by

$$\eta = \sigma \dot{\gamma} \quad (1.4)$$

Since both Hooke's law and Newton's law do not apply to all liquids and solids, the term viscoelasticity was developed to characterize the behaviour that lies between the ideal elastic behaviour (Hooke's law) and the ideal viscous behaviour (Newton's law).

The most common models for viscoelastic materials are the Maxwell model and the Kelvin-Voigt model. The Maxwell model, put forth by James Clerk Maxwell in 1867, is a representation of the most basic viscoelastic liquid model and is made up of a spring and a dashpot connected in series. When subjected to an external load, the Maxwell material initially exhibits elastic behaviour that is controlled by the elastic modulus G ; but, over time, viscous behaviour takes over and is controlled by the viscosity η . As a result, there are two parts to the strain: an immediate elastic component that corresponds to the spring, and a viscous component that develops over time[32].

The Kelvin-Voigt model is used to describe the behaviour of solids with a viscous response, while the Maxwell model applies to liquids with an elastic response. These two models, however, are limited to assessing the viscoelastic behaviour of a real system.

That is why the Bingham model and the Burger model are suggested in this situation, to describe the behaviour of viscoelastic fluids.

4.2 Rheological parameters

4.2.1 Viscosity

Viscosity is defined as the measure of a fluid's resistance to flow and is best described by the Two-Plate Model in Figure 1-7 (Coghill, 2003; Paterson & Cooke, 2000 Slatter and al, 2002). Figure 1-7 describes the shearing of a fluid between two parallel plates. The space between two parallel plates, a distance (H) apart, is filled with fluid. The upper plate, with surface area (A), is moved with a velocity (V) under the force (F), while the lower plate remains stationary. The top layer of the fluid adjacent to the upper plate moves with the plate at a velocity (V), while the bottom layer of the fluid adjacent to the lower plate remains stationary at zero velocity. As a result, a velocity gradient (dV/dH) develops across the space between the two plates, where dV refers to the velocity differential between adjacent layers of fluid and dH refers to the differential thickness of a layer of fluid (Coghill,2003; Paterson & Cooke, 2000 and Slatter et al,2002)[36].

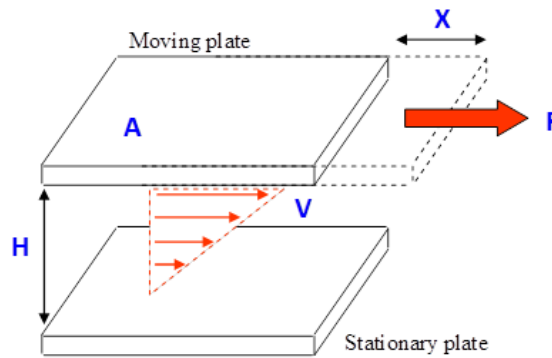


Figure 1. 7: The Two-Plate-Model Definition of Viscosity (Coghill, 2003; Paterson & Cooke, 2000 Slatter et al, 2002)[36].

4.2.2 Shear stress

During laminar shear motion, the layers are driven by relative motion concerning each other. This results in the development of stresses τ [Pa], which is exerted tangentially to the surface of the layer[37].

Consequently, we can define shear stress as the force applied per unit area of the fluid.

$$\tau = \frac{dF}{dS} \quad (1.5)$$

Where

dF : is a projection of the tangential frictional force.

dS : primary layer surface that has been sheared.

4.2.3 Shear rate

Let us consider a material as a set of parallel molecular layers, trapped between two parallel planes of surface S (separated by a distance dz). One of the planes is fixed, and the second one is moved by a distance dx at a constant speed of the norm V_0 .

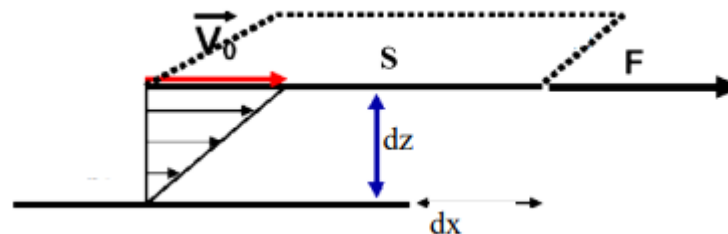


Figure 1. 8: Schematisation of shear rate.

Under the effect of the tangential force, the first molecular layer moves at the same speed. The lower layers will move in the same direction but with smaller and smaller speeds. A velocity gradient is created between the two planes. The displacement between the two planes is defined as the deformation, symbol following the relation:

$$\gamma = \frac{dx}{dz} \quad (1.6)$$

The norm of the constant velocity gradient throughout the sample is defined as the shear rate [38].

4.2.4 Yield stress

The yield stress represents a material characteristic that delineates the shift from solid-like to fluid-like behaviour. It signifies the minimum stress required for a fluid to exhibit viscous flow. The presence of inter-particle forces among solids within a suspension gives rise to yield stress, which must be surpassed to initiate flow. When the applied stress falls below the yield stress, the material undergoes deformation akin to a solid rather than flowing.

The determination of yield stress presents a significant challenge. Theoretically, as the yield stress is approached, the apparent viscosity of the material transitions from a finite value to infinity, necessitating an infinite test duration. Before reaching the yield stress, yield stress fluids exhibit an elastic response. This transition from linearity to non-linearity in material behaviour occurs, accompanied by the presence of residual stress following the peak stress. Consequently, establishing a definitive definition for yield stress is subject to debate[39].

4.3 Types of Fluids

4.3.1 Newtonian fluid

It is an exclusively viscous fluid body whose flow occurs as soon as a constraint is applied. The Newtonian fluid has a linear relationship between the shear stress τ (Pa) and the shear rate (s^{-1}). The behaviour of this fluid is determined solely by the dynamic viscosity (Pas).

The shear stress τ represents, as it were, the frictional force due to the force applied to the fluid. The strain or shear rate is defined as the gradient of the strain rate across the fluid layers. At constant temperature and pressure, the viscosity of a Newtonian fluid is not affected by the shear rate: it remains shear rate: it remains constant.

The relationship between the shear stress and the shear rate becomes linear as shown in the following equation:

$$\tau = \mu \dot{\gamma} \quad (1.7)$$

Where:

τ : the shear stress [Pa]

$\dot{\gamma}$: the shear rate [1/s]

μ : the viscosity [Pa.s]

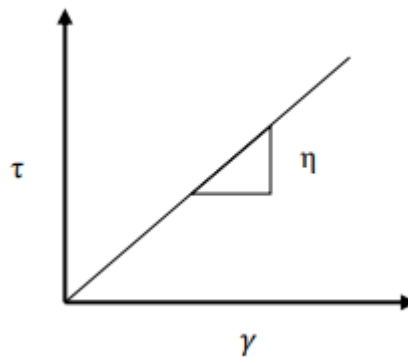


Figure 1. 9: The Newtonian model.

4.3.2 No-Newtonian fluid

Non-Newtonian fluids do not obey Newton's linear law of friction. These fluids are typically very viscous, and their elastic characteristics are also crucial.

The viscosity of non-Newtonian fluids is frequently influenced by the shear rate. These non-linear characteristics result from the existence of items in the fluid that are bigger than the atomic scale but yet less than the flow's standard dimension. Under deformation, these objects rearrange themselves and endow the fluid with non-Newtonian characteristics[40].

4.3.3 Time Independent Fluid

A time-independent fluid refers to a fluid that exhibits a constant viscosity over time, implying that its flow rate remains unchanged regardless of the duration of flow.

Time-independent fluids can be categorized as either Newtonian or non-Newtonian fluids, that classification depends on its specific flow characteristics and the relationship between shear stress and shear rate under dynamic conditions.

Time-independent fluids are often classified into two categories:

- **Shear-thinning fluids**

Shear-thinning fluids do not have yield stress at zero strain rate and are characterized by a progressively decreasing ratio of shear stress to shear rate, hence decreasing apparent viscosity [41].

$$\tau = \mu \dot{\gamma} \quad (1.8)$$

The power law is the simplest of the empirical equations that have been used to describe pseudoplastic fluids (Hughes and Brighton 1967):

$$\tau = k \dot{\gamma}^n \quad (1.9)$$

Where n is a measure of the deviation from Newtonian behaviour (in this case $n < 1$), and k is a measure of the "consistency" of the fluid.

- **Shear-thickening fluids**

Like shear-thinning fluids, shear-thickening fluids have no yield stress at zero strain rate, but the apparent viscosity increases with increasing shear rate. The same relationships apply to Shear-thickening fluids as to shear-thinning fluids except that in this case $n > 1$ [41].

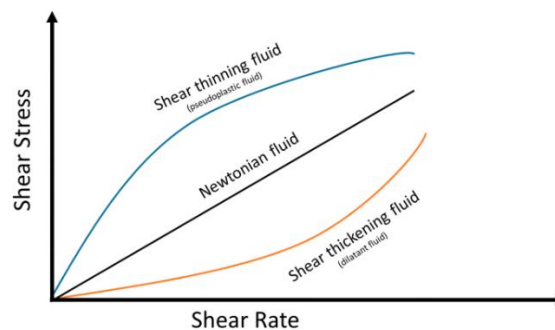


Figure 1. 10: Schematisation of shear stress-shear strain plot for Newtonian and Non-Newtonian fluids[42].

4.3.4 Time-Dependent Fluid

These fluids are very difficult to model. Their behaviour is such that for a constant shear rate $\dot{\gamma}$ and at constant temperature the shear stress s either increases or decreases monotonically concerning time, towards an asymptotic value $\tau(\dot{\gamma})$.

The fluids regain their initial properties sometime after the shear rate has returned to zero [43].

- **Thixotropic Fluid**

The term thixotropy is used in rheology to identify a material whose viscosity decreases with time when applying external shear stress. It is by definition a reversible phenomenon.

For non-Newtonian fluids, it is also possible to describe the thixotropic character as a function of the effort required to maintain the flow. Thus, once the shear threshold is crossed, if the effort required to maintain a constant flow decreases with time, the material is then said to be thixotropic[44].

For instance, the thixotropic properties of cement paste result from the flocculation and deflocculating of the paste's suspended cement particles. Figure 1.11 provides a schematic illustration of a cement paste without additives. As the shear rate increases, the flocculated particles are broken apart, and further increases in shear rate may cause the individual cement particles to reflocculate with non-Newtonian properties to the fluid [40].

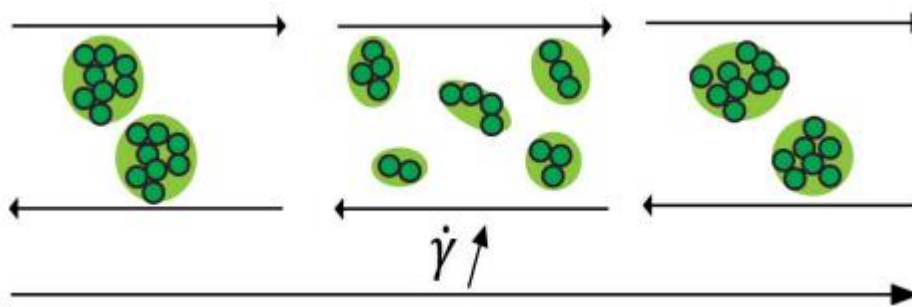


Figure 1. 11:Evolution of the structure of a cement paste without additives under various shear rates[40].

- **Non-Thixotropic Fluid**

Rheopexy, also known as anti-thixotropy or negative thixotropy, is the term used to describe the time-dependent shear-thickening tendency that is the opposite of thixotropy. The time-dependent rise in viscosity during flow is typically brought on by aggregation brought on by the flow. Figure I.12 illustrates the distinction between thixotropy and anti-thixotropy behaviours. Anti-thixotropic substances are substantially less prevalent.

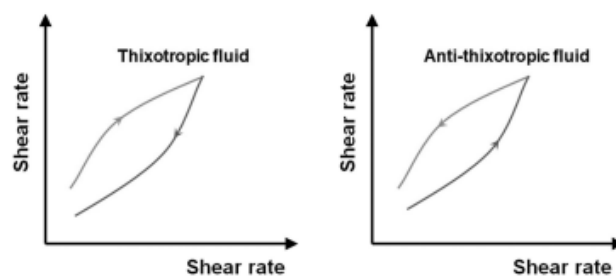


Figure 1. 12: Thixotropy versus anti-thixotropy.[32]

5 Rheology of cement pastes

Cement paste is a colloidal suspension of cement particles in water. It is a non-Newtonian fluid, meaning that its viscosity (resistance to flow) changes with the shear rate. The rheological properties of cement paste are important for its workability, durability, and strength.

The rheological properties of cement paste are affected by several factors, including the water-to-cement ratio, the type of cement, the particle size distribution of the cement, and the presence of admixtures

The study of cement paste rheology encompasses intricate aspects that remain largely unexplored. Nevertheless, enhanced comprehension of cement paste rheology has the potential to facilitate the advancement and innovation of concrete materials.

5.1 Rheological Models for cement pastes

Rheological models are extensively employed in elucidating the flow characteristics of cementitious materials. These models facilitate comprehension and anticipation of material behaviour in specific circumstances, such as mixing, pumping, and pouring.

Various rheological models have been developed to depict the flow behaviour of cement pastes, each incorporating distinct assumptions and mathematical formulations. Among the frequently employed models are:

5.1.1 The Bingham model

The Bingham model is a viscoplastic model that assumes that the material behaves like a solid below a value of critical stress (i.e., the shear threshold), and flows like a viscous liquid when this stress is exceeded, and describes this flow using a linear trend between the shear stress and shear rate, its mathematical equation (1.10) is as followed:

$$\tau = \tau_0 + \mu\dot{\gamma} \quad (1.10)$$

where τ is the shear stress [Pa], τ_0 is the yield stress, $\dot{\gamma}$ [s^{-1}] is the shear rate, and μ is the plastic viscosity.

However, this model falls short in describing the rheological behaviour of a fluid that exhibits shear thickening or shear thinning, where the relationship between shear stress and shear rate requires the use of additional parameters to represent rheological data.

That's why the rheological behaviour of dense cement-based materials can be better represented by the Herschel-Bulkley model since it can model the shear thinning behaviour that is observed (De Larrard et al. 1998) [39].

5.1.2 The Herschel-Bulkley model

When a material's viscosity, measured at or above the shear threshold, depends on the applied shear rate, it is described by non-linear laws such as the Herschel-Bulkley model. Once the applied shear rate exceeds the Herschel-Bulkley threshold, the relationship between viscosity and shear rate can be expressed by an exponential equation:

$$\tau = \tau_0 + k\dot{\gamma}^n \quad (1.11)$$

Herschel-Bulkley's law is empirical, it is a combination of the Bingham and the extrapolation of the power-law models. This law does not provide a value of viscosity but rather K and n which are respectively the coefficients of consistency and the flow index.

De Larrard proposed a method to use the Herschel-Bulkley model with only two parameters, according to his proposal, the yield stress can be determined using the Herschel-Bulkley equation, while the plastic viscosity can be calculated using a different equation [45]:

$$\mu' = \frac{3k}{n+2} \dot{\gamma}_{max}^{n-1} \quad (1.12)$$

where $\dot{\gamma}_{max}$ is the maximum shear rate reached in the test.

5.1.3 The power law model

The Power-Law model, also known as the Ostwald-de Waele model, assumes a power-law relationship between stress and deformation rate. It is described by the equation:

$$\tau = K \cdot \dot{\gamma}^n \quad (1.13)$$

5.1.4 Modified Bingham Model:

The Modified Bingham model extends the Bingham model by including a second-order term to account for the non-linearity observed at low shear rates. This model can capture the yield stress and the shear-thinning behaviour of cementitious pastes [46].

$$\tau = \tau_0 + \mu \cdot \dot{\gamma} + K \cdot \dot{\gamma}^2 \quad (1.14)$$

Where:

τ is the shear stress

τ_0 is the yield stress

μ is the plastic viscosity

K is the second-order coefficient

$\dot{\gamma}$ is the shear rate

5.1.5 The Sisko model

The Sisko model is a versatile model that can be used to describe a wide range of non-Newtonian fluids, it's validated against experimental data for a variety of non-Newtonian fluids. It has been shown to be accurate for a wide range of shear rates and shear stresses[47].

The Sisko model can be described by the following equation:

$$\tau = \tau_0 + k \cdot \dot{\gamma}^n \quad (1.15)$$

5.1.6 The Generalized Casson model

A generalised Casson fluid is a non-Newtonian fluid that is a generalisation of the classical Casson fluid. The classical Casson fluid is a fluid that liquefies under shear and has infinite viscosity at zero shear rate. This implies that the fluid behaves like a solid until the shearing stress reaches a certain value, at this point the fluid starts to flow[48].

The mathematical model for a generalized Casson fluid is given by the following equation:

$$\tau = \mu \cdot (|\dot{\gamma}| + m|\dot{\gamma}|^q) \quad (1.16)$$

Where τ is the shear stress, μ is the viscosity, $\dot{\gamma}$ is the shear rate, m is a constant that determines the strength of the memory effects and q is a constant that determines the degree of retardation.

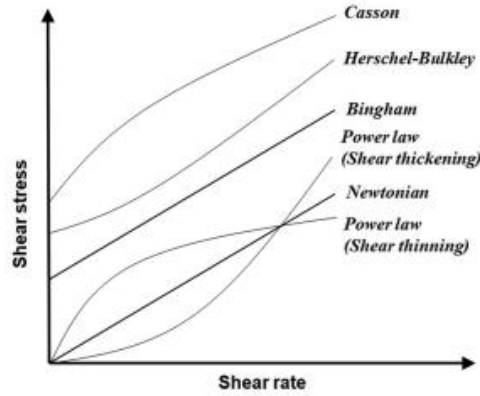


Figure 1. 13: Typical common constitutive models for non-Newtonian fluids[32].

Table 1. 3: Summary of rheological equations for non-Newtonian fluids[32].

Model	Equation	References
Power	$\tau = A\dot{\gamma}^n$	Ostwald (1929)
Bingham	$\tau = \tau_0 + \mu\dot{\gamma}$	Bingham (1917)
Modified Bingham	$\tau = \tau_0 + a\dot{\gamma} + b\dot{\gamma}^2$	Feys et al. (2007), Feys et al. (2008)
Herschel–Bulkley	$\tau = \tau_0 + a\dot{\gamma}^b$	Herschel and Bulkley (1926)
Casson	$\tau^{1/2} = \tau_0^{1/2} + \mu^{1/2}\dot{\gamma}^{1/2}$	Papo and Piani (2004)
Generalized Casson	$\tau^m = \tau_0^m + [\eta_\infty\dot{\gamma}]^m$	Papo and Piani (2004)
Papo–Piani	$\tau = \tau_0 + \eta_\infty\dot{\gamma} + K\dot{\gamma}^n$	Papo and Piani (2004)
De Kee	$\tau = \tau_0 + \eta\dot{\gamma}e^{-\alpha\dot{\gamma}}$	Yahia and Khayat (2003)
Vom Berg	$\tau = \tau_0 + B \sinh^{-1}(\dot{\gamma}/C)$	Vom Berg (1979)
Eyring	$\tau = a\dot{\gamma} + B \sinh^{-1}(\dot{\gamma}/C)$	Atzeni et al. (1985)
Roberston–Stiff	$\tau = a(\dot{\gamma} + C)^b$	Yahia and Khayat (2003)
Atzeni	$\dot{\gamma} = a\tau^2 + b\tau + \delta$	Atzeni et al. (1983)
Williamson	$\tau = \eta_\infty\dot{\gamma} + \tau_f \frac{\dot{\gamma}}{\dot{\gamma} + \Gamma}$	Papo (1988)
Sisko–Ellis	$\tau = a\dot{\gamma} + b\dot{\gamma}^c \quad (c < 1)$ $\eta = \eta_\infty + K\dot{\gamma}^{n-1}$	Papo (1988)
Shangraw–Grim–Mattocks	$\tau = \tau_0 + \eta_\infty\dot{\gamma} + \alpha_1 [1 - \exp(-\alpha_2\dot{\gamma})]$	Papo (1988)
Yahia–Khayat	$\tau = \tau_0 + 2(\sqrt{\tau_0\eta_\infty})\sqrt{\dot{\gamma}e^{-\alpha\dot{\gamma}}}$	Yahia and Khayat (2003)

As we mentioned earlier, the rheological behaviour of cement pastes may be influenced by a variety of variables, including temperature and chemical or mineral additions. However, a potential influence that the test protocol and/or the rheological model may have been yet not fully understood. Nehdi and Rahman. [49] used rheometers with coaxial cylinders (smooth and vane) and parallel plates (smooth and serrated) to study the effects of rheological models (Bingham, modified Bingham, Herschel-Bulkley, Casson, Sisko, and Williamson) on the rheological characterization of cement pastes with a water/binder ratio of 0.40 and 0.50.

To estimate rheological qualities, several cement pastes were tested using various rheological test geometries, and the flow curves that resulted from those tests were fitted using a range of rheological stress models. The yield stress, viscosity, and standard error values for the various models were attempted to empirically correlate. These inferences can be made based on the investigation's findings.

For the parallel plates test geometries, the correlations between the Bingham model yield stress values and those of the Modified Bingham, Herschel-Bulkley, and Casson models appeared to be linear. For vane rotor flow testing, the Modified Bingham, Herschel-Bulkley, and Casson models' yield stress values showed parabolic relationships with the Bingham model's yield stress [50].

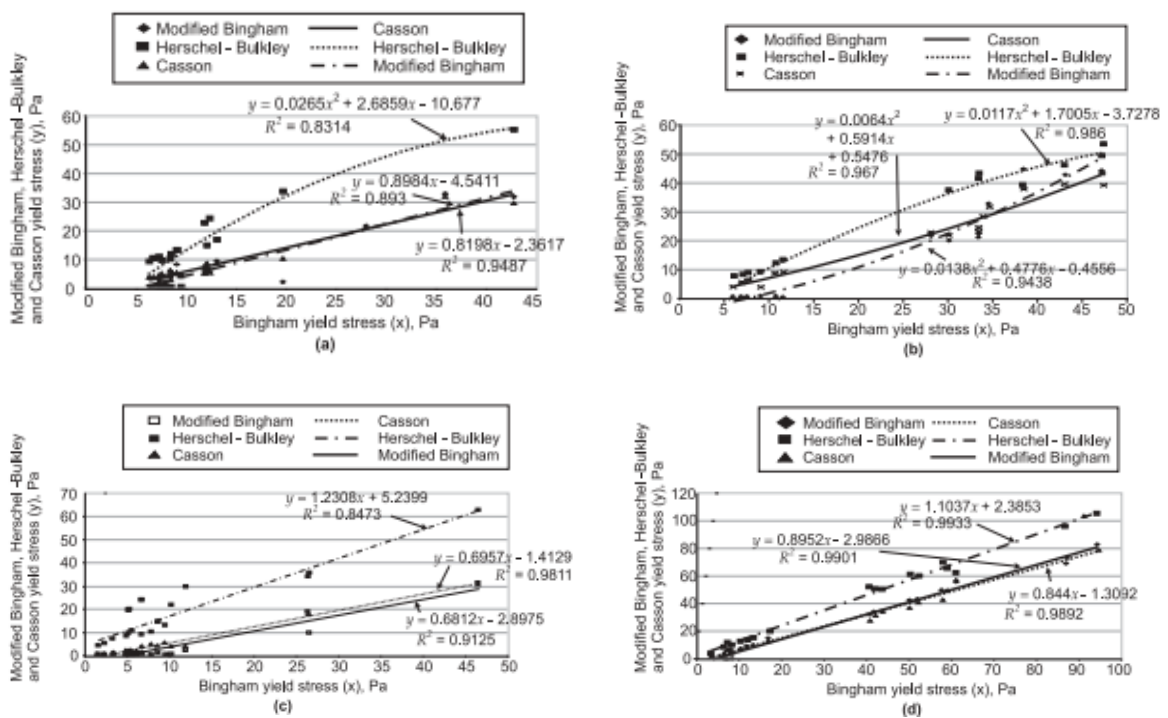


Figure 1. 14: Correlation between the Bingham yield stress and that estimated by the Modified Bingham, Herschel-Bilkley, and Casson models (a) tested by coaxial cylinders, (b) tested by vane rotor, (c) tested by smooth plate, (d) tested by serrated plate[50].

Meanwhile, figure 1-15 represents correlations between the Modified Bingham, Herschel-Bulkley, and Casson model yield stress that show a linear behaviour for the serrated plate test geometry, however, the relationship between the Casson and Modified Bingham yield stress values for coaxial cylinders revealed a parabolic behaviour [50].

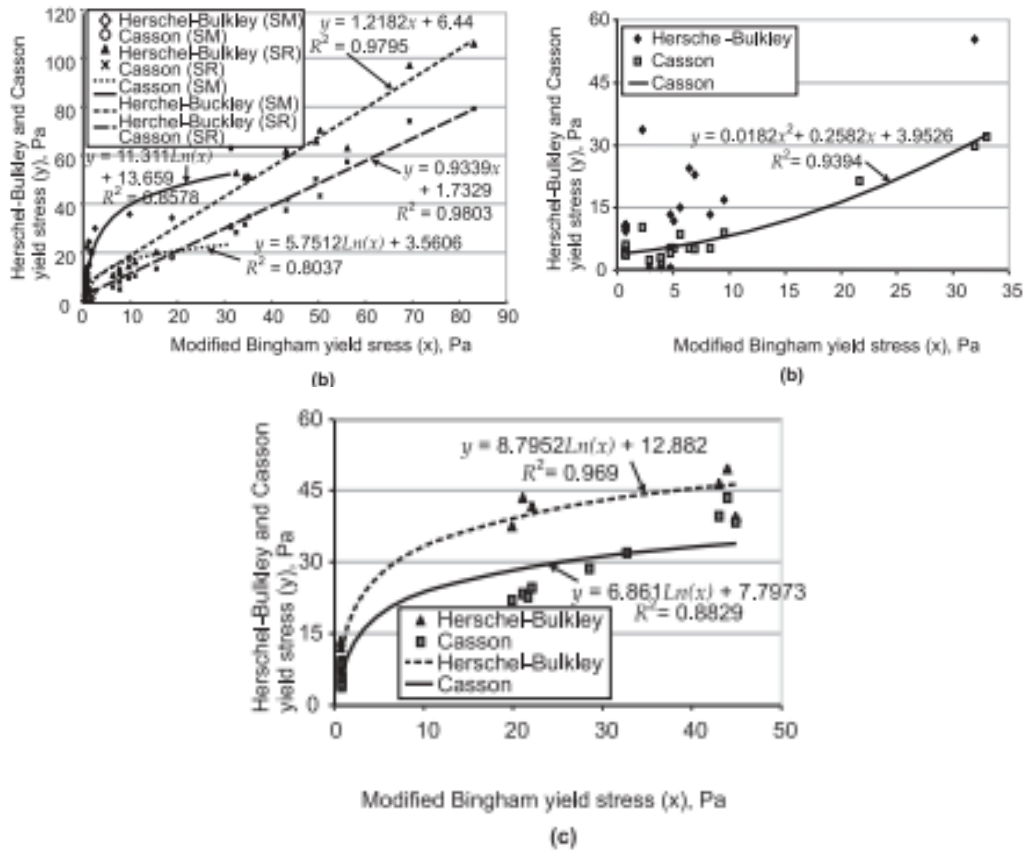


Figure 1. 15: Correlation between the modified Bingham, and Herschel Bulkley and Casson model yield stress for parallel plates test geometries. Herschel-Bulkley and Casson model yield stress versus modified Bingham model yield stress (b) tested by coaxial cylinders[50].

Slag, fly ash, and silica fume, along with welan gum and naphthalene sulphonate superplasticizer were evaluated in cement pastes. The authors discovered that the variations in rheological properties were caused by the geometry, gap, and surface of the rheometric equipment as well as the rheological models used to derive rheological properties from the flow curves [51].

Part B: Generality about Modelling

1 Generalities

Modelling is an operation which allows to obtain, to create the model of a complex system by another one easier to apprehend, in order to carry out a more convenient study of this system by measuring the variations of such or such of its component elements, to analyse it, to explain it and to predict certain aspects of it.

The model thus constructed is based on hypotheses and input data that can be adjusted or validated using observed data. The results obtained with the model can be used to better understand the functioning of the real system, to anticipate its evolution, to evaluate action strategies or to provide forecasts. Modelling is widely used in many scientific fields such as many fields such as physics, economics, biology, it is common to have to understand and analyse phenomena whose behaviour is known only by experimental measurements. Therefore, it is often useful to create a mathematical model that reproduces the behaviour of the real phenomenon. This approach also makes it possible to explore the influence of certain parameters of which knowledge may be limited. By synthesising such a model, it is therefore possible to better understand and study the phenomenon, as well as to highlight the impact of these little-known parameters.

2 Regression and Modelling

Regression analysis is a statistical method employed to examine, establish, determine, and simulate the correlation between variables. The utilization of regression is wide-ranging and spans various disciplines, such as engineering, physical and chemical sciences, economics, and management.

Therefore, it is often useful to create a mathematical model that reproduces the behaviour of the real phenomenon, which is a fundamental concept in regression analysis. In this context, a model represents a mathematical equation formulated to explain and understand the patterns or fluctuations in a particular variable of interest. The ultimate goal is to discover an appropriate equation that accurately captures the provided data.

Equations are commonly employed by engineers and scientists to summarize or depict a collection of data. In this regard, regression analysis proves to be beneficial as it aids in the development of these equations.

Furthermore, regression methods can be employed to solve parameter estimation problems.

2.1 Model Building

The process of model building involves several key steps. Firstly, there is data gathering and exploring that may involve conducting experiments, surveys, or gathering existing datasets.

Then, the subsequent step involves making assumptions, which reflect our understanding of how the system functions. These assumptions serve as statements about the underlying principles guiding the system. In future analyses of the system, these assumptions are treated as true, and the validity of the results relies on the accuracy of these assumptions. In certain cases, if the assumptions are specific enough, they can directly lead to the mathematical equations that govern the system.

After determining the structure of a model, the subsequent step involves selecting appropriate mathematical equations to characterize the system. It is crucial to exercise caution and deliberate thought when choosing these equations since they can potentially have unforeseen impacts on the model's behaviour. This process often entails referring to existing literature to identify relevant equations that have been previously established, which in our case includes choosing the best equations that best describe the rheological behaviour of cement pastes.

Next, analogies from physics, physicists have extensively employed mathematical models to describe various systems, drawing analogies from the field of physics. In many cases, these systems can be precisely defined, allowing for the relatively straightforward application of mathematical equations[52].

2.2 Simple Linear Regression

In simple linear regression, we attempt to model the relationship between two variables, in this case, and where the relationship can be represented linearly, a model in the following format is employed:

$$y = \beta_0 + \beta_1 x + \varepsilon \quad (1.17)$$

where y is the dependent or response variable and x is the independent or predictor variable, and the random variable ε is the error term in the model[53].

2.3 Multiple Linear Regression

When the response variable y is frequently influenced by multiple predictors variables, the linear model has the form[53] :

$$y = \beta_0 + \beta_1x_1 + \beta_2x_2 + \dots + \beta_kx_k + \varepsilon \quad (1.18)$$

Where:

$\beta_0, \beta_1, \dots, \beta_k$: are called regression coefficients.

ε : the error.

k : number of variables.

2.4 Nonlinear regression

Nonlinear regression involves the consideration of functions that cannot be expressed as linear combinations of the parameters. Such functions are often derived from theoretical principles. The following is a representation of the nonlinear regression model:

$$y_n = f(x_n, \theta) + z_n \quad (1.19)$$

where

f : is the expectation function.

x : is a vector of associated regressor variables or independent variables.

The parameters of a nonlinear model are referred to as θ to highlight the distinction between linear and nonlinear models. The vectors x_n (where n extends from 1 to N) are assumed as fixed while evaluating a particular dataset, and the reliance of the predicted responses on θ is the main emphasis.

We create the N -vector $\eta(\theta)$ with its n th element represented as:

$$\eta_n(\theta) = f(x_n, \theta) \quad (1.20)$$

and write the nonlinear regression model as: θ

$$y = \eta(\theta) + z \quad (1.21)$$

with Z assumed to have a spherical normal distribution[52].

3 Choice of model

The selection of an appropriate statistical model is a critical step in conducting data analysis and drawing meaningful conclusions. It involves choosing a model that best captures the underlying relationship between variables and provides accurate predictions. Making an informed choice of model requires considering various factors, including the quality of fit, model assumptions, and interpretability.

One key aspect in evaluating the choice of model is the examination of statistical measures such as the standard error and coefficient of determination

3.1 Coefficient of Determination

The measure R^2 ($0 < R^2 < 1$) is called the coefficient of determination, we may interpret R^2 as the proportionate reduction of total variation associated with the use of the predictor variable X . Thus, the larger R^2 is, the more the total variation of Y is reduced by introducing the predictor variable X [54].

$$R^2 = \frac{SSR}{SST} = \frac{\sum_{i=1}^n (\hat{y}_i - \bar{y})^2}{\sum_{i=1}^n (y_i - \bar{y})^2} \quad (1.22)$$

Where:

SSR: is the regression sum of squares

SST: is the total sum of squares.

Values of R^2 that are close to 1 indicate that useful predictions can be made and that the regression fits the data perfectly.

3.2 The error

The error is the measure of the difference between the predicted and actual data. A lower error indicates a closer fit of the model to the data.[55]

The error is evaluated using the following formula:

$$S = \sqrt{\frac{\sum_i^n (\bar{y} - y_i)^2}{n - p}} \quad (1.23)$$

Where:

\bar{y} = measured value.

y_i = calculated value.

n = number of data points.

p = number of coefficients in a model.

The error and correlation coefficient combined can be used to estimate the validity of a model in general. A model with a low error and a high correlation coefficient is more likely to match the data properly.

3.3 Identification of the model parameters

The identification of model parameters is a fundamental task in statistical modelling and data analysis. Model parameters represent the unknown quantities that govern the relationship between variables and play a crucial role in describing and understanding the underlying mechanisms within a system. Accurate estimation of these parameters is vital for making reliable predictions, drawing meaningful inferences, and gaining insights from the data.

The process of parameter identification involves determining the values of the model's unknown parameters that best align with the observed data. This task often relies on statistical estimation techniques, such as maximum likelihood estimation or least squares estimation. Through these methods, the parameters are estimated by optimizing an objective function that measures the goodness of fit between the model and the observed data.

- **The least square method**

The objective of finding the least squares estimates can be succinctly described in geometric terms. Given a data vector y , an expectation function $f(x_n, \theta)$, and a set of design vectors x_n (where $n = 1, \dots, N$), the process involves two steps:

- 1) find the point $\hat{\eta}$ on the expectation surface which is closest to y , and then
- 2) determine the parameter vector $\hat{\theta}$ which corresponds to the point $\hat{\eta}$.

To get estimates for the parameters θ , the sum of the squared deviations should thus be minimized[56].

$$s(\underline{\theta}) = \sum_{i=1}^n (y_i - \eta_i(\underline{\theta}))^2 \quad (1.24)$$

- **Gauss-Newton Algorithm**

One approach, proposed by Gauss, involves utilizing a linear approximation of the expectation function to iteratively enhance an initial estimate θ^0 for θ . The process continues to refine the estimates until no further changes occur. Specifically, we expand the expectation function $f(x_n, \theta)$ using a first-order Taylor series around the point θ^0 , yielding the following expression:

$$f(x_n, \theta) \approx f(x_n, \theta^0) + v_{n1}(\theta_1 - \theta_1^0) + v_{n2}(\theta_2 - \theta_2^0) + \dots + v_{np}(\theta_p - \theta_p^0) \quad (1.25)$$

Where

$$v_{np} = \left. \frac{\partial f(x_n, \theta)}{\partial \theta_p} \right|_{\theta^0} \quad (1.26)$$

Incorporating all N cases, we write

$$\eta(\theta) = \eta(\theta^0) + v^0(\theta - \theta^0) \quad (1.27)$$

Where v^0 is the $N \times P$ derivative matrix with elements (v_{np}) . This is equivalent to approximating the residuals, $z(\theta) = y - \eta(\theta)$, by

$$z(\theta) \approx y - [\eta(\theta^0) + v^0 \delta] = z^0 - v^0 \delta \quad (1.28)$$

Where $z^0 = y - \eta(\theta^0)$ and $\delta = \theta - \theta^0$

We then calculate the Gauss, increment δ^0 to minimize the approximate residual sum of squares $\|z^0 - v^0 \delta\|^2$ using

$$v^0 = QR = Q_1 R_1$$

$$w_1 = Q_1^T z^0$$

$$\hat{\eta}^1 = Q_1 w_1$$

$$R_1 \delta^0 = w_1$$

At this stage, the point $\hat{\eta}^1 = \eta(\theta^1) = \eta(\theta^0 + \delta^0)$ is expected to be closer to y compared to $\eta(\theta^0)$. Consequently, we transition to this improved parameter value $\theta^1 = \theta^0 + \delta^0$ and initiate another iteration. In this iteration, we calculate new residuals $z^1 = y - \eta(\theta^1)$, a new derivative matrix v^1 , and a fresh increment. This iterative process continues until

convergence is achieved, meaning that the increment becomes sufficiently small, resulting in negligible changes to the elements of the parameter vector [56].

- **Maximum Likelihood Estimation**

This method seeks to find the parameter values that maximize the likelihood of the observed data given the model. It assumes that the observed data follows a particular statistical distribution.

The joint distribution across the observations is what is referred to as the likelihood and can only be determined if the probability of Y is known. If we have this knowledge, the probability is given by:

$$L(y_1, \dots, y_n | \theta) \equiv f(y_1, \dots, y_n | \theta) \quad (1.29)$$

The maximum likelihood estimator of θ is the value that maximizes the likelihood of the data[54]:

$$\hat{\theta} = \operatorname{argmax}_{\theta} L(y_1, \dots, y_n | \theta) \quad (1.30)$$

Conclusion

In conclusion, this chapter has provided an overview of key concepts related to cement, superplasticizers, different rheological behaviours and modelling approaches. Through an extensive literature review, we have gained valuable insights into the fundamentals and characteristics of cement pastes and superplasticizers. In addition, we have reviewed the different rheological behaviours of cement pastes and explored the different modelling methods employed in this field. The knowledge acquired in this chapter provides the basis for the following chapters and contributes to a better understanding of the rheological behaviour of cement pastes containing superplasticizers.

Chapter 2: Test and experimental

1 Introduction

Several factors can affect the rheology of superplasticized cement paste. These factors are mainly connected to the type of chemical and phase compositions and fineness of cement, the chemical nature of the superplasticizer, its dosage, and the addition method.

Our work is based on the experimental results carried out on cementitious admixtures, which deal with their rheological behaviour. We are interested in understanding how these cementitious admixture pastes behave when subjected to various mechanical stresses, such as viscosity and plasticity. To evaluate the rheological behaviour of cementitious admixture pastes, we prepared the pastes by mixing specific proportions of cement, admixtures and water. Then we carry out a series of experimental tests to assess their rheology.

2 Rheological test

2.1 Types of viscometer:

Devices for measuring the rheological characteristics of fluids are called rheometers, and they vary depending on the geometry of the measuring instrument and the way the fluid is stressed. There are wide varieties of rheometers available.

2.1.1 Dynamic Shear Rheometer (DSR):

Is a viscometer used to measure the rheological properties of materials, including fresh cement paste. It applies a dynamic oscillatory shear strain to the material and measures the resulting stress response. The DSR is useful in understanding how cement paste behaves under different conditions, as it can measure properties like yield stress, viscosity, and viscoelastic behaviour at a range of frequencies and temperatures. The test involves applying a sinusoidal shear strain and measuring the resulting shear stress, which is used to calculate the storage and loss moduli and other properties.[57]

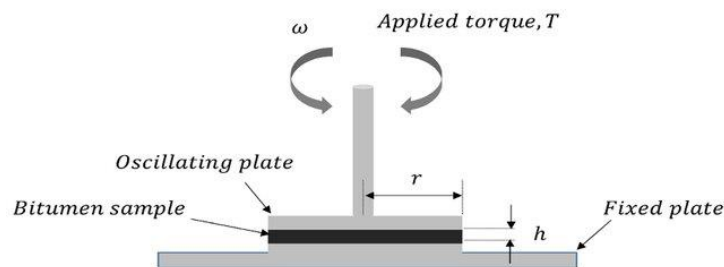


Figure 2. 1: The DSR testing configuration.

2.1.2 Oscillating rheometer

Type of viscometer used to measure the rheological properties of materials, including cement paste. It applies a sinusoidal strain to the sample and measures the resulting stress response, making it useful for measuring viscoelastic properties such as storage and loss moduli [58].

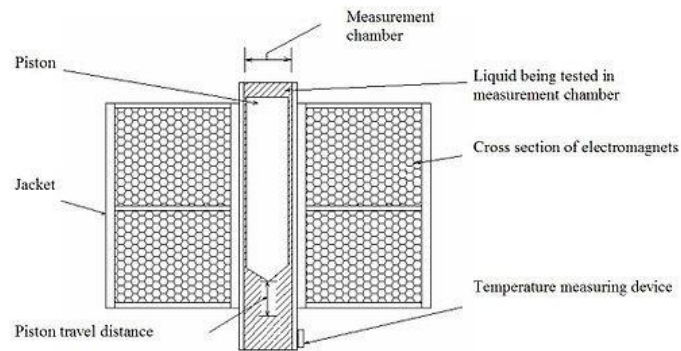


Figure 2. 2: Cross-section of Oscillating Piston Viscometer.

2.1.3 Ultrasonic Rheometer:

Viscometer used to measure the rheological properties of fluids and semi-solids, including cement paste. It works by measuring the velocity of ultrasonic waves as they pass through the sample, which is related to the rheological properties of the sample.

The ultrasonic rheometer is often used to measure the shear viscosity of fresh cement paste. Case of cement the test involves applying ultrasonic waves to the sample and measuring the velocity of the waves as they pass through it. The velocity is then used to calculate the viscosity of the sample[59].

2.1.4 Coaxial cylinder rheometer:

Commonly utilized to evaluate the rheological features of cement paste and concrete, such as viscosity and flow properties. The Brookfield viscometer and the rheometer are some examples of rotary viscometers that are commonly used for these applications. These instruments measure the torque required to maintain the rotation of a spindle or rotor inside the sample, and this data is then used to calculate the rheological properties of the cementitious material.

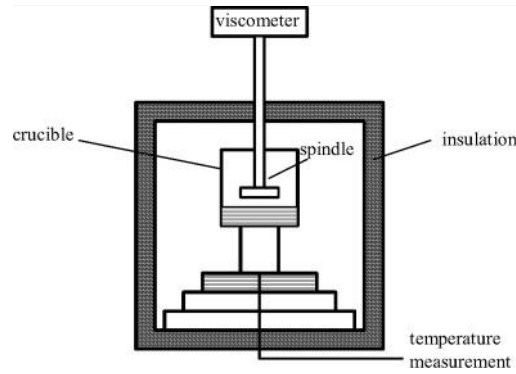


Figure 2. 3: Rotational viscometer.

A coaxial cylinder rheometer is a type of rotational rheometer used to measure the rheological properties of fluids and soft materials. It consists of two concentric cylinders, with the inner cylinder rotating while the outer cylinder remains stationary. The sample is placed between the two cylinders, and the torque and angular velocity of the inner cylinder is measured as a function of time [2].

The operating principle of this rheometer consists in shearing the substance between two coaxial cylinders between two cylinders of revolution, coaxial of radius R_1 and R_2 , and height H (Figure 2.3).

The laminar shearing motion is obtained by imparting to one of the cylinders a uniform rotation, speed ω_0 , the other cylinder remaining stationary or also rotating at an angular speed different from ω_0 .

The characterization of the rheological behaviour of the sheared substance is obtained by the determination of the curve $(\tau - \gamma)$; from the torque values provided by the rheometer, which are respectively the resistive moment M and the rotational speed of the mobile ω_0 . In the uniform laminar flow regime, we can easily calculate the stress of shear stress at the wall of a cylinder:

$$\tau = \frac{M}{2\pi \cdot R^2 \cdot H} \quad (2.1)$$

Where

R: respectively the radius

H: height of the cylinder.

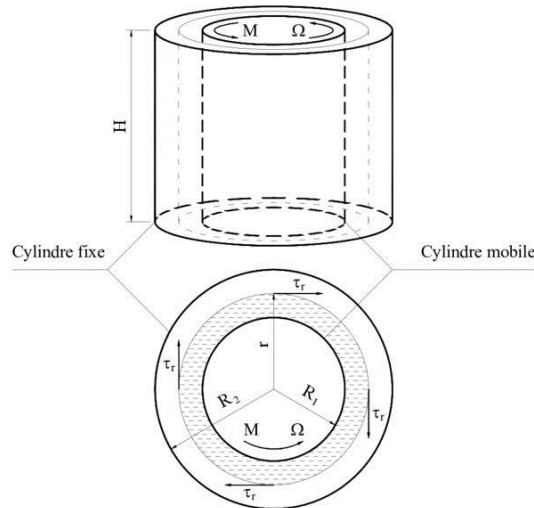


Figure 2. 4: Schematic representation of the operating principle of rotary rheometers with coaxial cylinders.

Determining the velocity gradient $\dot{\gamma}$ (also known as shear rate) is a more complicated task, as it depends on the material's rheological characteristics. The formula for calculating this parameter is as follows:

$$\dot{\gamma}(r) = r \frac{d\omega}{dr} \quad (2.2)$$

The expression for determining the velocity gradient $\dot{\gamma}$ requires knowledge of the angular displacement velocity, $d\omega$, between two layers positioned at a radial distance r and separated by dr . However, knowing only ω is insufficient for determining $\dot{\gamma}(r)$. It is also necessary to know the distribution law of angular velocity, $\omega(r)$, which is a function of the material's rheological properties. Thus, there is a circular dependency where determining the material's rheological behaviour requires prior knowledge of it. This circular dependency poses a significant challenge in experimental rheology, and various experimental procedures and mathematical approximations are adopted to overcome it.

3 Equipment and materials

3.1 The experimental instrument used

The study can be summarized as an exploration of the relationship between shear stress τ and shear rate $\dot{\gamma}$. This relationship is being investigated using a rotary viscometer with coaxial cylinders, which allows for continuous viscosity evaluation as the speed of rotation of a cylinder immersed in a grout is increased.

Here we review the different geometries used in this study. The tests of this study were carried out using the HAAKE Viscometer 550 from Thermo Scientific it's a rotary viscometer with coaxial cylinders, which makes it possible to continuously evaluate the viscosity while increasing the speed of rotation of a cylinder immersed in a grout. His apparatus is intended to analyse the rheological characteristics of liquid to semi-solid[60].

The substance to be measured is located in the measuring gap of the sensor system. The rotor rotates at a predefined speed (n). The substance to be measured exerts resistance to this rotational movement (due to its viscosity) which becomes apparent as a (braking) torque value.

The built-in computer to calculate the relevant measuring values for the following factors uses the measured variables of speed, torque, and sensor geometry.

Viscosity η in mPas.

Shear rate $\dot{\gamma}$ in s^{-1} .

Shear stress τ in Pa.

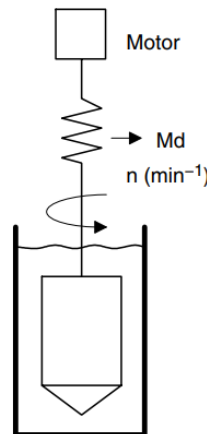


Figure 2. 5: Functional principle of the instrument used[60].

System factors – Calculation procedure:

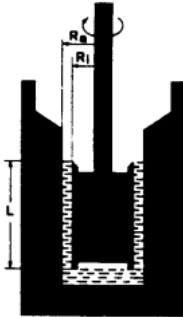
By definition, viscosity describes the relationship between shear stress (τ) and shear rate ($\dot{\gamma}$).

$$\eta = \frac{\tau}{\dot{\gamma}} \quad (2.3)$$

The calculation considers the geometric characteristics of various sensor systems through system factors, starting with the measured values for "torque Md" and "speed n." Equation (2.3) can now be supplemented as follows:

$$\eta = \frac{f \cdot Md}{M \cdot n} \quad (2.4)$$

Characteristic of the instrument



Inner Cylinder (Rotor)	Radius Ri (mm)	Height L (mm)
	10.1	61.4
Outer Cylinder (Cup)	Radius Ra (mm)	
	11.55	

3.2 Materials used

3.2.1 Cement

The CEMI 42.5 (Msila) and the CEMII A 42. (Mascara) were used in this study.

The two types of cement examined display contrasting chemical and mineralogical compositions, as presented in Table 2.1 and Table 2.2, rendering them suitable for conducting a comparison analysis of the planned tests.

Table 2. 1: Chemical analysis of the two cements.

	Chemical analysis	
	CEMII A 42.5	CEMI 42.5
Loss on ignition (%)	8.00 – 10.00	0.5–3
Insoluble residues (%)	0.7 – 1.5	>0.7
Sulfur trioxide SO ₃ (%)	2.10 – 2.50	1.8–3
Magnesium oxide MgO (%)	1.00 – 1.30	1.2–3
Chloride (%)	0.01 – 0.03	0.01–0.05

Table 2. 2: Mineralogical composition of the two cements.

	Clinker composition	
	CEMII A 42.5	CEMI 42.5
Tricalcium silicate C ₃ S (%)	55.00 - 62.00	< 61.00
Dicalcium silicates C ₂ S (%)	13.00 - 22.00	< 16.00
Tricalcium aluminate C ₃ A (%)	6.50 – 8.20	< 3.00
Tetracalcium aluminoferrite C ₄ AF (%)	10.00 – 13.00	< 13.00

The CEMI 42.5 cement (sulphate-resistant cement) is made of:

- 95% clinker, secondary constituents (from 0 to 5%) can be incorporated in this cement.
- Calcium sulfate in the form of gypsum is added as a setting regulator.

It was chosen for its ability to resist chemical aggressions and for the fact that all the works in concrete buried are made with this cement.

The CEMII A 42.5 cement comprising of at least 65% clinker and not more than 35% of other constituents: blast furnace slag, silica fume, natural pozzolan, fly ash, and limestone. This cement is adapted for the current concretes and all works of civil engineering which do not require high constraints, the works of masonry, the realization of pavements, the confection of coatings, the prefabrication with or without heat treatment, the road works, treatments of gravels, tracks, ..., concrete ready to use as well as all works of concreting in a big mass.

3.2.2 Superplasticizers

Superplasticizers are chemical admixtures added to concrete or cement pastes to improve their workability and flowability which can also modify their rheological properties such as yield stress and plastic viscosity[61].

We used three different types of superplasticizers from various manufacturers. We name:

- SP1, this next-generation non-chlorine superplasticizer based on acrylic copolymer technology is a versatile admixture that can be used in a wide range of applications. Its recommended dosage range is 0.2 to 3.0% by weight of cementitious materials.

- SP2, a new generation of non-chlorine superplasticizer based on modified polycarboxylic ether is a high-performance concrete admixture that reduces water content, improves workability, and increases strength. Its recommended dosage range is from 0.3 to 2.0% by weight of cementitious materials.
- SP3, is a synthetic polymer-based superplasticizer used to improve the resulting material's workability, strength, and durability. This type of superplasticizer is highly effective at reducing the water which allows for obtaining a very low W/C ratio, the recommended use range for SP3 is between 1.0 and 2.5% by weight of cementitious materials.

4 Mixture proportion

Cement pastes were prepared using the two types of cement and superplasticizer from the three different families mentioned earlier with a water binder ratio of 0.4.

As for the superplasticizer's dosage used in the experimentation, it was defined as the mass of the dry extract of the superplasticizer relative to the mass of the initial anhydrous cement in the mixture. The dosage varies according to the recommended range of use for each particular superplasticizer = 0.5, 1, 1.5, 2, and 2.5%. To ensure a fair comparison of the results, the same dosage was used for both types of cement used in the experimentation

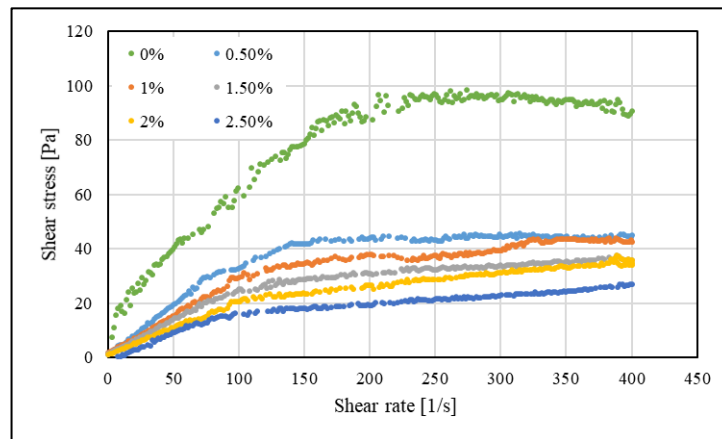
5 Results and Discussion

5.1 Rheological Curves

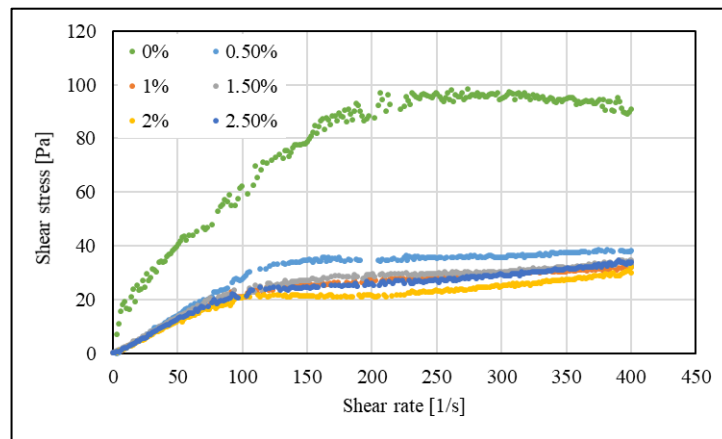
The analysis of the rheograms depicted in Figure 2.6 and Figure 2.7 intuitively allowed us to conclude that cement pastes exhibit non-Newtonian fluid behaviour. The evaluation of shear stress as a function of shear rate clearly demonstrates a nonlinear behaviour with a yield stress, which indicates a complex rheological response exhibited by the material.

The effect of the different superplasticizers is also well reflected by the rheological curves, with the increase of the different superplasticizers' dosages the resulting shear stress during the measurement decreases.

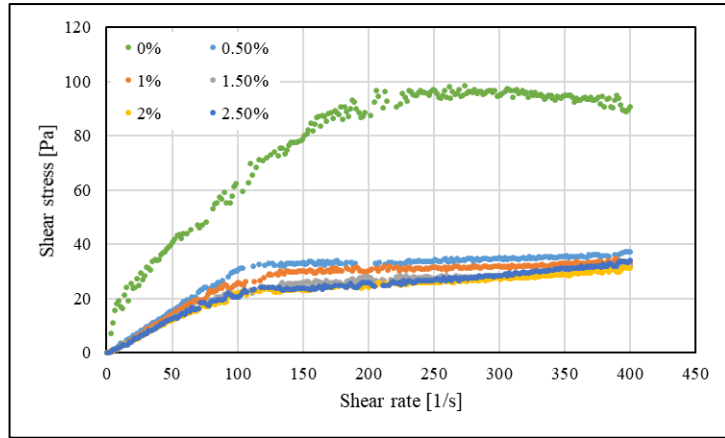
However, we can clearly see from the shape of the curves of the two types of cement pastes that the effect of incorporating the superplasticizers into them is completely different. The divergences observed in the curves between the two types of cement pastes highlight the influence of various factors, including cementitious compositions (such as the types and amount of cement mineral admixtures)



(a)

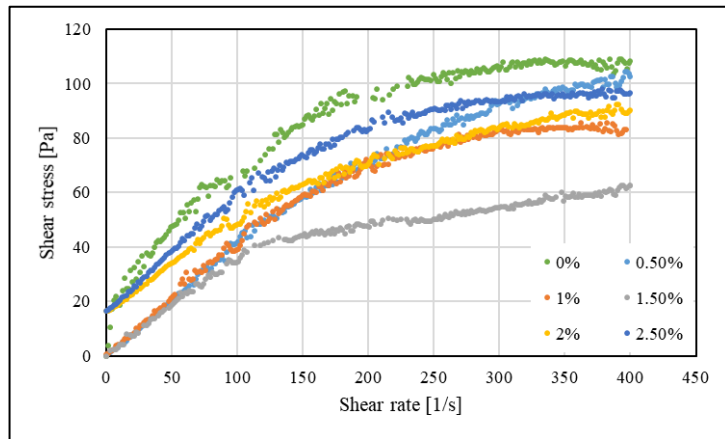


(b)

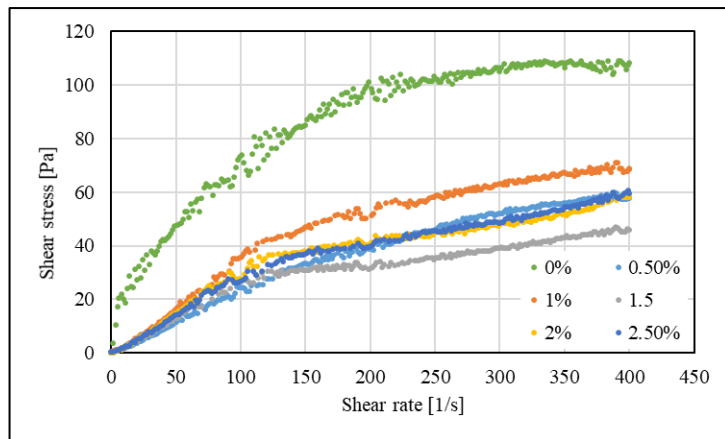


(c)

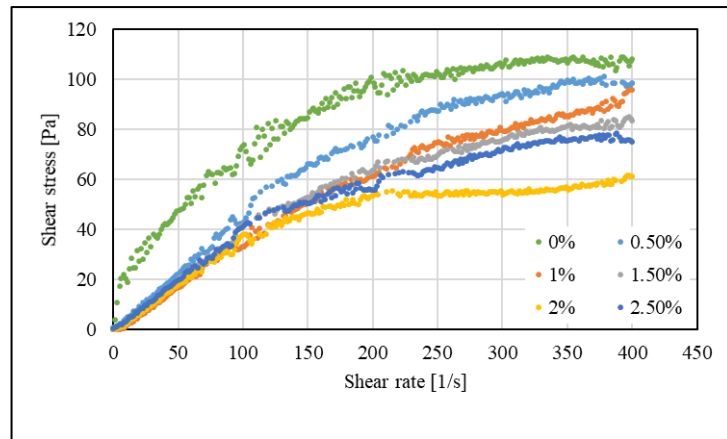
Figure 2. 6: Comparative analysis of Shear rate -Shear stress behaviour in cement paste 1 with different superplasticizers: (a) SP1, (b) SP2, (c) SP3.



(a)



(b)

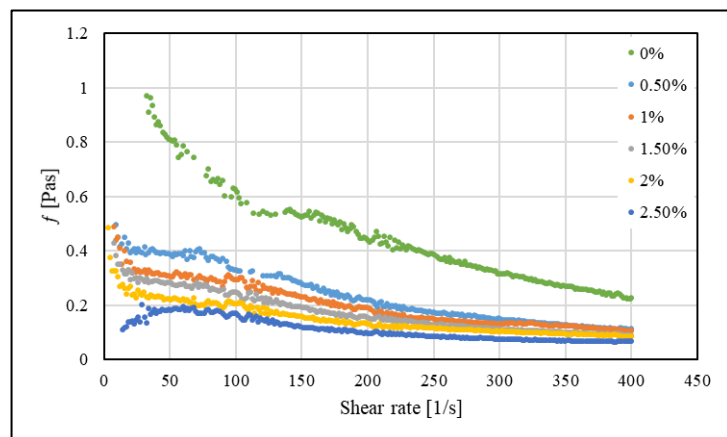


(c)

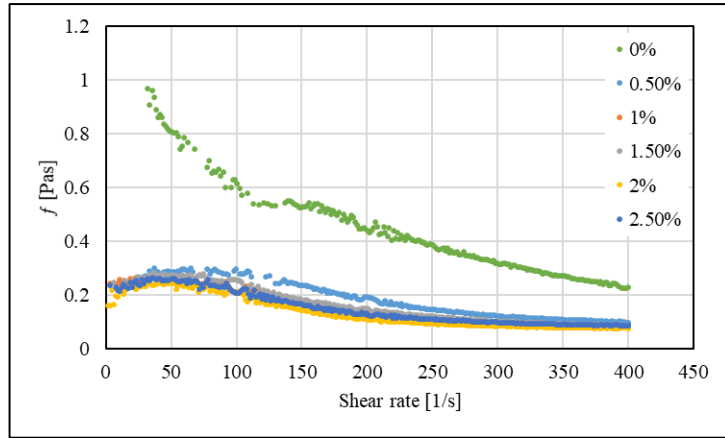
Figure 2. 7: Comparative analysis of Shear rate -Shear stress behaviour in cement paste 2 with different superplasticizers: (a) SP1, (b) SP2, (c) SP3.

The Figure 2.8 and Figure 2.9 shows us the viscosity of the cement past with different superplasticizers. Which we see the effect of SP on the viscosity obtain compared with 0% paste is by increasing the percentage of SP dosages used is reflected by decrease of viscosity of the paste in function of the shear rate $\dot{\gamma}$.

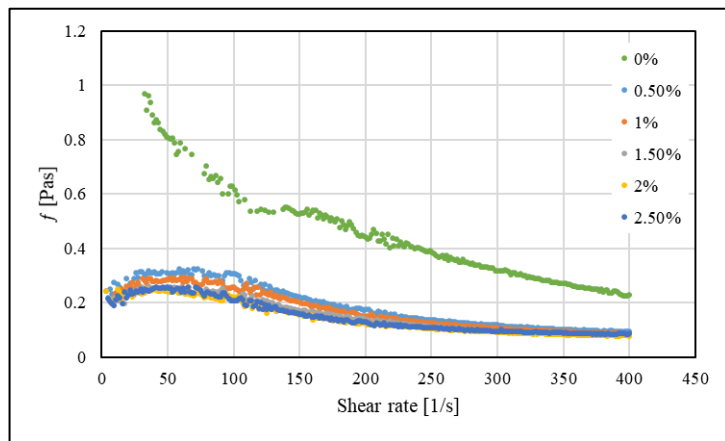
Several factors can contribute to a decrease in the viscosity of cement paste. Increasing the water content reduces viscosity because the water acts as a lubricant between the cement particles, facilitating flow. The duration and intensity of mixing influences viscosity by spreading the cement particles, which reduces binding. Chemical admixtures such as water reducers can reduce viscosity while maintaining the desired water/cement ratio, which promotes fluidity. Temperature also plays a role, with higher temperatures reducing viscosity and lower temperatures increasing it.



(a)

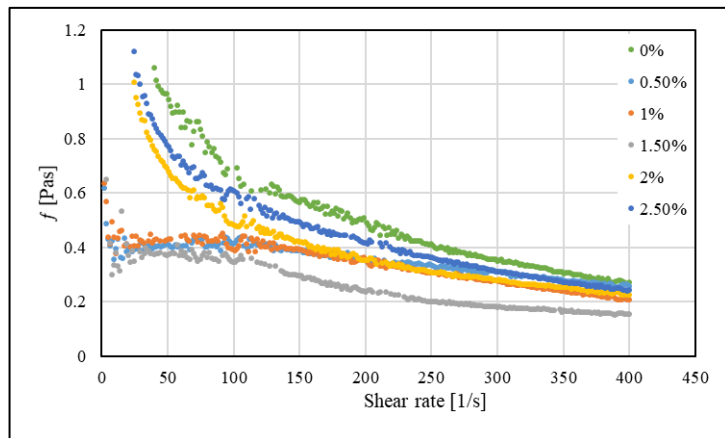


(b)

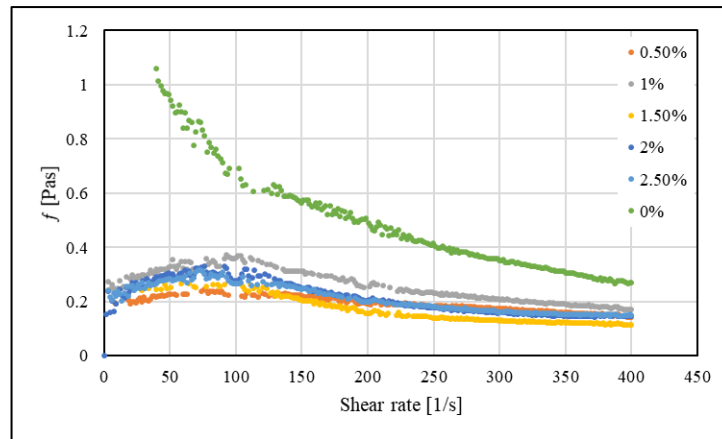


(c)

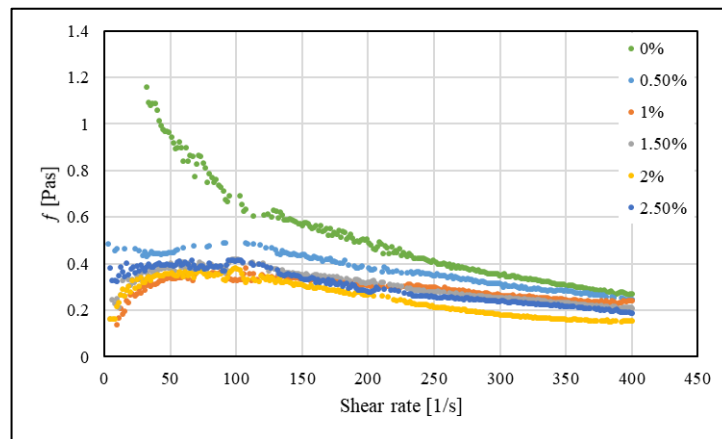
Figure 2. 8: Viscosity behaviour for cement paste 1 with different superplasticizers: (a) SP1, (b) SP2, (c) SP3.



(a)



(b)

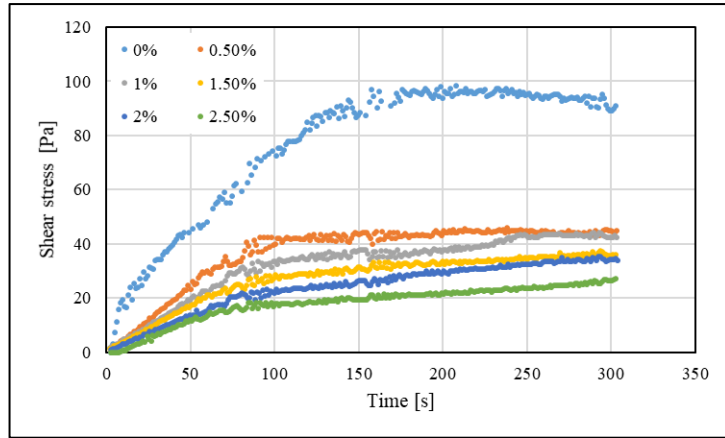


(c)

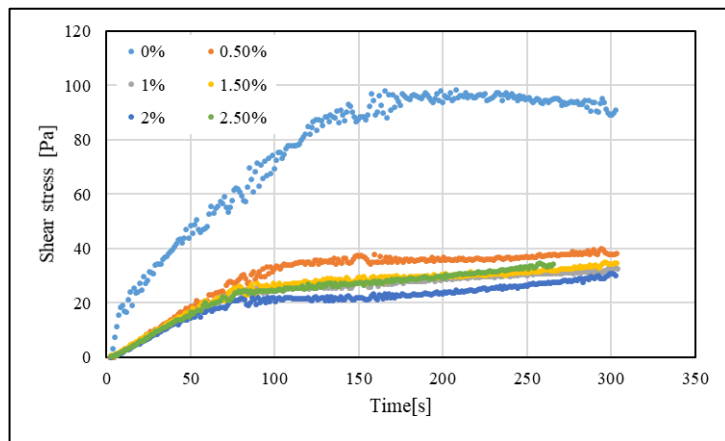
Figure 2. 9: Viscosity behaviour for cement paste 2 with different superplasticizers: (a) SP1, (b) SP2, (c) SP3.

The Figure 2.10 and Figure 2.11 showed that the shear stress of both cement pastes with various dosage of SP does increase over time 0 to 300s, for the cement 1, the shear stress does not necessarily increase rapidly over time in terms of rheology unlike cement 2 that we see big jump of the shear stress. On the contrary, the rheological behaviour of cement paste changes over time due to the continuous process of hydration and setting process. This is due to the process of thixotropy, which is the reversible increase in viscosity of a fluid when it is sheared.

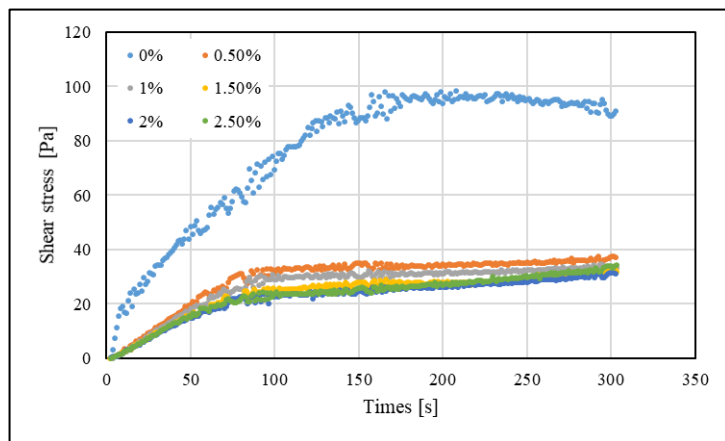
A number of different factors, including type of cement, water/cement ratio, additive used, and shear rate, effects the thixotropic yield strength of cement paste.



(a)

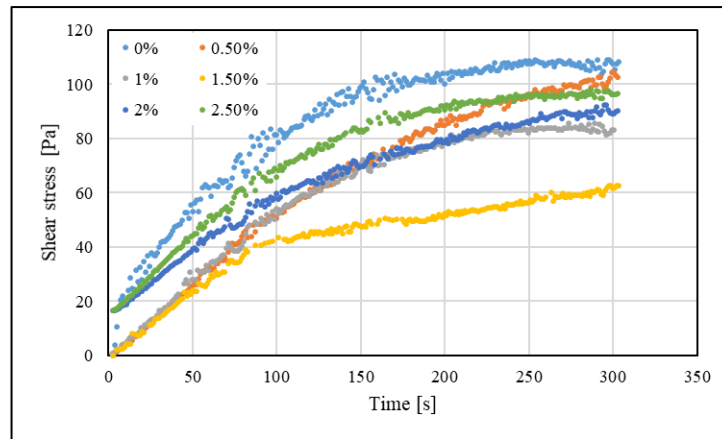


(b)

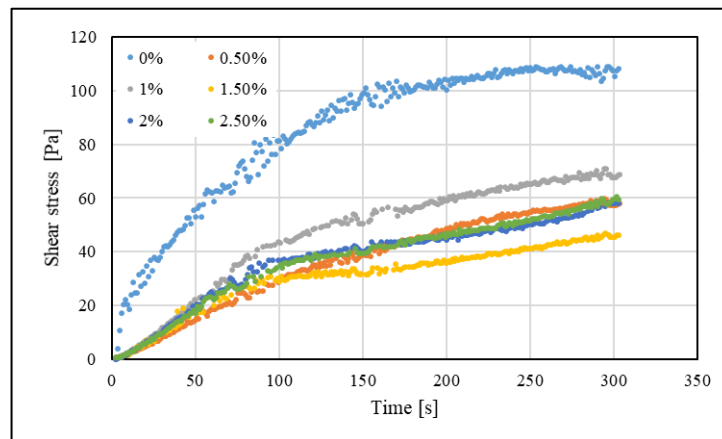


(c)

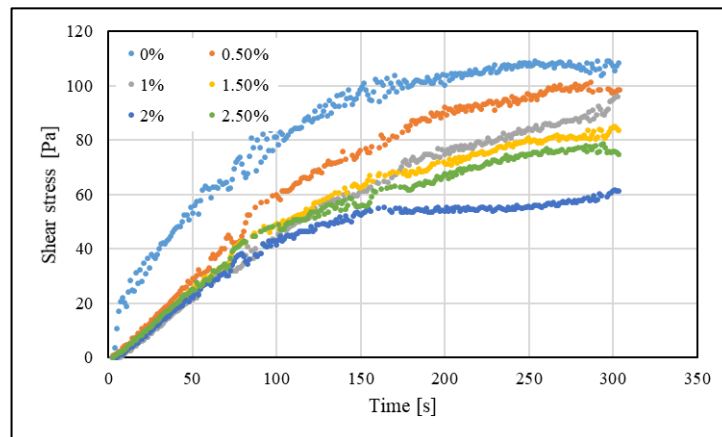
Figure 2. 10: Evolution of the shear stress in function of time for cement paste 1 with different superplasticizers: (a) SP1, (b) SP2, (c) SP3.



(a)



(b)



(c)

Figure 2. 11: Evolution of the shear stress in function of time for cement paste 2 with different superplasticizers: (a) SP1, (b) SP2, (c) SP3.

A number of different factors, including type of cement, water/cement ratio, additive used, and shear rate, effects the thixotropic yield strength of cement paste.

The type of cement used can affect the overall rheological properties of the paste, including its yield strength. Different types of cement have varying particle sizes and chemical

compositions, which can influence the paste's thixotropic behaviour. The choice and dosage of superplasticizers, can modify the rheological properties of the cement paste. Superplasticizers are commonly used to enhance workability and followability, and their presence can affect the thixotropic yield strength. The dosage of the additive is particularly important, as higher dosages can lead to increased flow and lower the viscosity.

Conclusion

In this chapter we focused on carrying out tests and experiments to examine the rheological behaviour of cement pastes containing superplasticizers. HAAKE 550 viscometers were used, along with specific materials, two types of cement and three types of superplasticizer, and measurement techniques to collect the data. The results obtained were analysed and correlated with the curing conditions. These experimental results provided valuable information on the influence of superplasticizers on the rheological properties of cement pastes. Examination of the data obtained during the experiments has enabled us to gain a better understanding of the actual behaviour of the material, which has facilitated the development and validation of the rheological model.

Chapter 3: Modelling and Interpretation

1 Introduction

A mathematical model is a simplified representation of a real system that uses equations and mathematical relationships to describe its behaviour. It may be based on known physical laws, statistical principles or other scientific concepts.

Experimental measurements are used to adjust the model's parameters and ensure that it adequately reproduces actual observations.

Once the model has been built and validated, it can be used to analyze different situations and predict the results of new experiments or conditions.

It can also be used to make predictions and hypotheses about phenomena that cannot be directly observed or measured.

2 The choice of model

When it comes to describing the rheological behaviour of cement pastes, various models are used and explored to capture the complex rheological properties of these fluids, we named in the first chapter some of these models, which are the Herschel-Bulkley model, the modified Bingham model, the Generalized Casson model, and the Sisko model.

To determine which model best fits the goal of our study, we tented to compare the performances of each one of them, and several requirements had to be considered and satisfied to select the suitable model, these criteria include:

- Coefficient of determination R^2 : which is a measure of how well the model fits the data. It is calculated by squaring the correlation coefficient between the model predictions and the actual data. A higher R^2 value indicates a better fit.
- Shape of the curves: the shape of the curves can be used to assess the model's ability to predict the behaviour of the system
- Rheological parameters: rheological parameters are quantitative measures of the flow behaviour of a fluid. They can be used to describe a fluid's viscosity, yield stress, and thixotropy.

Based on these factors, and by examining the obtained results, we aim to choose the model that best aligns with our data to better understand the flow behaviour of examined cement pastes.

2.1 The choice based on R²

As we mentioned earlier, the coefficient of determination plays a significant role in choosing the right rheological model for cement paste analysis. By evaluating the R-square values obtained from various rheological models fitted to our experimental data of cement pastes, we can determine the model that best represents the behaviour of the material.

In the following table, we present the results of the R-square for each considered model:

Table 3. 1: The coefficient of determination R² for rheological models tested.

		%	Sisko	Generalized Casson	Herschel-Bulkley	Bingham	Modified Bingham
Cement 1	SP1	0.5	0.980	0.984	0.897	0.684	0.951
		1	0.975	0.975	0.951	0.817	0.950
		1.5	0.987	0.989	0.957	0.806	0.962
		2	0.991	0.991	0.983	0.897	0.978
		2.5	0.976	0.976	0.972	0.857	0.948
	SP2	0.5	0.963	0.974	0.904	0.707	0.937
		1	0.981	0.981	0.954	0.788	0.948
		1.5	0.975	0.979	0.945	0.774	0.937
		2	0.944	0.951	0.943	0.805	0.888
		2.5	0.964	0.965	0.963	0.834	0.931
	SP3	0.5	0.957	0.965	0.890	0.667	0.907
		1	0.967	0.970	0.903	0.677	0.923
		1.5	0.968	0.970	0.936	0.750	0.926
		2	0.969	0.974	0.950	0.789	0.927
		2.5	0.966	0.961	0.961	0.827	0.926
Cement 2	SP1	0.5	0.991	0.996	0.992	0.955	0.999
		1	0.981	0.991	0.967	0.873	0.997
		1.5	0.984	0.987	0.972	0.863	0.967
		2	0.991	0.996	0.972	0.928	0.995
		2.5	0.990	0.994	0.968	0.870	0.998
	SP2	0.5	0.992	0.996	0.992	0.959	0.998
		1	0.985	0.992	0.978	0.904	0.989
		1.5	0.976	0.976	0.974	0.882	0.957
		2	0.979	0.982	0.974	0.886	0.965
		2.5	0.988	0.990	0.987	0.930	0.980
	SP3	0.5	0.984	0.992	0.979	0.918	0.997
		1	0.990	0.995	0.991	0.957	0.997
		1.5	0.987	0.995	0.983	0.919	0.995
		2	0.971	0.985	0.941	0.796	0.973
		2.5	0.989	0.994	0.984	0.913	0.991

It is evident in Table 3.1, that all the models but the Bingham one resulted in high values of R^2 (all above 0.9) indicating that they accurately predict the data.

The reason why the Bingham model was not as effective as the other models, and yielded a low coefficient of determination results could be related to the fact that the model assumes a linear relationship between the shear rate and shear stress of a fluid, which is not the case for our data as we saw in the previous chapter, where the evolution of shear stress shear rate curves represented in the previous chapter exhibited a non-linear behaviour.

Comparatively, on the other hand, the Generalized outperformed the other models by delivering superior results, followed by the Sisko model, which demonstrated a commendable level of performance, while both the Herschel-Bulkley and the Modified Bingham models exhibited relatively lower performance, the results remained commendable and within acceptable limits.

However, the coefficient of determination alone cannot determine the suitability of a model to the experimental data, it is important to analyse the extracted parameters to enable us to identify the appropriate model.

2.2 The choice based on the model parameters

The study of the acquired results is the key that plays a pivotal role in fostering a deeper understanding of the rheological behaviour of cement pastes and is an essential prerequisite for choosing the right model.

Figure 3.1 represent the flow curves of both cement pastes with a 1.5% dosage of SP1, it highlights the correlation between the predicted curve and the experimental one, which can serve as an indicator of the model's excellence.

Upon visual examination of the figure, the pronounced similarity between the shape of the experimental curve and the predicted one using the aforementioned models is well demonstrated.

However, regardless of the resemblance between the shapes of curves, we cannot determine the model's suitability to our experimental data based solely on that factor.

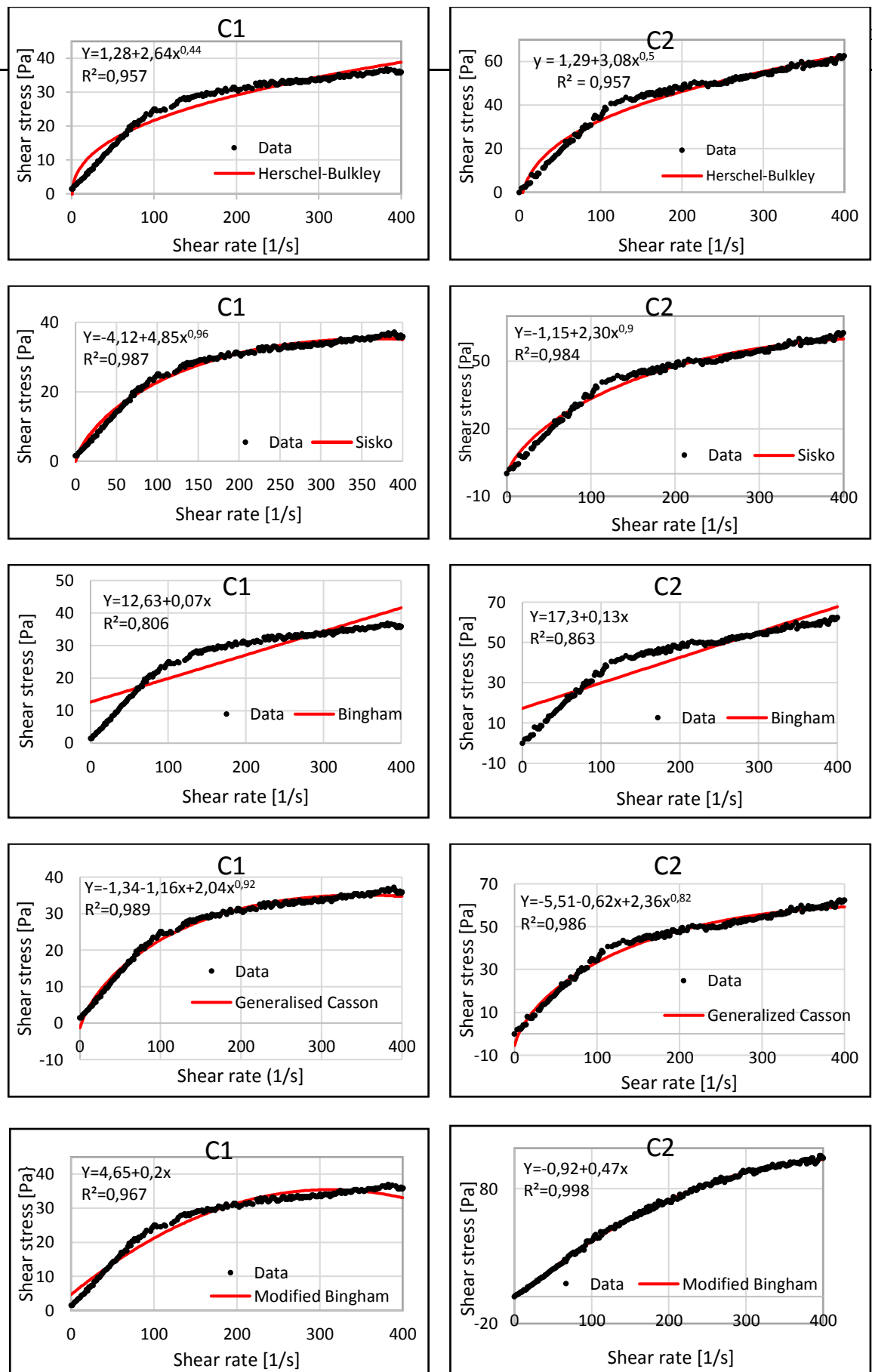


Figure 3. 1: Curves of C1 and C2 with a 1.5% dosage of SP1 followed by the predicted curve of the rheological models.

As explained previously, since the Bingham model describes a linear relationship between shear rate and shear stress, it was the least likely to fit the experimental curves and to follow the same shape, and for that, we excluded this model from further analysis in our study and we devoted our attention to the remaining models.

The conclusive step to selecting the appropriate model, which serves our study, involved analysing and thoroughly studying the extracted parameters from the models.

This step allows us to comprehend the models' performance and evaluate their suitability for our study.

Table 3.2 and Table 3.3 summarized the yield stress resulting from each model, and it is well shown that each model estimated different values of the parameter and delivered distinct outcomes.

Table 3. 2: Tested Rheological models Yield Stress for C1.

C1		Herschel-Bulkley	Generalized Casson	Modified Bingham	Sisko
SP1	0,5	1,61	-4,986	5,789	-7,435
	1	1,32	14,510	5,383	2,810
	1,5	1,28	-1,334	4,778	-4,128
	2	1,05	-0,578	3,501	-1,817
	2,5	1,01	-5,102	2,666	-0,522
SP2	0,5	1,34	-4,737	3,220	-11,010
	1	1,27	-1,224	4,448	-1,176
	1,5	1,34	-6,0245	4,786	-3,546
	2	1,13	0,824	5,431	-0,116
	2,5	1,15	-0,300	4,887	2,757
SP3	0,5	1,48	-6,532	5,173	-5,385
	1	1,39	-3,963	4,436	2,702
	1,5	1,25	-1,755	4,262	1,906
	2	1,16	-0,790	4,535	-0,494
	2,5	1,14	-0,285	4,990	-0,235

Table 3. 3: Tested Rheological Model Yield Stress for C2.

C2		Herschel-Bulkley	Generalized Casson	Modified Bingham	Sisko
SP1	0,5	1,04	-8,07	-0,892	-13,832
	1	1,17	-11,432	-0,341	-6,687
	1,5	1,29	-5,511	5,606	-5,327
	2	1,595	8,228	17,334	-0,165
	2,5	1,779	5,421	16,950	-1,521
SP2	0,5	0,975	-4,737	-0,5021	-11,010
	1	1,080	-9,929	-0,542	-17,849
	1,5	1,06	-2,473	3,605	-1,075
	2	1,123	-2,969	3,0970	1,084
	2,5	1,042	-2,450	2,645	-2,999
SP3	0,5	1,107	-12,386	-1,582	-6,303
	1	0,994	-8,653	-2,325	-4,458
	1,5	1,08	-10,238	-0,370	-5,399
	2	1,282	-10,080	1,523	-11,323
	2,5	1,126	-7,670	2,000	-4,187

The following histograms represent the yield stress results obtained by the different models

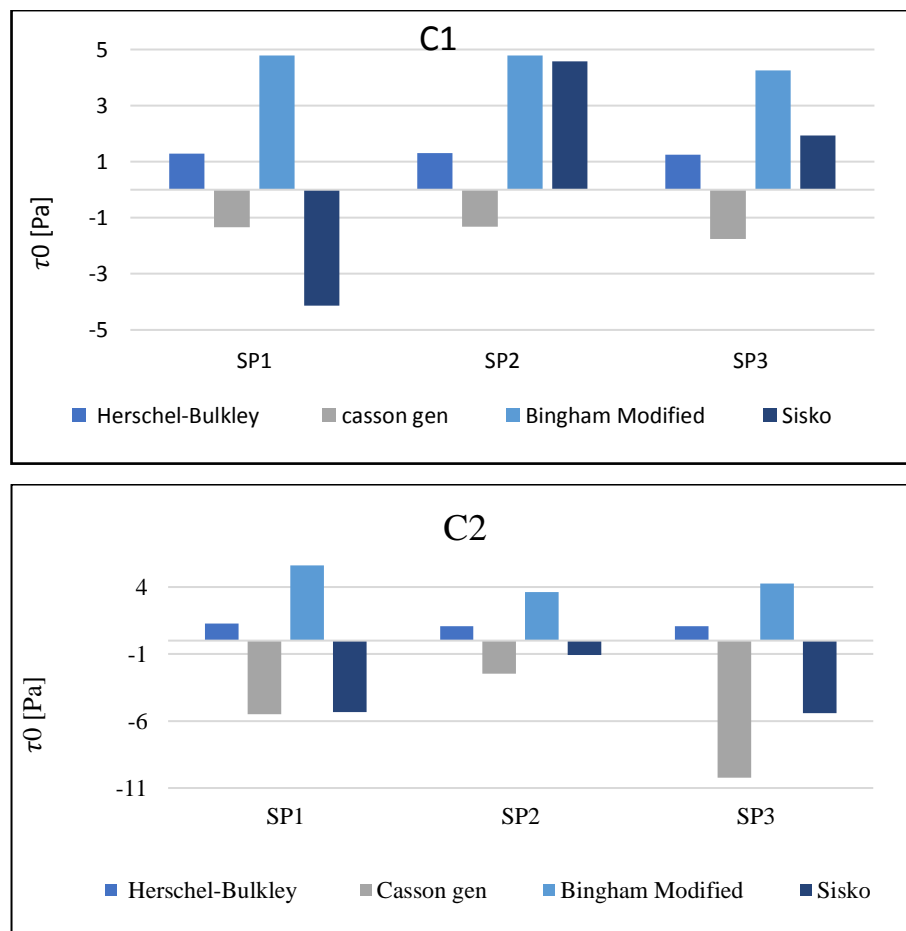
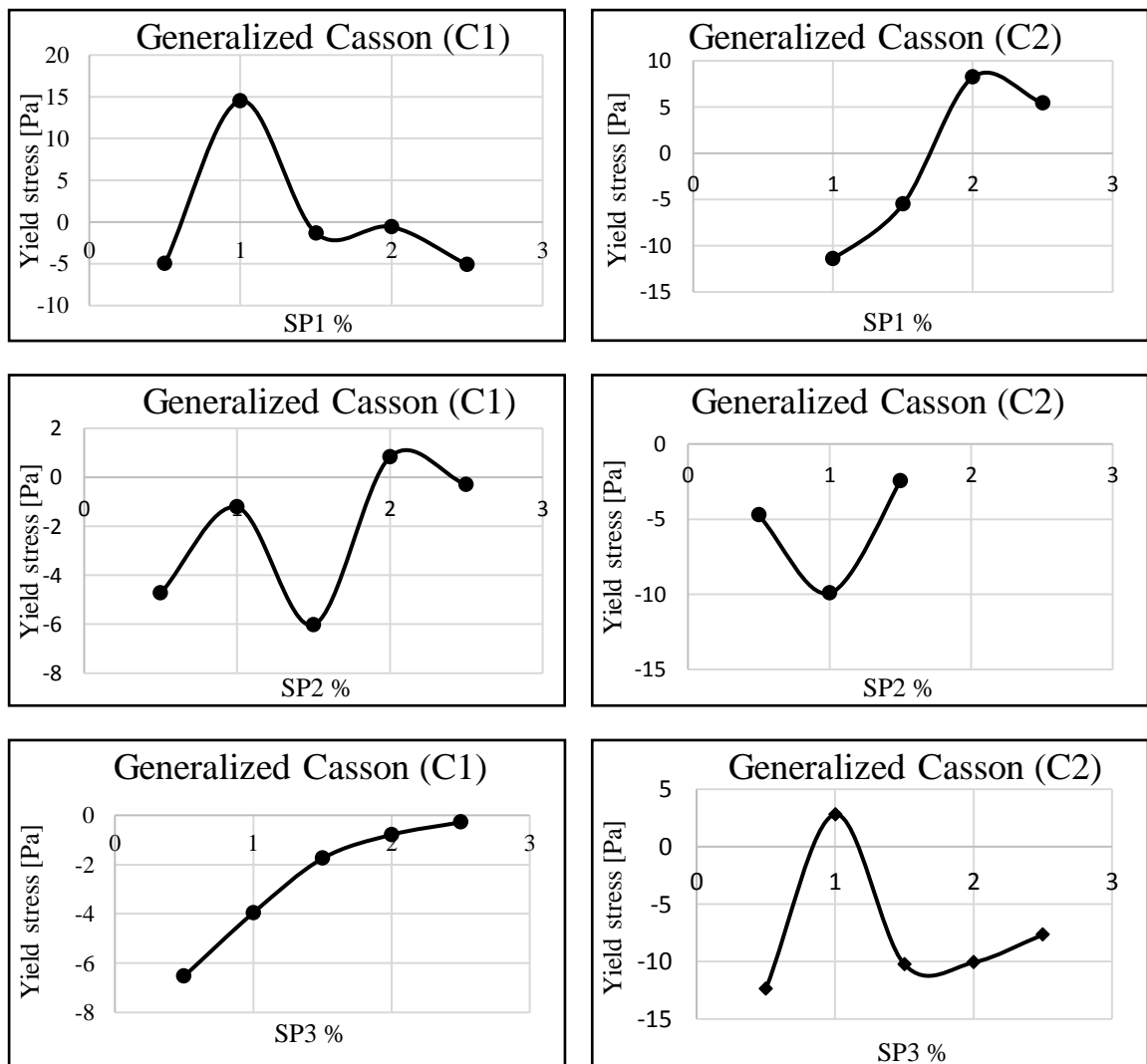


Figure 3. 2: Yield stress histogram of C1 and C2 with a 1.5% dosage of SP1 obtained by rheological model tested.

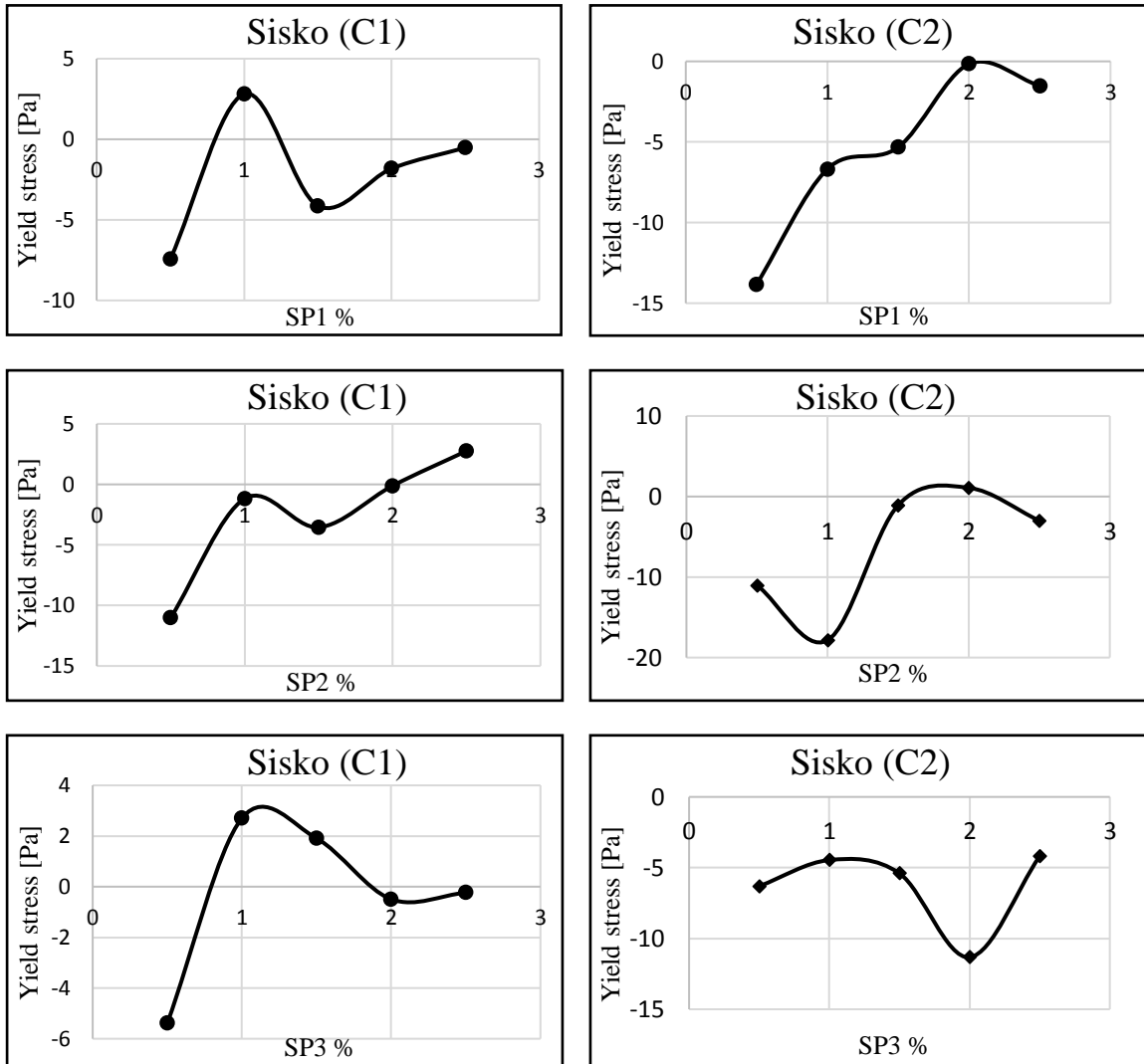
Tables 3.2 and 3.3 show that the models presented significantly uncommon results, while the yield stress is the minimum stress that must be applied for the paste to flow, the Sisko, the modified Bingham, and the Generalized Casson model anticipated negative values of this parameter, which is contradictory to its physical meaning.

The obtained results allowed us to present graphically the yield stress as a function of the superplasticizer dosage, which as can be shown, the curves cannot provide a significant insight or meaningful conclusion making them unreliable and unfit for use in our study.

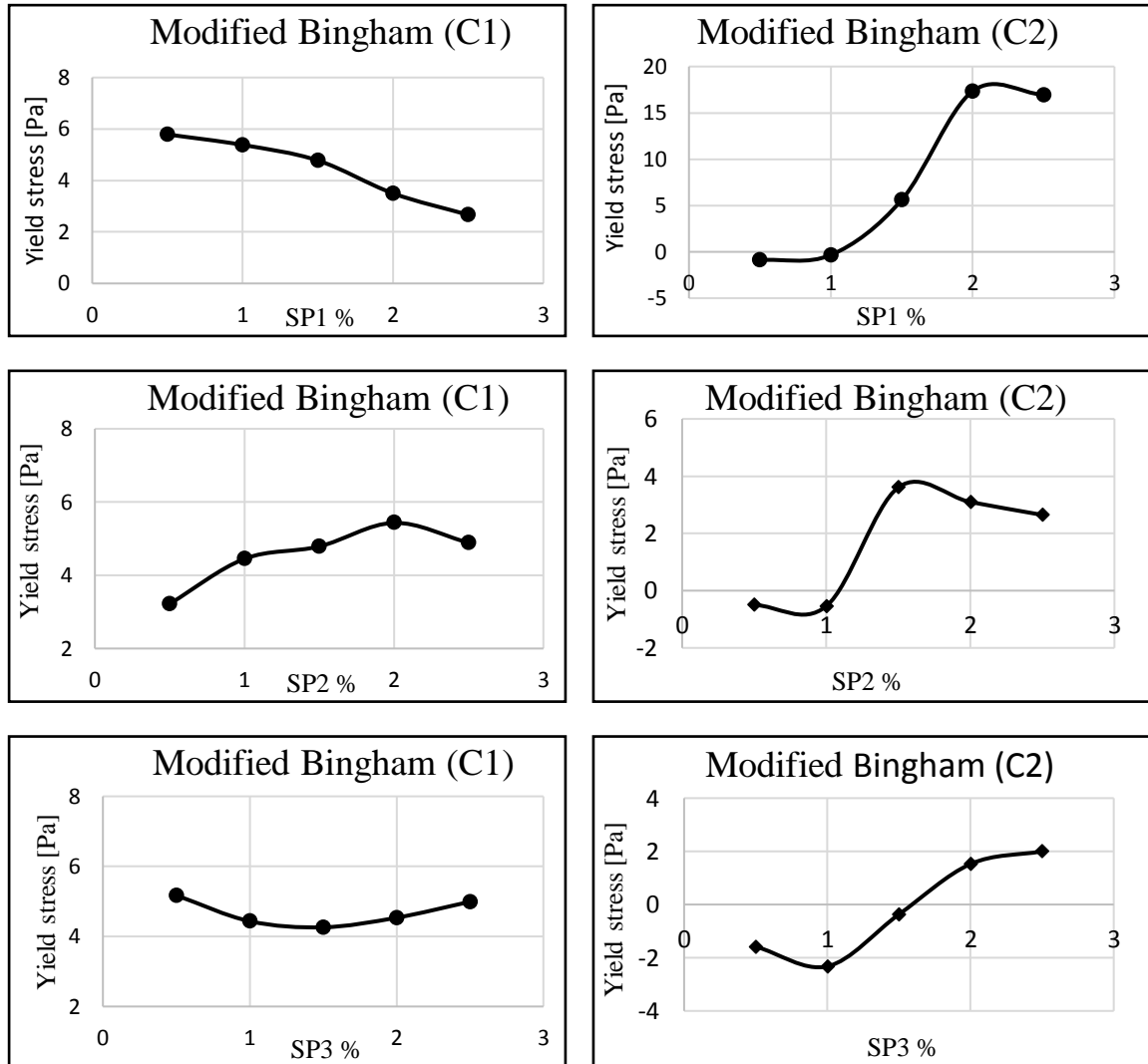
Figure 3.3 displays the distinct curves representing the resulting yield stress from the models for both cement pastes incorporating various superplasticizers.



(a)



(b)



(c)

Figure 3. 3: Yield Stress Curves for C1 and C2 with Different Superplasticizers:(a) Generalized Casson, (b)Sisko, (c)Modified Bingham.

The Herschel-Bulkley was the only model that well explained the behaviour of our cement pastes and revealed remarkable results, not only were they the exclusive positive results, but also as it will be presented in Figure 3.4, the model well reflected the presence of superplasticizers on our cement paste 1, where the values of yield stress decrease with the increase of the SP dosage.

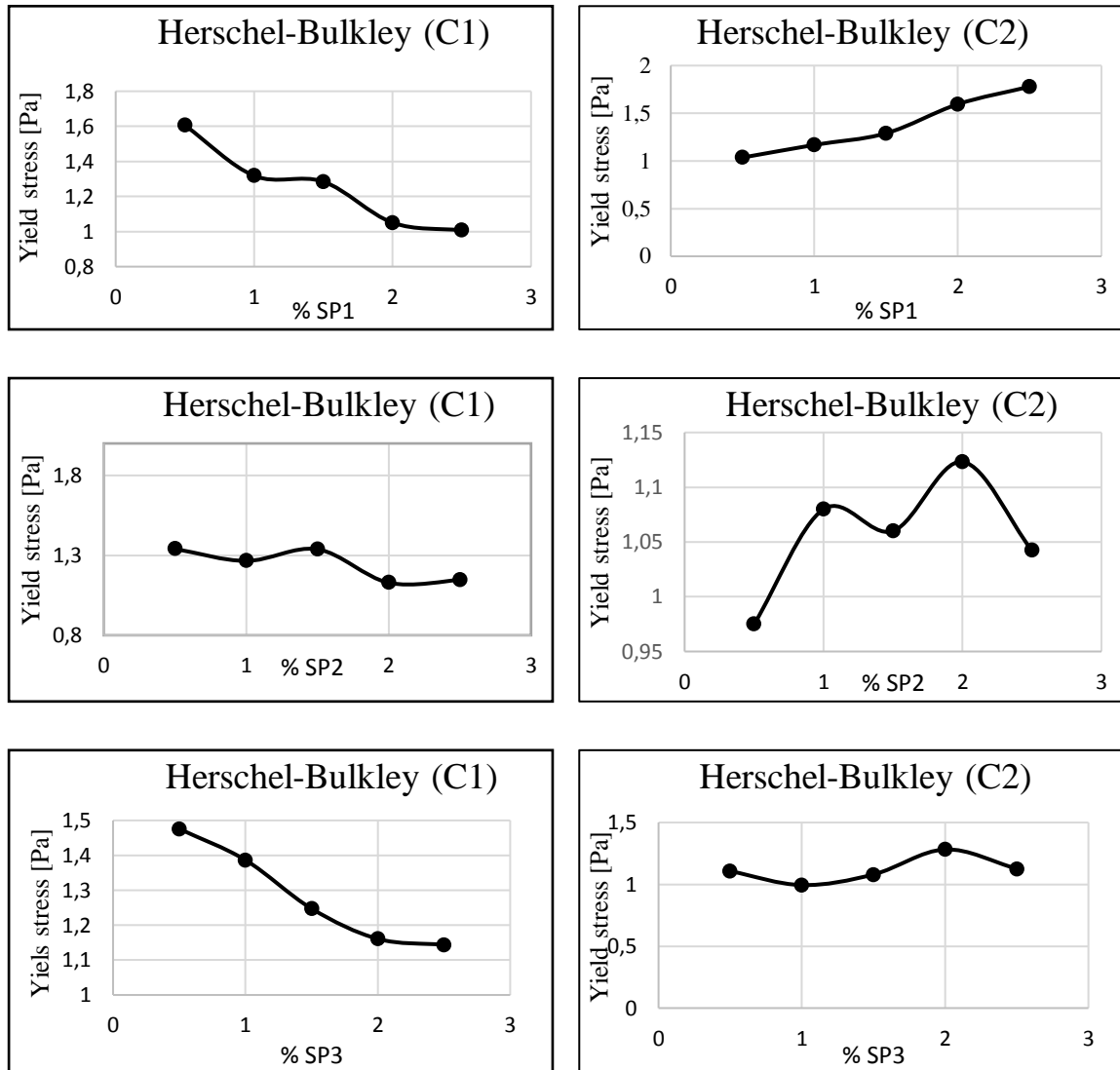


Figure 3. 4: Herschel-Bulkley yield Stress Curves for C1 and C2 with Different Superplasticizers.

3 The chosen model

As was shown in the results, the Herschel Bulkley model was the only model that well represented the behaviour of cement pastes and the only model that satisfied the criteria mentioned earlier.

Similar results were observed in a study of the combination of superplasticizers with hydroxypropyl guar, effect on cement-paste properties[62] where they selected the Herschel-Bulkley model as the model that accurately describes the behaviour of cement pastes, where the results show a non-linear reduction of yield stress values by adding PCE (Polycarboxylate Ether Superplasticizers) into the cement pastes.

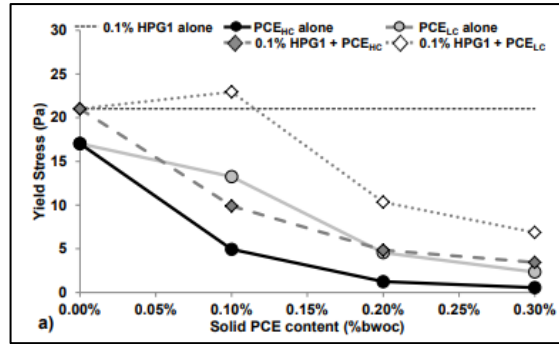


Figure 3. 5: Yield stress as a function of solid PCE content [62].

Figure 3.6 shows another study that captured the same behaviour of the Herschel-Bulkley model on cement pastes[63].

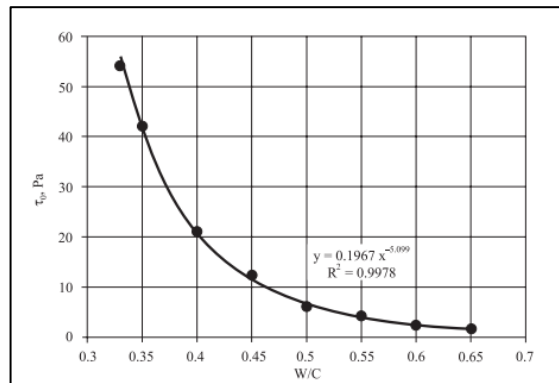


Figure 3. 6: Yield stress as a function of W/C [63].

Moreover, another study displayed parallel characteristics for the remaining two parameters of the models (the consistency index and the flow index, which will be elaborated on later) that aligns perfectly with our results.

After careful consideration and analysis of the results delivered by the models, we conclude that the Herschel-Bulkley model showed its fitting compacity to our experimental data and its effectiveness to well describe and determining the rheological behaviour of our cement pastes.

By satisfying all the measurements mentioned previously, we carried out our study using the Herschel-Bulkley model with the aim of gaining a more nuanced understanding of the behaviour exhibited by our cement pastes.

Figures 3.7, 3.8, 3.9 show the evolution of shear stress as a function shear rate of both cement pastes with the predicted values from applying the Herschel-Bulkley model.

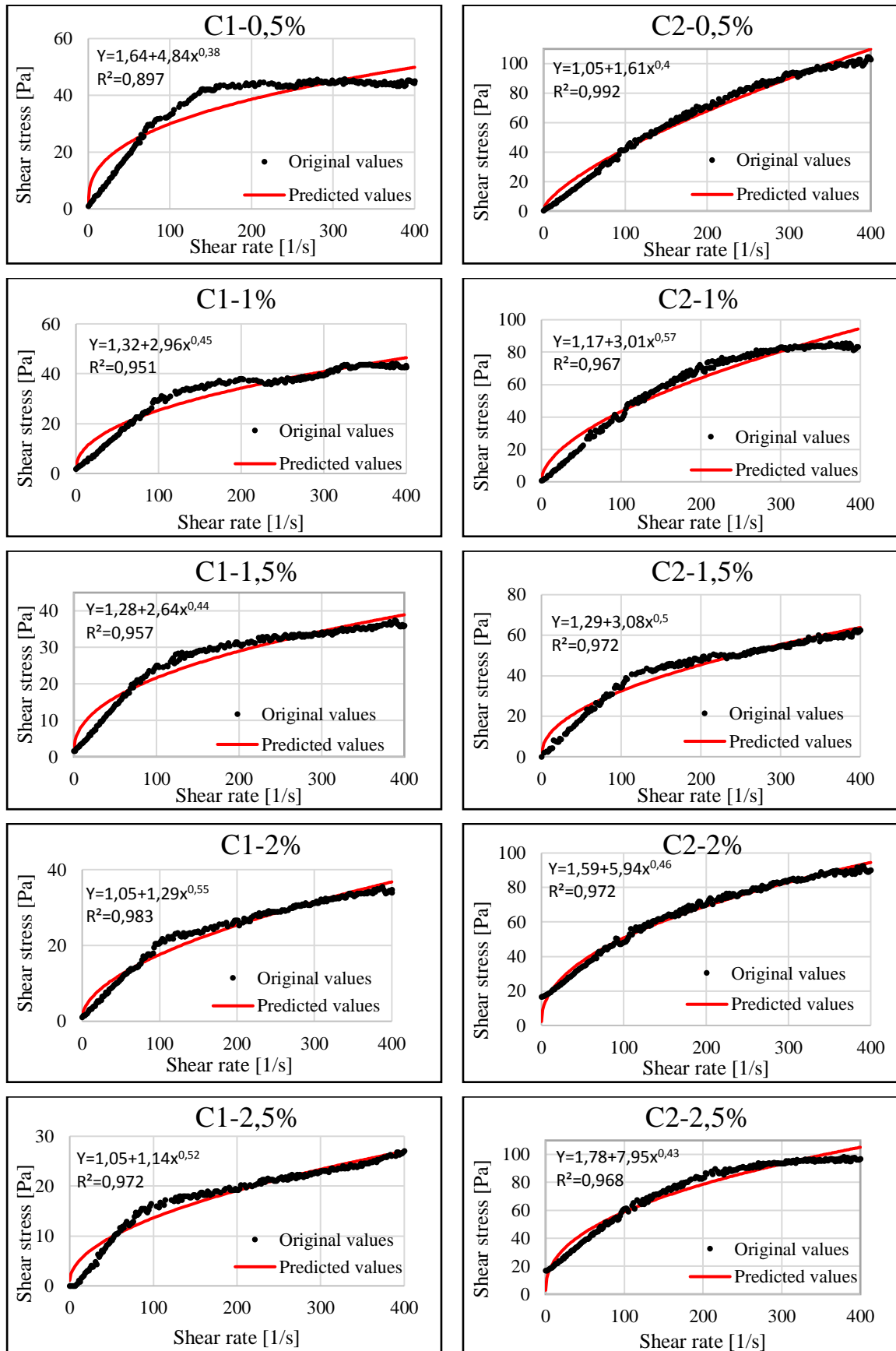


Figure 3. 7: Experimental and predicted Herschel-Bulkley curves for C1 C2 SP1.

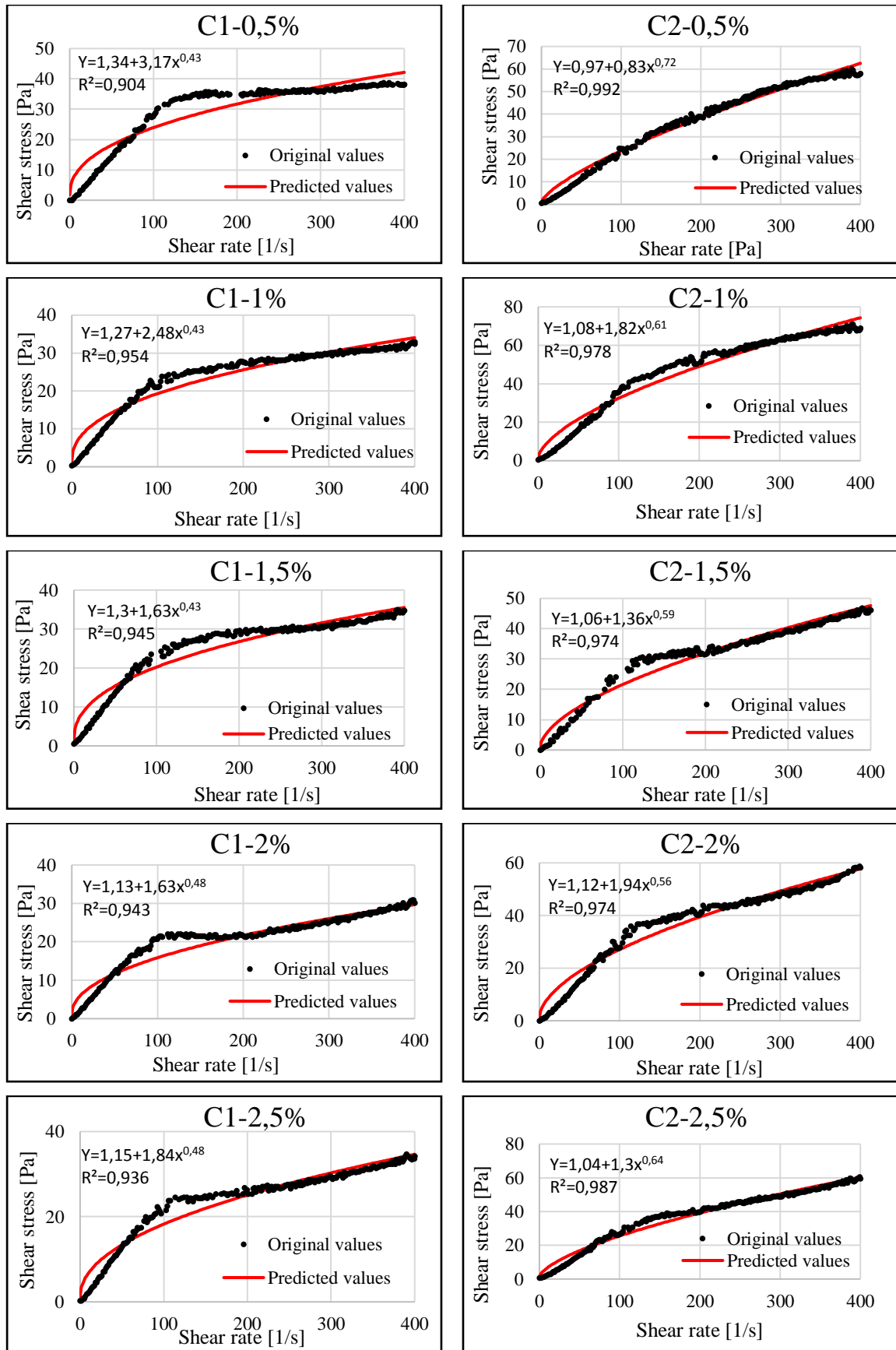


Figure 3. 8: Experimental and predicted Herschel-Bulkley curves for C1 C2 SP2.

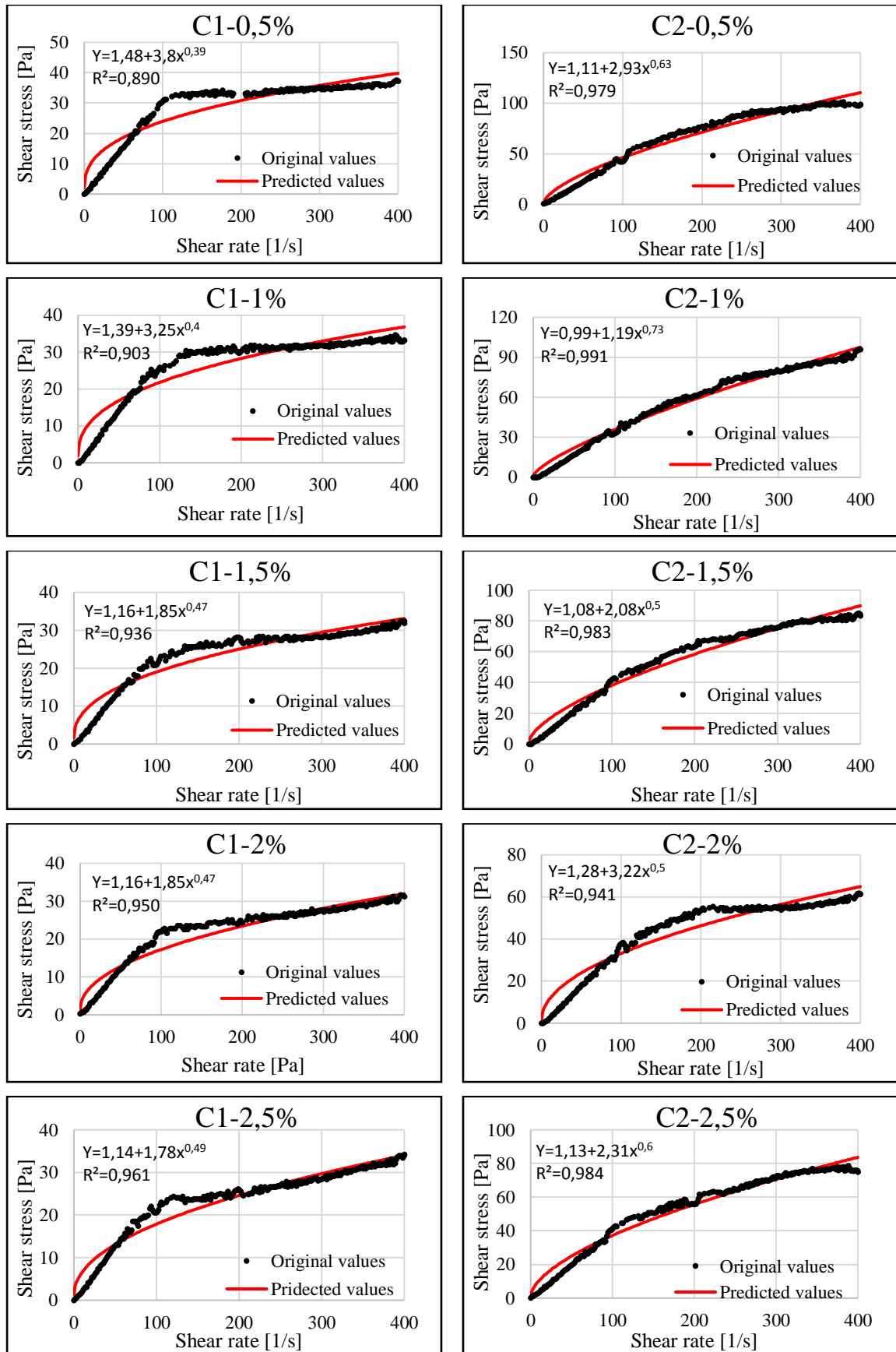


Figure 3. 9: Experimental and predicted Herschel-Bulkley curves for C1 C2 SP3.

4 The model parameters

The model parameters were identified by optimization using the non-linear least square method, which consists in minimizing, for a given shear rate, the SSR (sum square residual) between the observed value of the stress and that is calculated by the model.

Table 3.4 and 3.5 summarizes the results of the Herschel-Bulkley parameters obtained for both cement pastes 1 (C1) and cement paste 2 (C2) with different dosage of the three types of superplasticizers (SP).

Table 3. 4: Herschel-Bulkley parameters results obtained for C1 with different dosages of the three types of superplasticizers.

Herschel-Bulkley Model $\tau = \tau_0 + k\dot{\gamma}^n$		Cement paste 1		
		τ_0	k	n
SP1	0.5%	1.64	4.84	0.38
	1%	1.32	2.96	0.45
	1.5%	1.28	2.64	0.44
	2%	1.05	1.29	0.55
	2.5%	1.01	1.14	0.52
SP2	0.5%	1.34	3.17	0.43
	1%	1.27	2.48	0.43
	1.5%	1.3	2.66	0.43
	2%	1.13	1.63	0.48
	2.5%	1.15	1.84	0.48
SP3	0.5%	1.48	3.80	0.39
	1%	1.39	3.25	0.40
	1.5%	1.25	2.54	0.42
	2%	1.16	1.85	0.47
	2.5%	1.14	1.78	0.49

Table 3. 5: Herschel-Bulkley parameters results obtained for C2 with different dosage of the three types of superplasticizers.

Herschel-Bulkley Model $\tau = \tau_0 + k\dot{\gamma}^n$		Cement paste 2		
		τ_0	k	n
SP1	0.5%	1,04	1,61	0,7
	1%	1,17	3,01	0,57
	1.5%	1,29	3,08	0,5
	2%	1,59	5,94	0,46
	2.5%	1,78	7,95	0,43
SP2	0.5%	0,97	0,83	0,72
	1%	1,08	1,89	0,61
	1.5%	1,06	1,36	0,59
	2%	1,12	1,94	0,56
	2.5%	1,04	1,3	0,64
SP3	0.5%	1,11	2,39	0,63
	1%	0,99	1,19	0,73
	1.5%	1,08	2,04	0,63
	2%	1,28	3,22	0,5
	2.5%	1,13	2,31	0,6

The data presented in Table 3.4 demonstrates that an increase in the dosage of various superplasticisers results in a reduction in the yield stress of cement paste 1 which shows the dispersing effect of SPs on the cement paste. In other words, the addition of SP helped promote the flow of the cement paste.

These results match the results found by Berra et al [64], where in their study they observed reduction of the yield stress caused by the increase of superplasticizer dosages, which highlights the contribution of sp additives in the rheological properties of cement pastes.

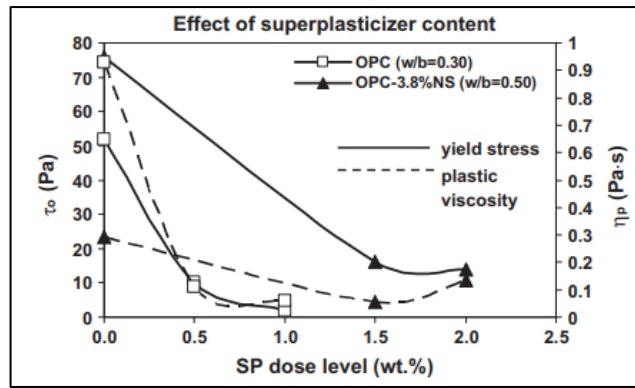
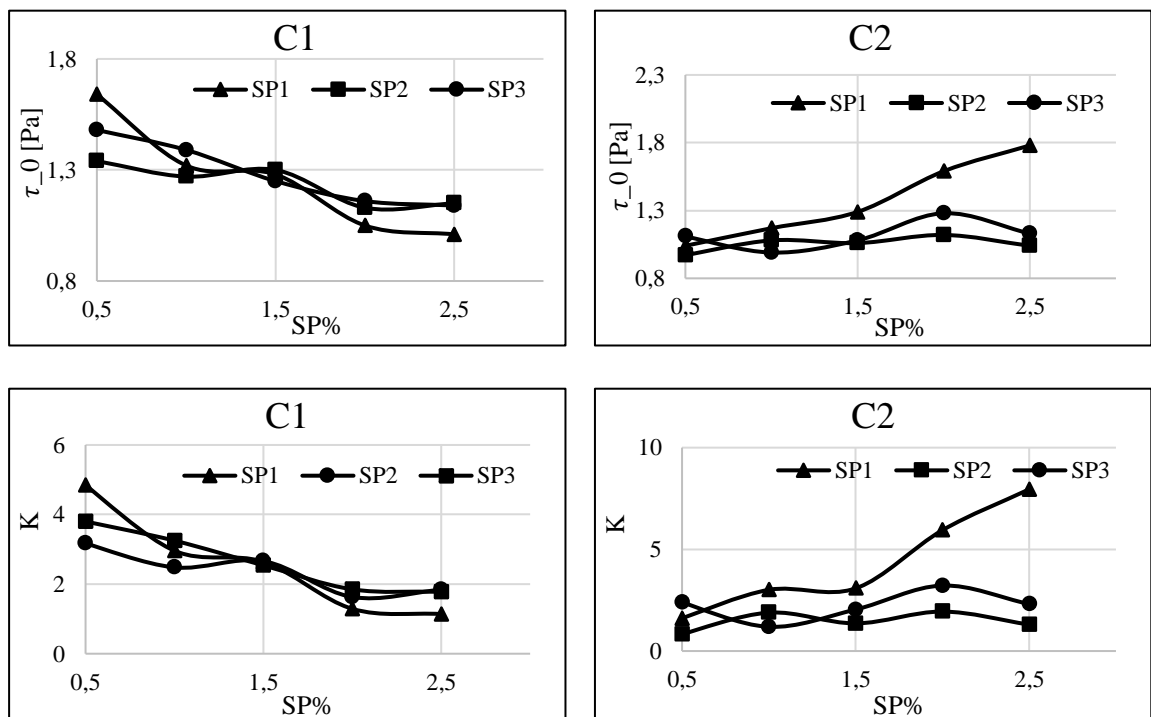


Figure 3. 10: Yield stress as a function of SP dose level [64].

The flow index “n” signifies the fluid’s flow behaviour, as presented in the table, the parameter exhibits values below 1 across all instances ($0.38 < n < 0.73$). Furthermore, followed by the viscosity findings discussed in the preceding chapter, where it was evident in the curves that the viscosity decreased with increasing shear, in this case, it can be concluded that the fluid is pseudoplastic with shear-thinning characteristics[65]. The shear stress and shear rate curves provide further evidence of this behaviour.

Figures 3.11 illustrate the rheological parameters variation due to the superplasticizer dosage for the Herschel-Bulkley model.



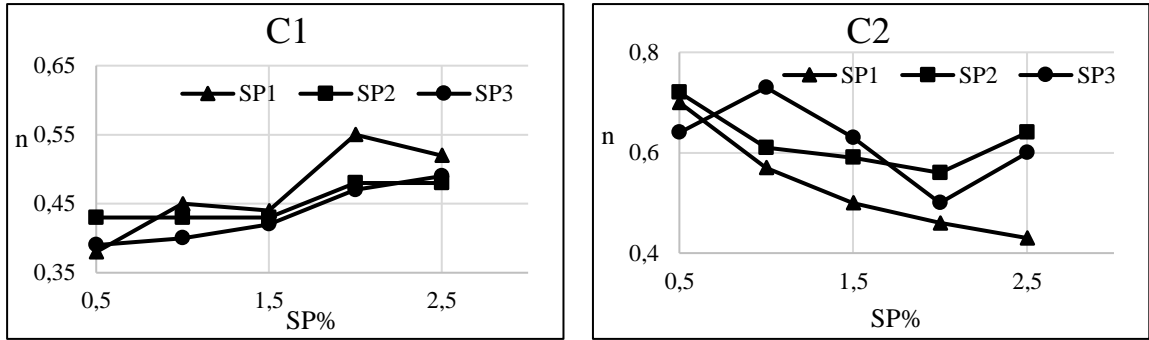


Figure 3. 11: Curves of Herschel-Bulkley model rheological parameters of C1 and C2 with the superplasticizer dosage.

4.1 The yield stress " τ_0 "

The yield stress values obtained using the Herschel-Buckley model on cement pastes with different dosages of different types of superplasticizer appear to be well-described by an exponential function, which is expressed as:

$$\tau_0 = a + \exp^{-b*x} \tag{3.1}$$

Where a and b are the parameters of the model.

Table 3.6 encapsulates the obtained results

Table 3. 6: The parameters of the suggested model for the yield stress.

$\tau_0 = a + \exp^{-b*x}$		a	b	R ²	s
C1	SP1	0.93	0.86	0.97	0.06
	SP2	1.12	2.31	0.85	0.12
	SP3	0.92	0.77	0.95	0.07
C2	SP1	1.4	50.13	0.74	0.3
	SP2	1.14	43.44	0.88	0.23
	SP3	1.16	43.84	0.87	0.21

After analysing the data presented in Table 3.6, and drawing upon the evidence, the model showed higher performance when it comes to C1, the correlation between the analysed parameters expressed by the coefficient of determination R² was stronger in C1 than C2, (between 0,85 and 0,97 for C1, and 0,74 and 0,88 for C2).

The relationship between dosage and yield stress is graphically represented in Figure 3.12.

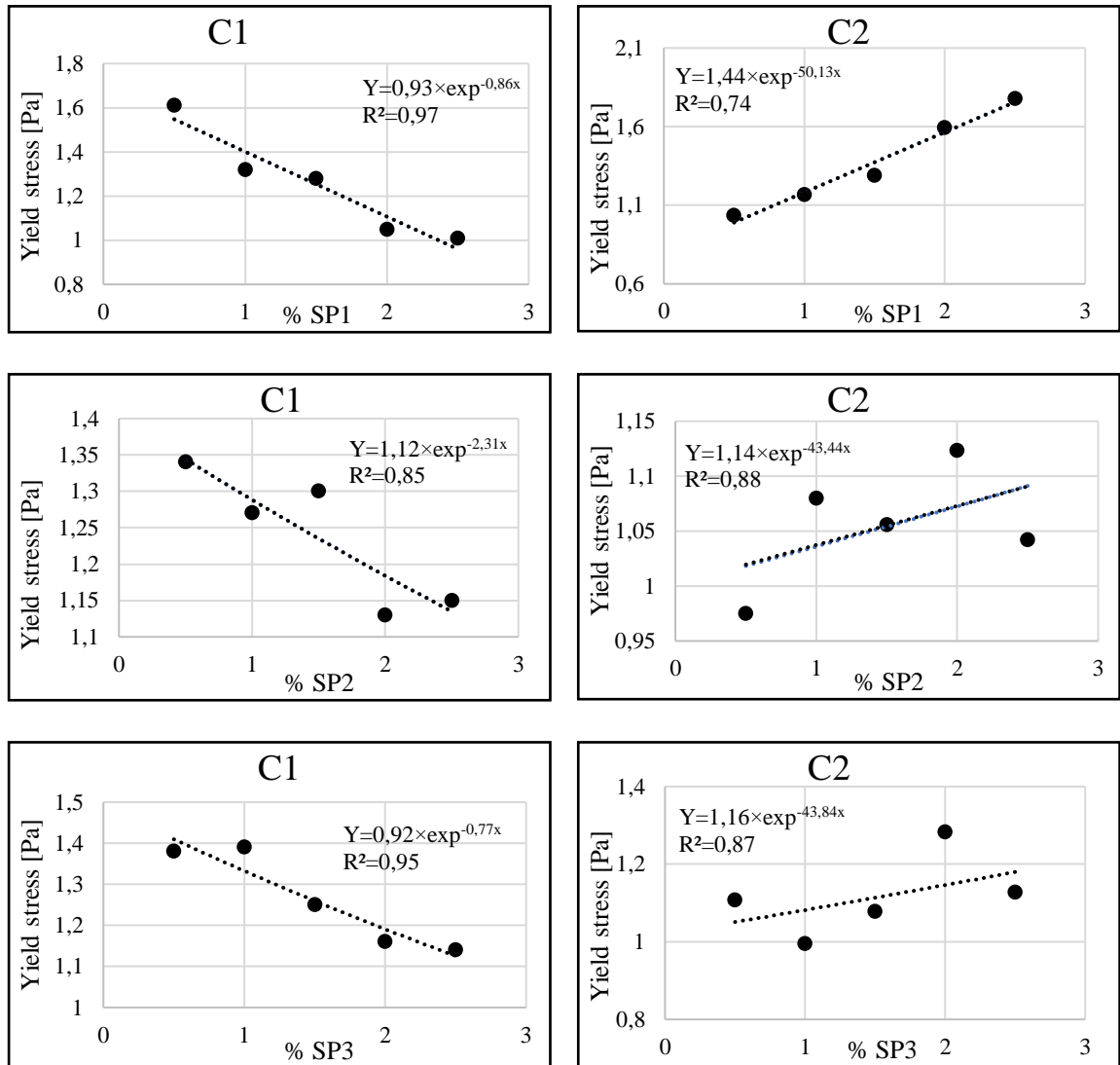


Figure 3. 12: Yield stress in relation to the SP dosages.

As we can observe, the two cement pastes' yield stress exhibited dissimilar patterns. While the parameter decreases in C1, with all the three SPs, in C2 it didn't follow the same behaviour, where the results didn't offer a substantial significance.

This can be attributed to the differential impact of the superplasticizer on the two types of cement pastes. The effect of the superplasticizer on each cement paste was distinct.

4.2 The consistency index “k”

When it comes to cement paste 1, the consistency index also exhibited similar behaviour to the yield stress, where as it is shown in Figure 13, the consistency index tends to non-linearly decrease with the raise of superplasticizers dosages.

As stated by the authors, the consistency index k describes the viscosity of cement paste, which as we mentioned earlier, is experiencing a reduction[63] which reflects perfectly the superplasticizers function.

Nevertheless, we cannot make the same statement for cement paste 2, since it did not display the same response. While cement paste 2 consistency increased by increasing the SP1 dosage, the other two remaining superplasticisers couldn't provide the same assessment, which made it impossible to be modelled and represented by a specific equation.

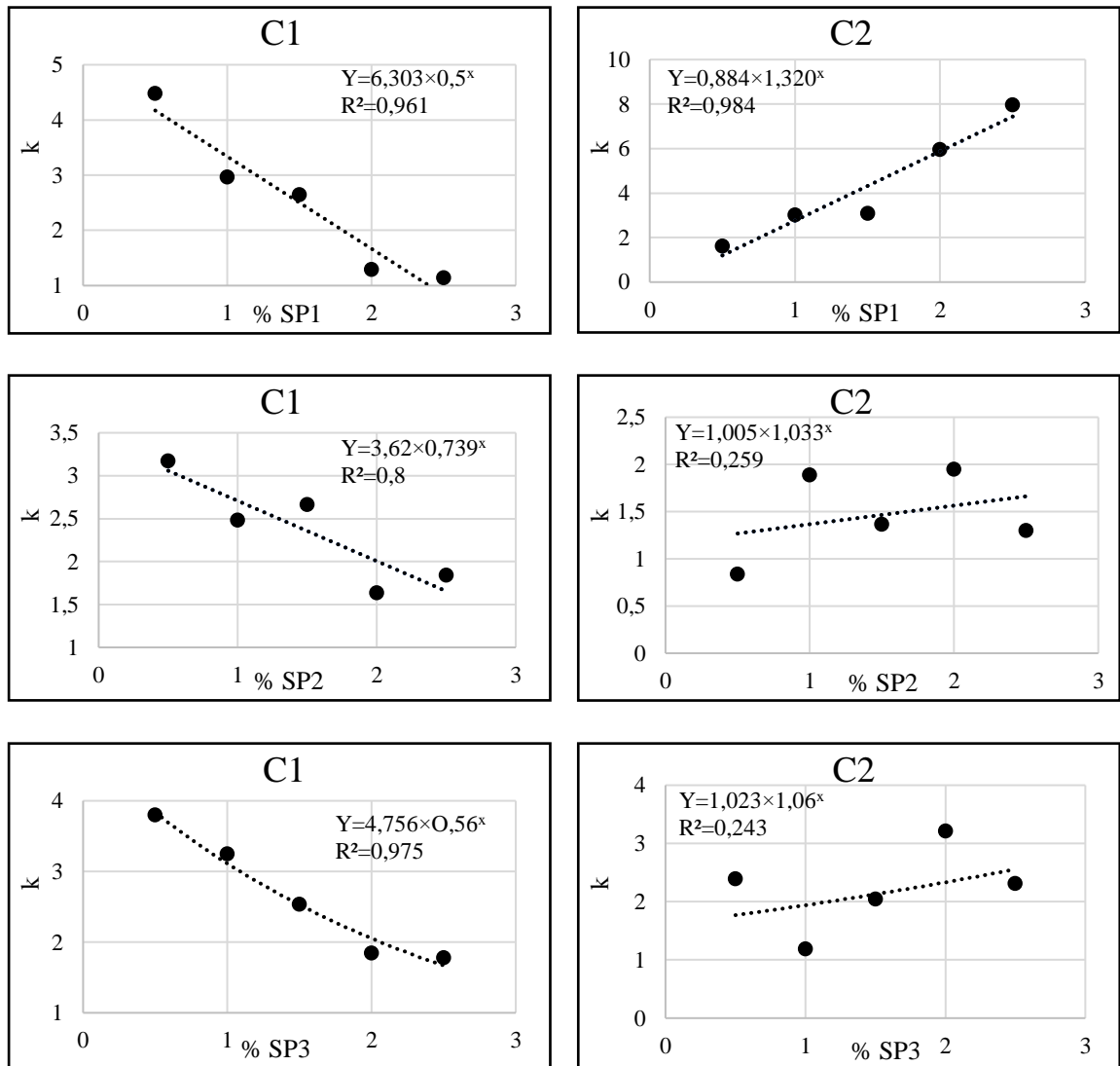


Figure 3. 13: The Consistency Index k with 3 Superplasticizer Dosage for C1 and C2.

We were able to establish a model for the consistency index of the first cement paste, however, this same model failed to represent cement paste 2.

The correlation between the analysed parameters is represented in Table 3.7 and Table 3.8. The model is expressed as follows:

$$k = c \cdot d^x \tag{3.2}$$

Where c and d are the parameters of the model

Table 3. 7: The parameters of the model suggested for the consistency index.

$k = c \cdot d^x$		c	d	R ²	s
C1	SP1	6.302	0.50	0.961	0.31
	SP2	3.62	0.739	0.8	0.32
	SP3	4.756	0.56	0.975	0.156

$k = c \cdot d^x$		c	d	R ²	s
C2	SP1	0.884	1.320	0.984	0.043
	SP2	1.005	1.033	0.259	0.054
	SP3	1.023	1.060	0.243	0.115

As we can see, the model suggested for the consistency index failed to fit cement paste 2, the coefficient of determination for both SP 2 and SP3 were below 0,3.

4.3 The flow index “n”

In the Herschel-Bulkley model, the flow index is a parameter that characterizes the degree of shear-thinning behaviour of the fluid, as mentioned earlier, we were able to capture that behaviour from the results represented by the model.

The variation of the flow index “n” with the dosage of the 3 different SPs for both cement pastes is illustrated in Figure 3.14.

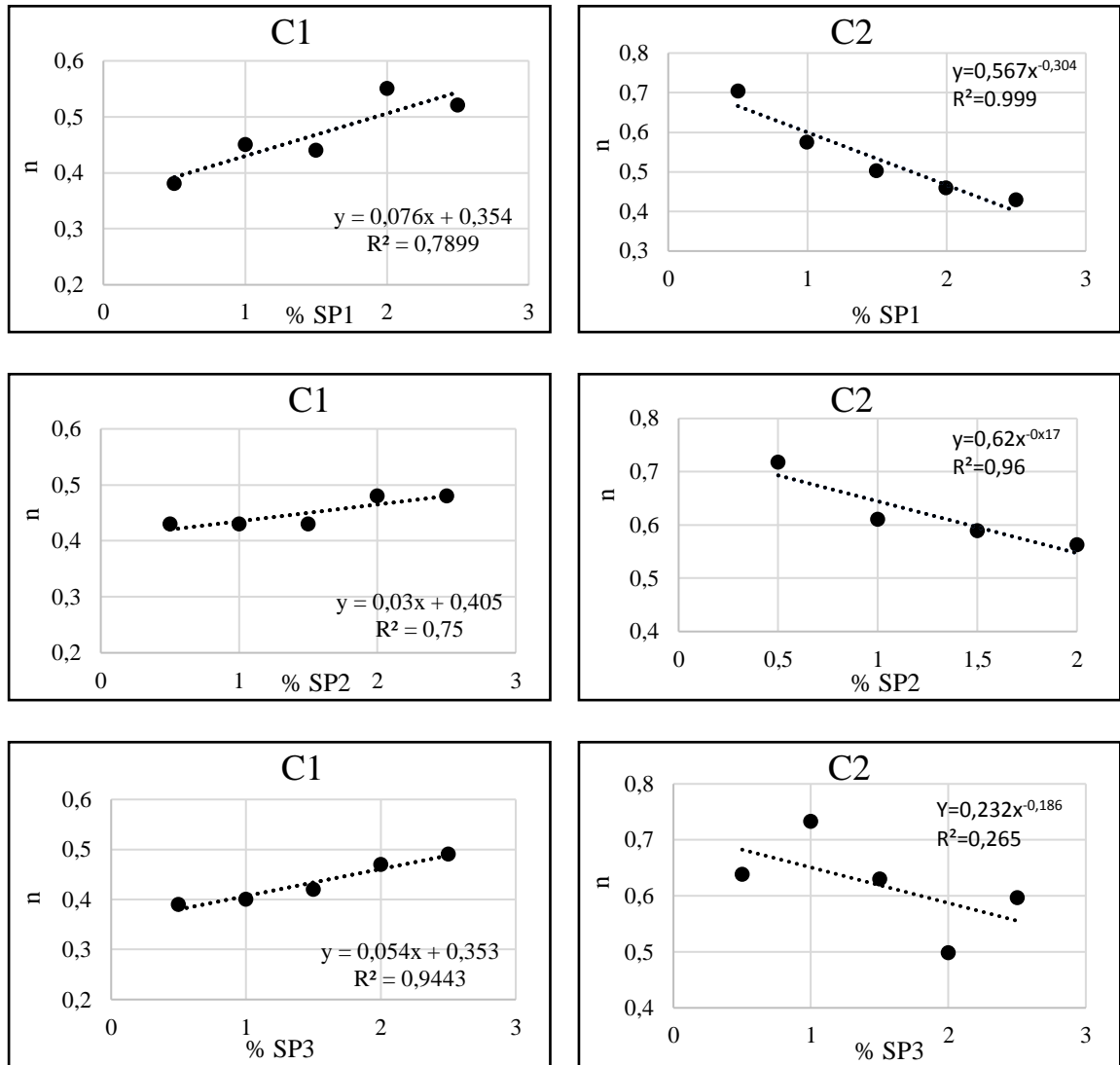


Figure 3. 14: Flow Index “n” Variation with 3 Superplasticizer Dosage in C1 and C2.

The significant discrepancy between the two cement pastes was also present and observed in the results of the flow index.

The C1 curves showed a linear progression, which can be explained by a linear equation, and that was not the case for C2.

As for C2, we can observe a similarity between the curves of cement paste that contains SP1 and SP2, where the flow index presented a non-linear decrease, contrary to the third curve that did not follow the same pattern (C2 with SP3).

This may indicate the fact that both SP1 and SP2 affected the cement paste in the same way.

To model the flow index parameter, two models represented by two equations were suggested.

Table 3. 8: The parameters of the model suggested for the flow index (C1).

$n = e.x + f$		e	f	R ²	S
C1	SP1	0.063	0.3781	0.781	0.074
	SP2	0.031	0.402	0.850	0.157
	SP3	0.054	0.353	0.9443	0.037

Table 3. 9: The parameters of the model suggested for the flow index (C2).

$n = e.x^{-f}$		e	f	R ²	s
C2	SP1	0.567	0.304	0.999	0.001
	SP2	0.62	0.17	0.96	0.014
	SP3	0.232	0.186	0.265	0.083

For C1, despite the linear shape of the curve and the suggestion of a linear equation to describe the parameter, the fitted model did not yield a high coefficient of determination (except for SP3).

In a study investigating the consistency of cement pastes and their rheological parameters, a similar approach was adopted. The curve representing the flow index exhibited a linear behaviour, resembling our findings. However, the model suggested by that study did not adequately account for the correlation between the flow index (n) and the water-to-cement ratio (W/C)[63].

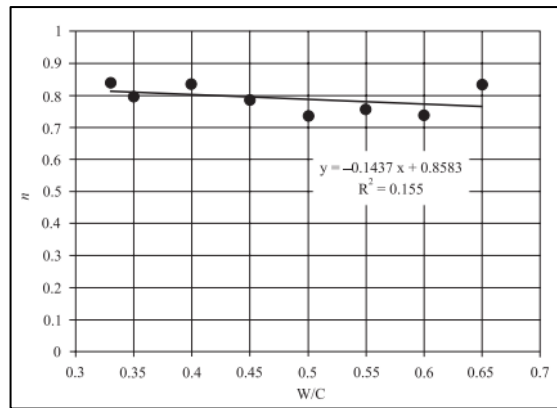


Figure 3. 15: Flow index as a function of W/C [63].

As for C2, the fitted model showed remarkable performance on cement paste with both SP1 and SP2, with a correlation expressed by a strong coefficient of determination ($0,96 < R^2 < 0,99$).

However, the model's effectiveness was not as pronounced for SP3 as it was for the first two superplasticizers, as shown by the coefficient of determination ($R^2 = 0,265$).

Conclusion

After analysing all the parameters, and fitting the different models to the obtained results, considering the outcomes, the conclusion can be inferred that the superplasticizers affected both cement pastes differently.

The incorporation of different superplasticizers led to the desired outcomes when it comes to C1 (CEMI 42.5), which was reflected by decreasing in the yield stress, the viscosity..., affirming their effectiveness in maintaining adequate levels of flowability of the cement paste.

However, that was not the case for C2 (CEMII A 42.5), where the results obtained were incongruous and deviated markedly from the initial findings, additionally, the extracted outcomes lacked significance and did not contribute to a comprehensible or meaningful understanding.

This urged us to conduct further research and investigation on the effect of superplasticizers on different types of cement, to grasp the essential factor governing the observed behaviour.

The fundamental dissimilarity between C1 and C2 is attributed to the higher concentration of C_3A in C2 (as mentioned in Chapter 2), while C_3A is the most reactive component in types of cement, a conducted investigation revealed that the chemical properties of cement have the ability to alter the overall statement regarding the reactivity of superplasticizers, where it was shown that all SPs delivered different findings in connection with the C_3A content[66].

According to a different research endeavour, while the dosage of superplasticizer increased, a positive impact on the rheological parameters of the mixture was observed, particularly at a low C_3A ratio, however an increase in C_3A content was found to have a deleterious effect on the rheological parameters of cement paste[67].

Conclusion

In conclusion, this Master's thesis focused on modelling the rheological behaviour of two types of cement pastes, CEM I and CEM II A, with three different types and dosages of superplasticizers ranging from 0.5% to 2.5%. The objective was to compare various rheological models including the generalized Casson; Bingham modified, Sisko, and Herschel-Bulkley models, and determine the most suitable model for accurately representing the rheological behaviour of the cement pastes with different superplasticizers.

Through a comprehensive series of experiments and data collection, data was generated on the rheological behaviour of cement pastes under different dosage of SP. These data were then used to calibrate and validate the rheological models mentioned above.

The results indicated that the Herschel-Bulkley model consistently provided a better fit to the experimental data compared to the other models. It effectively captured the behaviour, yield stress, flow and consistency index of the CEM I and CEM II A cement pastes with varying types and dosages of superplasticizers. The Herschel-Bulkley model demonstrated its robustness and accuracy in representing the complex rheological behaviour exhibited by these cement pastes.

In contrast, the generalized Casson, Bingham modified, and Sisko models showed limitations in accurately capturing the flow properties and yield stress of the cement pastes. These models could not adequately account for the non-Newtonian behaviour exhibited by the cement pastes, leading to poorer fits to the experimental data. The generalized Casson model, although widely used for non-Newtonian fluids, did not provide a satisfactory representation of the rheological behaviour of the cement pastes, it failed to capture the rheological nature of the pastes, where the viscosity decreases with increasing shear rate. This model assumes a constant viscosity, which is not suitable for describing the complex flow properties of cement pastes with varying superplasticizer dosages. Similarly, the Bingham modified model, it failed to accurately represent the non-linear relationship between stress and strain rate, resulting in deviations from the experimental data. Also, Sisko model, it's more complex rheological model that fell short in accurately describing the flow properties of the cement pastes.

The findings of this thesis highlight the importance of selecting an appropriate rheological model for accurately characterizing the rheological behaviour of cement pastes with different types and dosages of superplasticizers. The Herschel-Bulkley model emerged as the most

suitable choice for this particular study, providing reliable predictions and capturing the essential flow characteristics of the cement pastes.

Overall, this Master's thesis successfully demonstrated the superiority of the Herschel-Bulkley model in modelling the rheological behaviour of CEM I and CEM II A cement pastes with varying types and dosages of superplasticizers. The insights gained from this research contribute to the understanding of the flow properties of these cement pastes and provide valuable guidance for optimizing the selection and dosage of superplasticizers in cement-based materials. Moreover, this research emphasizes the significance of both the rheological model selection and the consideration of cement composition, particularly the percentage of C3A, when studying and modelling the rheological behaviour of cement pastes. The outcomes of this thesis provide a foundation for further studies and practical applications in the field of cement science and engineering, facilitating the development of improved cementitious materials with enhanced rheological properties and performance. This comprehensive approach integrating rheological modelling, superplasticizer optimization, and understanding of cement composition paves the way for advancements in cement science and engineering, enabling the development of innovative cement-based materials for a wide range of applications.

References List

- [1] G. . Bates, *Cement, a Century of Progress*. New York, NY: American, 1963.
- [2] A. Aspнас and T. Kallio, *Low-Carbon Transition in the Cement Industry : Technological and Political Trends and Challenges*. 2018.
- [3] O. Labahn and B. Kohlhaas, *Cement Engineers Handbook*. 1954.
- [4] J. W. Phair, “Green chemistry for sustainable cement production and use,” *Green Chem.*, vol. 8, no. 9, pp. 763–780, 2006, doi: 10.1039/b603997a.
- [5] M. S. Imbabi, C. Carrigan, and S. McKenna, “Trends and developments in green cement and concrete technology,” *Int. J. Sustain. Built Environ.*, vol. 1, no. 2, pp. 194–216, 2012, doi: 10.1016/j.ijjsbe.2013.05.001.
- [6] W. Kurdowski, *Cement and Concrete Chemistry*. 2013.
- [7] I. Soroka, *Portland Cement Paste and Concrete*. 1979. doi: 10.1007/978-1-349-03994-4.
- [8] G. Bye, *Portland Cement, Third edition*. 2011. doi: 10.1680/pc.36116.
- [9] F. Winnefeld, S. Becker, J. Pakusch, and T. Götz, “Effects of the molecular architecture of comb-shaped superplasticizers on their performance in cementitious systems,” *Cem. Concr. Compos.*, vol. 29, no. 4, pp. 251–262, 2007, doi: 10.1016/j.cemconcomp.2006.12.006.
- [10] C. Z. Li, N. Q. Feng, Y. De Li, and R. J. Chen, “Effects of polyethylene oxide chains on the performance of polycarboxylate-type water-reducers,” *Cem. Concr. Res.*, vol. 35, no. 5, pp. 867–873, 2005, doi: 10.1016/j.cemconres.2004.04.031.
- [11] C. Autier, “Etude de l ’ adjuvantation de pâtes cimentaires par différents polycarboxylates : la mésostructure : un lien entre interactions organo-minérales et propriétés macroscopiques.,” 2014.
- [12] F. LEA, *The Chemistry of Cement and Concrete*, Third Eddi. Edward Arnold, 1970.
- [13] A. M. Ley-hernandez, “Scholars ’ Mine Complexities observed during the development of a rheological testing procedure for small cement paste samples,” 2020.
- [14] B. Lu *et al.*, “A systematical review of 3D printable cementitious materials,” *Constr. Build. Mater.*, vol. 207, pp. 477–490, 2019, doi:

10.1016/j.conbuildmat.2019.02.144.

- [15] G. Ma and L. Wang, “A critical review of preparation design and workability measurement of concrete material for largescale 3D printing,” *Front. Struct. Civ. Eng.*, vol. 12, no. 3, pp. 382–400, 2018, doi: 10.1007/s11709-017-0430-x.
- [16] L. Ferrari, J. Kaufmann, F. Winnefeld, and J. Plank, “Interaction of cement model systems with superplasticizers investigated by atomic force microscopy, zeta potential, and adsorption measurements,” *J. Colloid Interface Sci.*, vol. 347, no. 1, pp. 15–24, 2010, doi: 10.1016/j.jcis.2010.03.005.
- [17] ACI Committee 212, “ACI PRC-212.3-16 Report on Chemical Admixtures for Concrete,” 2016.
- [18] I. Berkovitch, “Admixtures for Concrete.,” *Civ. Eng. London*, pp. 29–31, 1984, doi: 10.14359/8677.
- [19] Mamlouk, M. S. Zaniewski, and J. P., *Materials for Civil and Construction Engineers Fourth Edition In si units*. 2018.
- [20] T. Sekiguchi, Y. Okada, and T. Ulugai, “Relative effects of Ca-polystyrene sulfonate and Na-sulfonated-based superplasticizers on properties of flowing concrete,” *ACI Mater. J.*, pp. 157–170, 1989.
- [21] J.Zakka, Z.Carrasquillo, and D.L.Fabriarz., “Variables affecting the plastic and hardened properties of superplasticized concrete,” in *Internation Conference on Superplasticizers and Other Chemical Admixtures*, 1989, pp. 180–197.
- [22] M. Ben Aicha, *The superplasticizer effect on the rheological and mechanical properties of self-compacting concrete*. INC, 2020. doi: 10.1016/B978-0-12-818961-0.00008-9.
- [23] F. Huang, H. Li, Z. Yi, Z. Wang, and Y. Xie, “The rheological properties of self-compacting concrete containing superplasticizer and air-entraining agent,” *Constr. Build. Mater.*, vol. 166, pp. 833–838, 2018, doi: 10.1016/j.conbuildmat.2018.01.169.
- [24] M. Benaicha, O. Jalbaud, A. Hafidi Alaoui, and Y. Burtschell, “Marsh cone coupled to a plexiglas horizontal channel: Rheological characterization of cement grout,” *Flow Meas. Instrum.*, vol. 45, pp. 126–134, Oct. 2015, doi:

10.1016/j.flowmeasinst.2015.06.004.

- [25] C. Jianzhong, "Influence of water-reducing agents on rheological characteristics of fresh cement mortar and concrete," *J. SHH. Inst. Build. Mater.*, vol. 3, no. 2, pp. 283–289, 1989.
- [26] M. Benaicha, "Formulation of different concretes (SCC, HPC and UPFC) with a high mineral additions content: optimization to improve pouring, strength to young age and durability of concretes," Aix-Marseille university, 2014.
- [27] V.S. Ramachandran, R. F. Feldman, and J. J. Beaudoin, *Concrete science : treatise on current research*. London: Heyden, 1981.
- [28] S. Kasami, H. Ikeda, and T. Yamana, "Workability and pumpability of superplasticized concrete-experiences in Japan," in *Proceedings of the International Symposium Superplasticizers Concrete*, 1978, pp. 103-132.
- [29] G.Popescu, M.Muntean, B.Horia, I.Stelian, A.Dan-Florin, and A.Bujor, "Effect of superplasticizers on Portland cement mortars and pastes," *Cement*79, pp. 107–114, 1982.
- [30] M.Corradi, R.Khurana, and R.Magarotto, "User friendly self-compacting concrete in precast production," in *3rd International RILEM Symposium on Self-Compacting Concrete*, 2003, pp. 457–466.
- [31] R. J. Flatt and Y. F. Houst, "A simplified view on chemical effects perturbing the action of superplasticizers," *Cem. Concr. Res.*, vol. 31, no. 8, pp. 1169–1176, 2001, doi: 10.1016/S0008-8846(01)00534-8.
- [32] D. J. Qiang Yuan, Caijun Shi, *Rheology of Fresh Cement-Based materials : Fundamentals, Measurements, and Application*. 2022.
- [33] R. Durairaj, *RHEOLOGY - NEW CONCEPTS , APPLICATIONS AND Edited by Rajkumar Durairaj*. 114AD.
- [34] N. Roussel, *Understanding the Rheology of Concrete*. 2012. [Online]. Available: <http://www.sciencedirect.com/science/article/pii/B9780857090287500066>
- [35] J.Vosahlik, "Pumping of Concrete Mixtures: Rheology, Lubrication Layer Properties and Pumping Pressure Assessment," 2018. [Online]. Available:

<http://krex.k-state.edu/dspace/handle/2097/39134>

- [36] B. T. Zengeni, *BINGHAM YIELD STRESS AND BINGHAM PLASTIC VISCOSITY OF HOMOGENEOUS NON-NEWTONIAN SLURRIES* by Brian Tonderai Zengeni Student Number : 210233265 Dissertation submitted in partial fulfilment of the requirements for the degree and which counts towards 50 % of, no. October. 2016.
- [37] A. Poitou and G. Racineux, “A squeezing experiment showing binder migration in concentrated suspensions,” *J. Rheol. (N. Y. N. Y.)*, vol. 45, no. 3, pp. 609–625, 2001, doi: 10.1122/1.1366717.
- [38] K. Aït-mokhtar, “Effet des additions minérales et organiques sur le comportement rhéologique du béton Mhamed Adjoudj To cite this version,” 2016.
- [39] M. Rahman, “Rheology of cement grout – Ultrasound based measurement technique and,” p. 94, 2015.
- [40] A.-L. Vayssade, “2015 Flows of Herschel-Bulkley fluids in confined environments. Applications to the cementing of oil wells,” 2015.
- [41] C. j. Phillips, “Rheological investigation of debris flow materials,” *Researcharchive.Lincoln.Ac.Nz*, p. 227, 1988.
- [42] F. Rizzo, F. Pinto, and M. Meo, “Investigation of Silica-Based Shear Thickening Fluid in Enhancing Composite Impact Resistance,” *Appl. Compos. Mater.*, vol. 27, no. 3, pp. 209–229, 2020, doi: 10.1007/s10443-020-09805-7.
- [43] F. Irgens, *Rheology and Non-Newtonian Fluids*. 2014.
- [44] E. Crépault, “Rhéologie des bétons frais à base de ciment d’aluminat de calcium,” 2012.
- [45] L. Senff, D. Hotza, W. L. Repette, V. M. Ferreira, and J. A. Labrincha, “Rheological characterisation of cement pastes with nanosilica, silica fume and superplasticiser additions,” *Adv. Appl. Ceram.*, vol. 109, no. 4, pp. 213–218, 2010, doi: 10.1179/174367510X12663198542621.
- [46] E. C. Bingham, *Fluidity and plasticity*. New York, NY, USA: McGraw-Hill Book Co., 1922.
- [47] A. W. Sisko, “The Flow of Lubricating Greases,” *Ind. Eng. Chem.*, vol. 50, no. 12,

- pp. 1789–1792, 1958, doi: 10.1021/ie50588a042.
- [48] L. Fusi, “Lubrication flow of a generalized Casson fluid with pressure-dependent rheological parameters,” *J. Nonnewton. Fluid Mech.*, vol. 274, 2019, doi: 10.1016/j.jnnfm.2019.104199.
- [49] M. Nehdi and M. A. Rahman, “Estimating rheological properties of cement pastes using various rheological models for different test geometry, gap and surface friction,” *Cem. Concr. Res.*, vol. 34, no. 11, pp. 1993–2007, 2004, doi: 10.1016/j.cemconres.2004.02.020.
- [50] M. A. Rahman and M. Nehdi, “Empirical correlations between rheological properties of cement pastes from various models,” *Indian Concr. J.*, vol. 79, no. 10, pp. 52–60, 2005.
- [51] R. S. Campos and G. F. Maciel, “Test protocol and rheological model influence on determining the rheological properties of cement pastes,” *J. Build. Eng.*, vol. 44, p. 103206, 2021, doi: 10.1016/j.job.2021.103206.
- [52] M. J. Crawley, *Applied Linear Regression Models: Non-linear Regression*. 2012.
- [53] A. R. Kamel and M. R. Abonazel, “A Simple Introduction to Regression Modeling using R,” *Comput. J. Math. Stat. Sci.*, vol. 2, no. February, pp. 52–79, 2023, doi: 10.21608/cjmss.2023.189834.1002.
- [54] R. A. Gordon, “Regression Analysis for the Social Sciences,” *Regres. Anal. Soc. Sci.*, no. February, 2012, doi: 10.4324/9780203118092.
- [55] N. Bouleau, *Error Calculus for Finance and Physics*. Walter de Gruyter, 2003. doi: 10.1515/9783110199291.
- [56] T. Nonlinear and R. Model, “Nonlinear Regression : Iterative Estimation and Linear Approximations,” no. 32, pp. 32–66, 1988.
- [57] J. E. S. L. Teixeira, V. Y. Sato, L. G. Azolin, F. A. Tristão, G. L. Vieira, and J. L. Calmon, “Study of cement pastes rheological behavior using dynamic shear rheometer,” *Rev. IBRACON Estruturas e Mater.*, vol. 7, no. 6, pp. 922–939, Dec. 2014, doi: 10.1590/S1983-41952014000600003.
- [58] D. Feys, R. Cepuritis, S. Jacobsen, K. Lesage, E. Secrieru, and A. Yahia,

- “Measuring rheological properties of cement pastes: Most common techniques, procedures and challenges,” *RILEM Tech. Lett.*, vol. 2, pp. 129–135, 2017, doi: 10.21809/rilemtechlett.2017.43.
- [59] T. Yoshida, Y. Tasaka, and Y. Murai, “Quantitative evaluation of rheological properties for complex fluids using ultrasonic spinning rheometry,” pp. 5–8, 2016.
- [60] Thermo Fisher Scientific, “Instruction Manual HAAKE Viscotester 550,” 2007.
- [61] A. Papo and L. Piani, “Effect of various superplasticizers on the rheological properties of Portland cement pastes,” *Cem. Concr. Res.*, vol. 34, no. 11, pp. 2097–2101, Nov. 2004, doi: 10.1016/j.cemconres.2004.03.017.
- [62] A. Govin, M. C. Bartholin, W. Schmidt, and P. Grosseau, “Combination of superplasticizers with hydroxypropyl guar, effect on cement-paste properties,” *Constr. Build. Mater.*, vol. 215, pp. 595–604, 2019, doi: 10.1016/j.conbuildmat.2019.04.137.
- [63] M. Kasińska, J. Kempniński, and R. Świerzko, “the Consistency of Cement Pastes and Their Rheological Parameters,” *Acta Sci. Pol. Form. Circumiectus*, vol. 15, no. 3, pp. 71–81, 2017, doi: 10.15576/asp.fc/2016.15.3.71.
- [64] M. Berra, F. Carassiti, T. Mangialardi, A. E. Paolini, and M. Sebastiani, “Effects of nanosilica addition on workability and compressive strength of Portland cement pastes,” *Constr. Build. Mater.*, vol. 35, pp. 666–675, 2012, doi: 10.1016/j.conbuildmat.2012.04.132.
- [65] J. He, C. Cheng, X. Zhu, and X. Li, “Effect of Silica Fume on the Rheological Properties of Cement Paste with Ultra-Low Water Binder Ratio,” *Materials (Basel)*, vol. 15, no. 2, 2022, doi: 10.3390/ma15020554.
- [66] A. Schneider and H. Bruckner, “Impact of some parameters on rheological properties of cement paste in combination with PCE-based Plasticizers,” pp. 1–10, 2008.
- [67] K. Karakuzu, V. Kobya, A. Mardani, B. Felekoğlu, and K. Ramyar, “Effect of Different C3A Content on Rheological Parameters in Paste Mixtures,” *Key Eng. Mater.*, vol. 936, pp. 205–209, 2022, doi: 10.4028/p-v2bd0c.

Annex

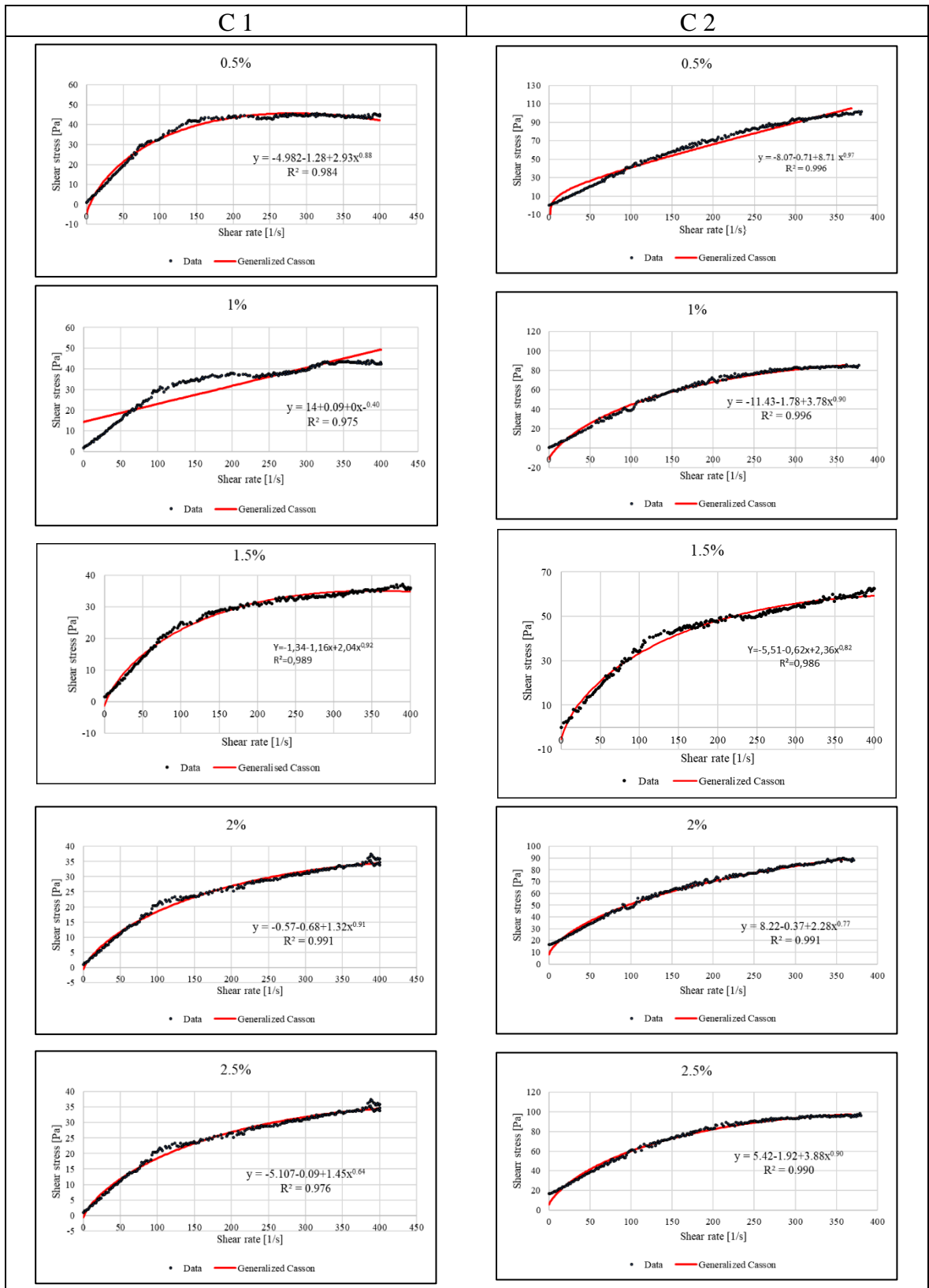


Figure 1: Generalized Casson model for SP1

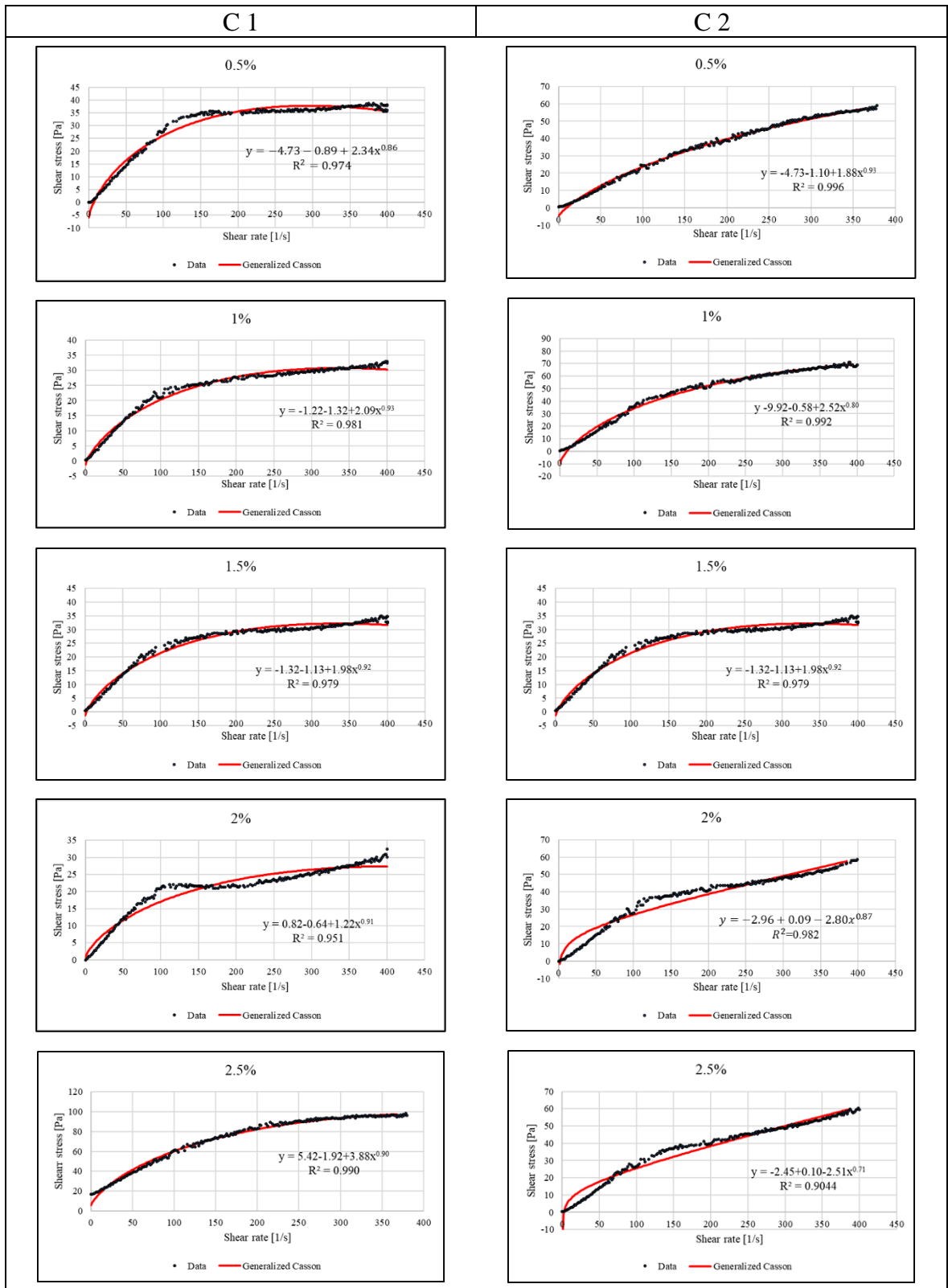


Figure 2: Generalized Casson model for SP2

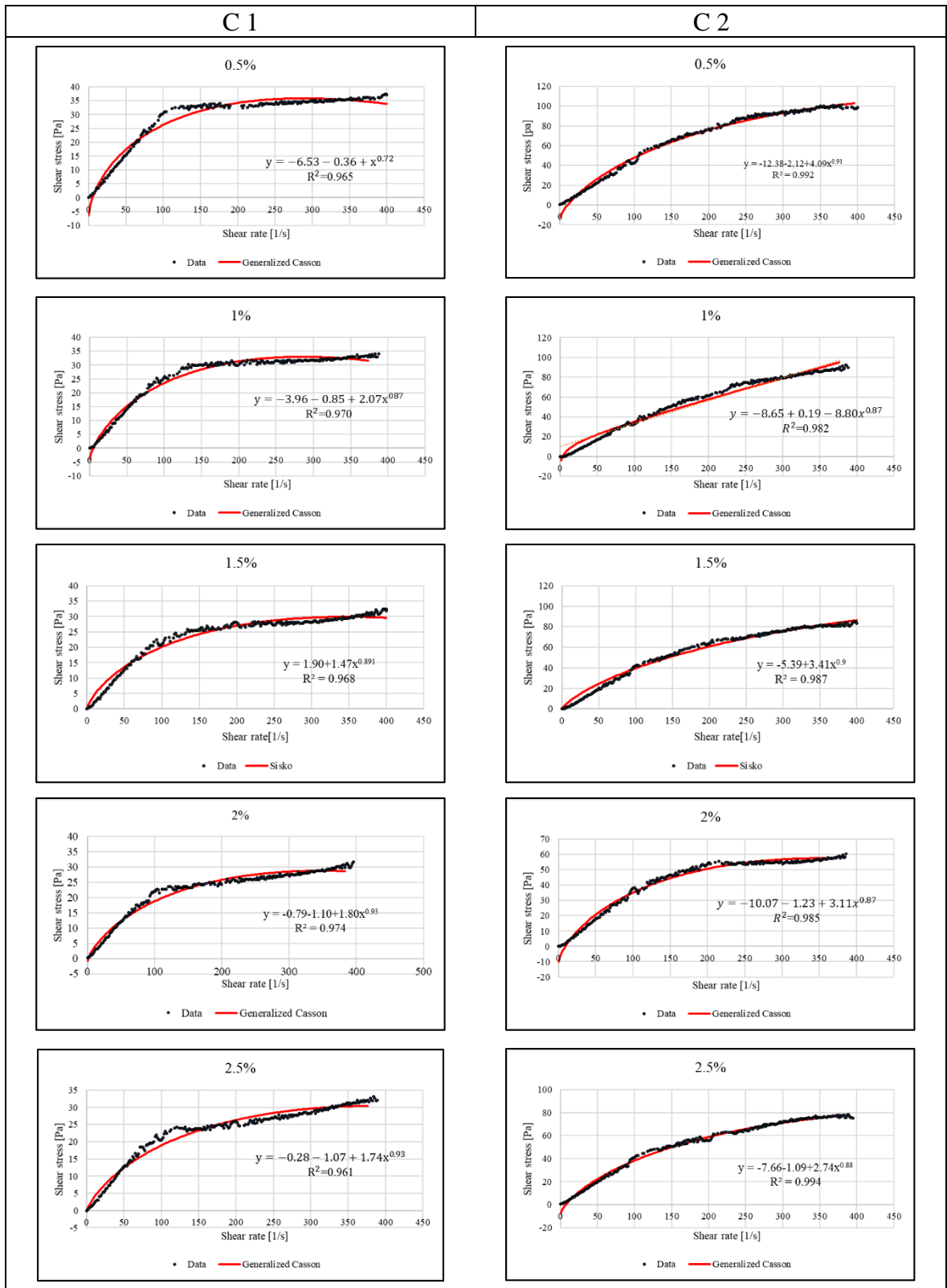


Figure 3: Generalized Casson model for SP3

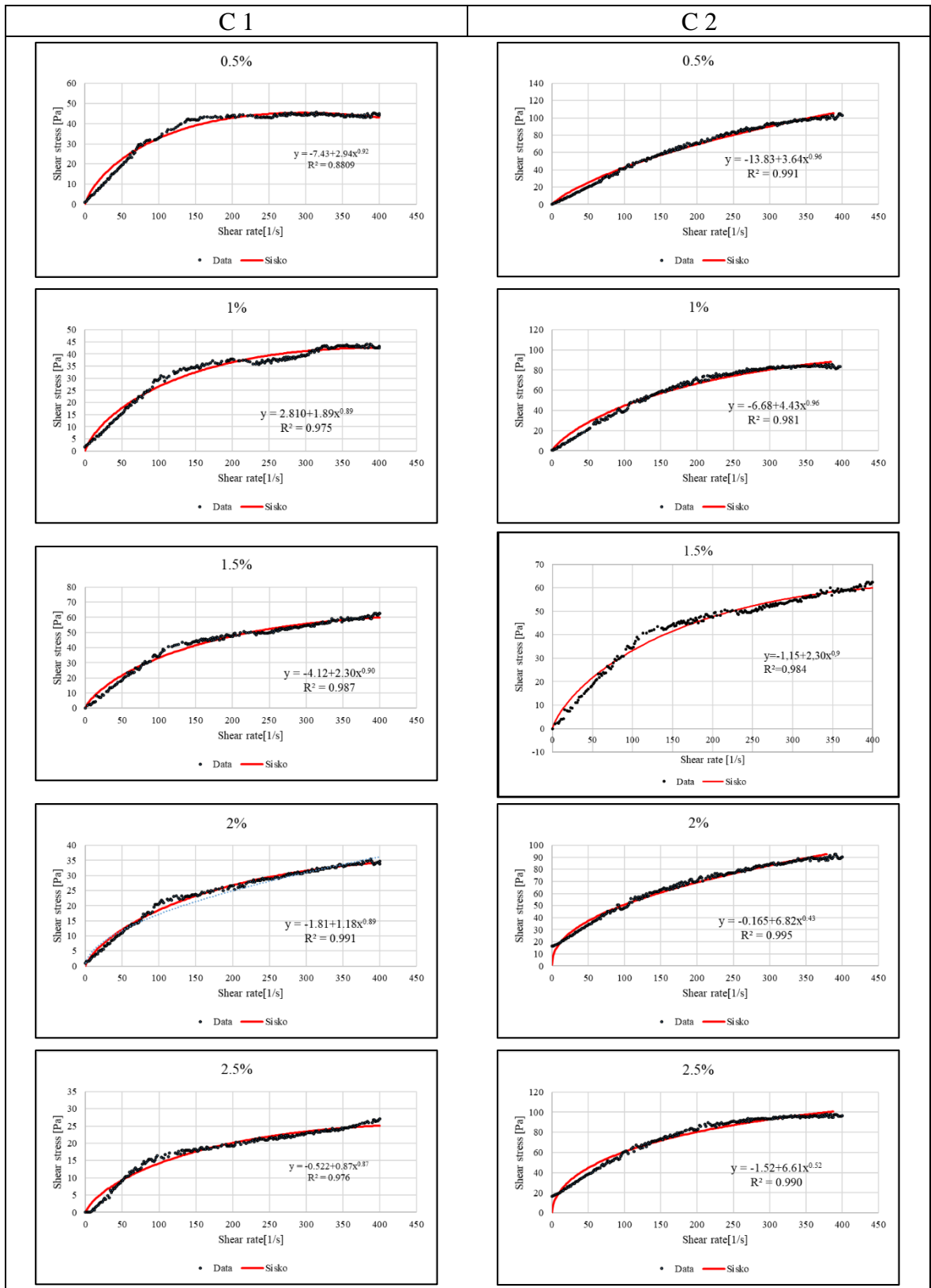


Figure 4: Sisko model for SP1

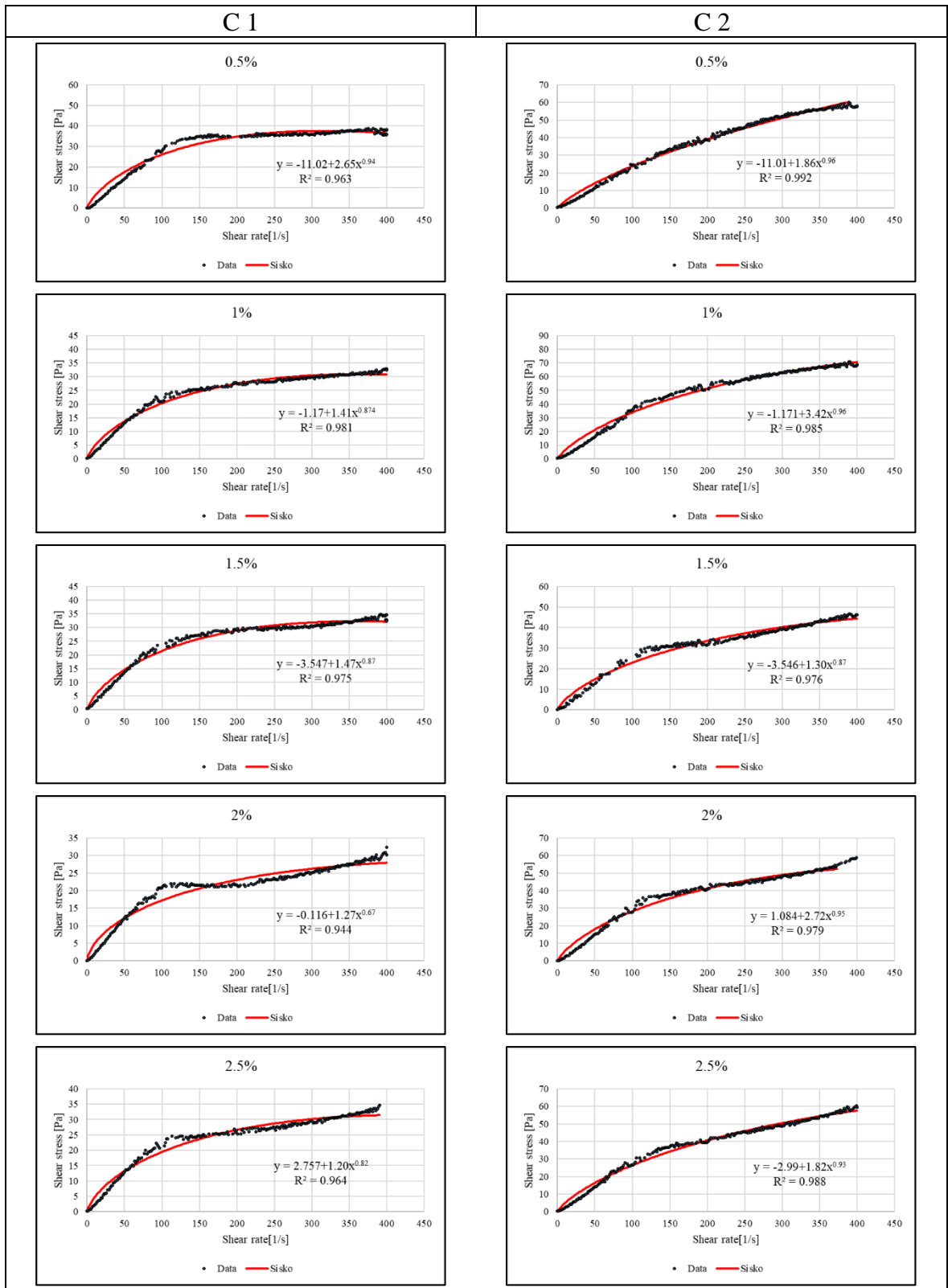


Figure 5: Sisko model for SP2

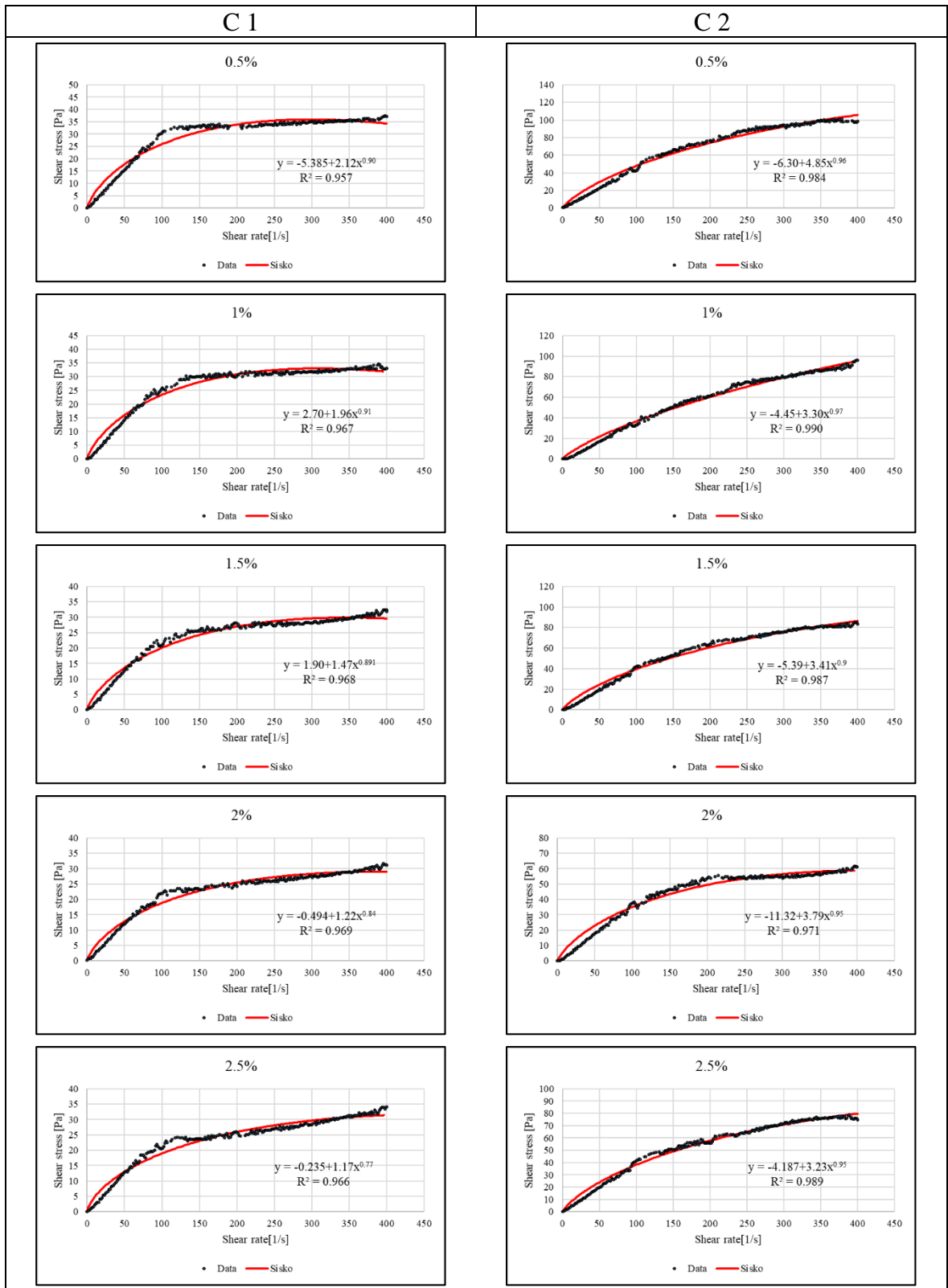


Figure 6: Sisko model for SP3

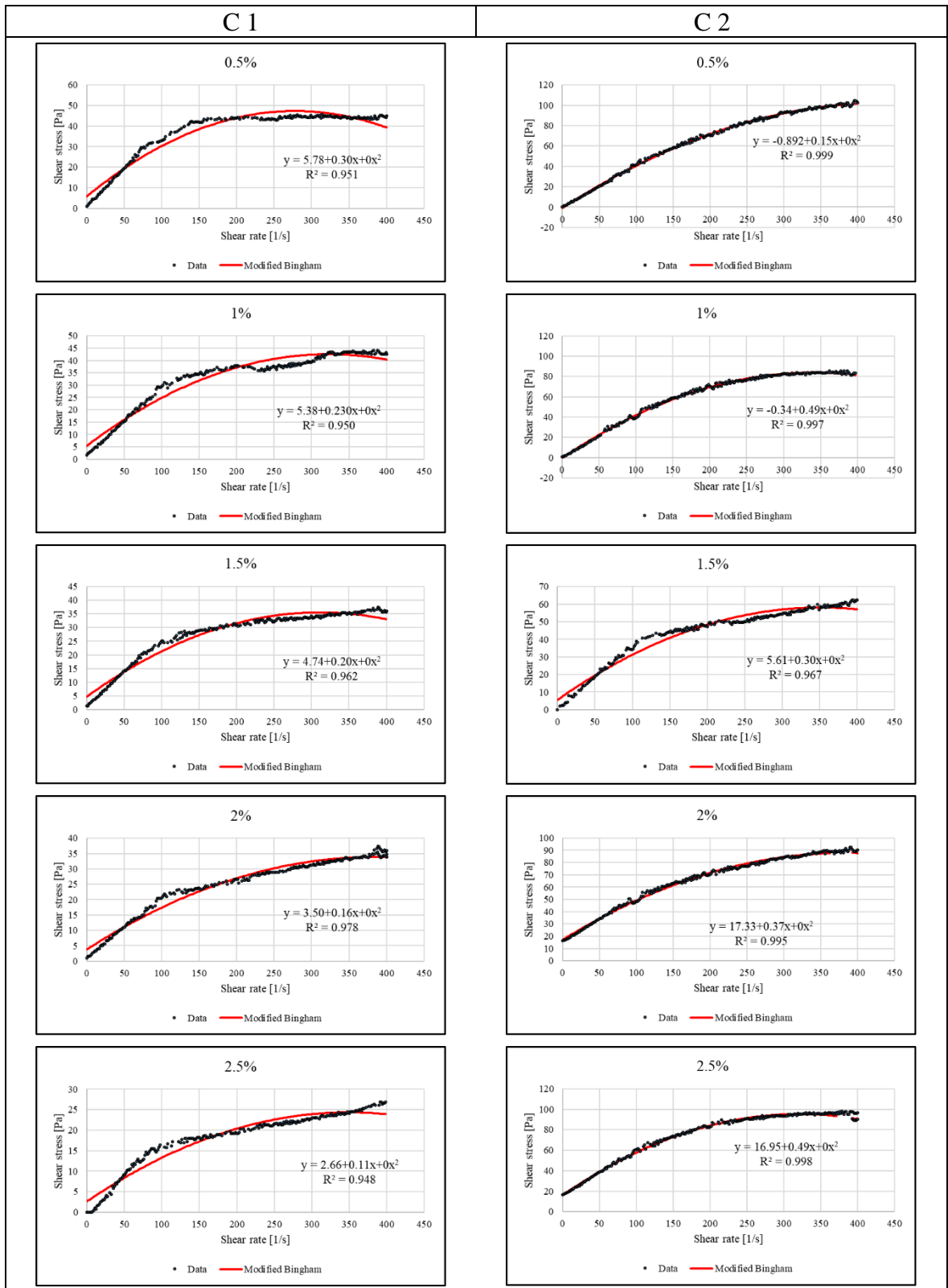


Figure 7: Modified Bingham model for SP1

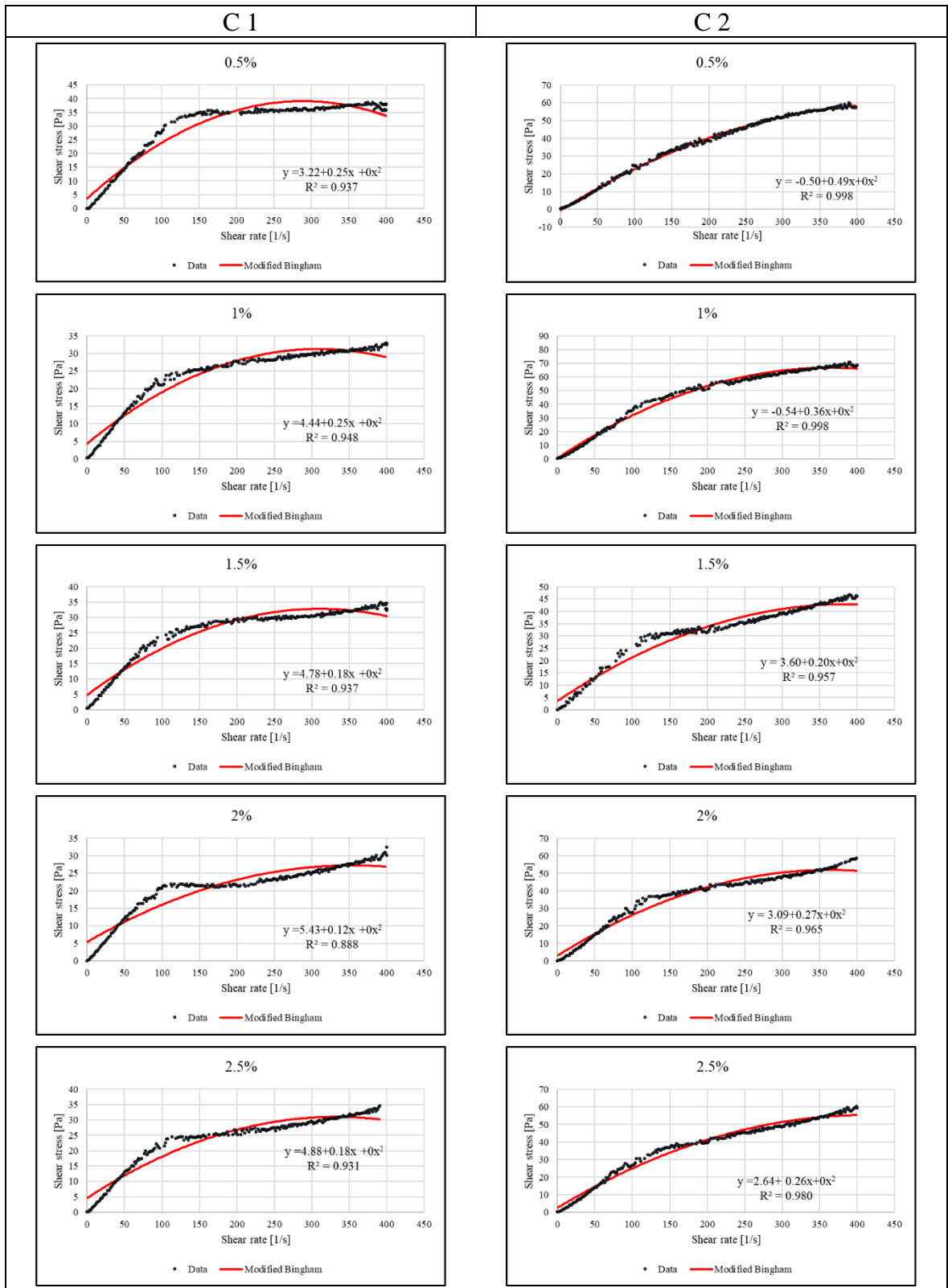


Figure 8: Modified Bingham model for SP2

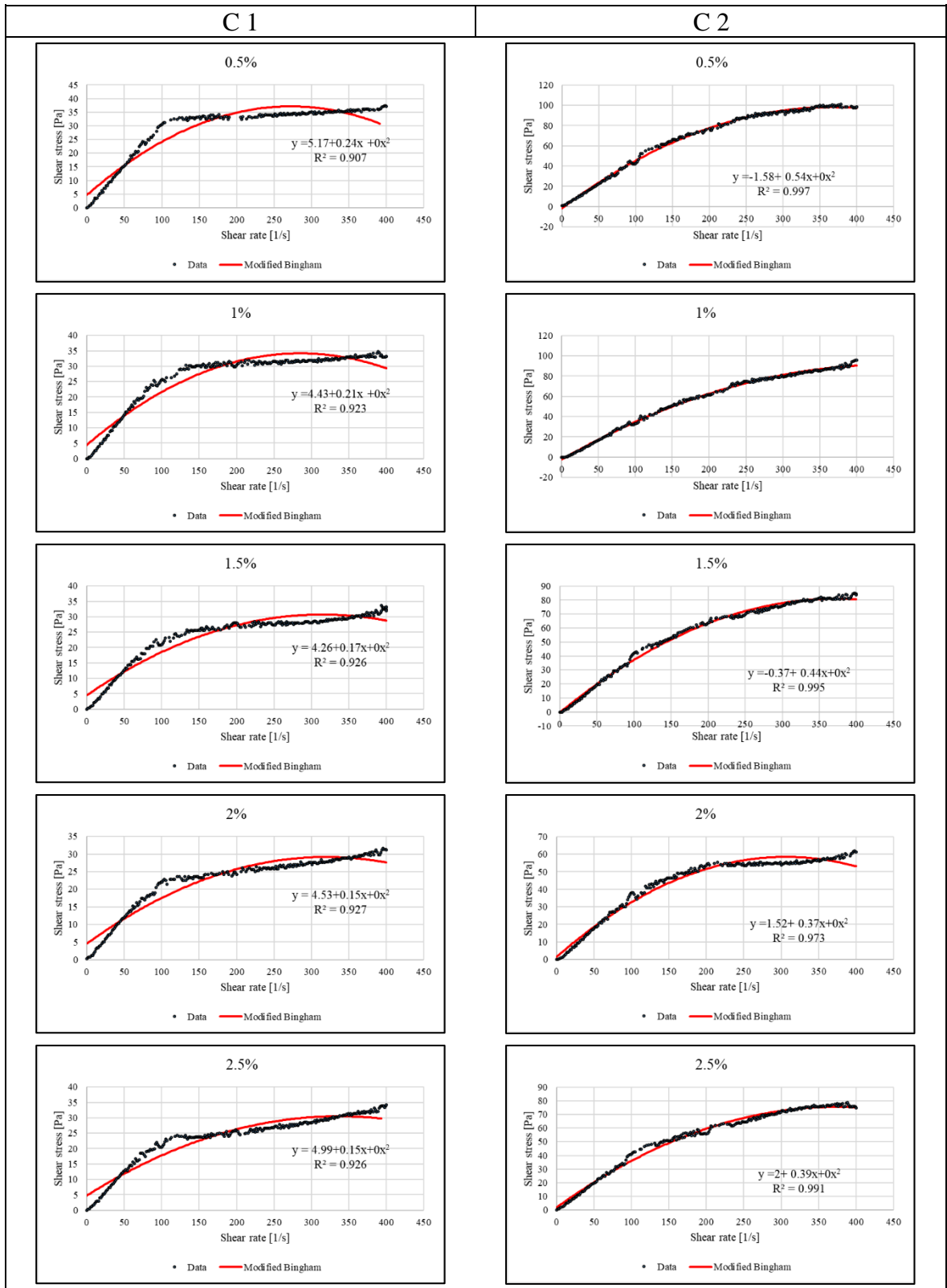


Figure 9: Modified Bingham model for SP3